UNIVERSITÄT ZU LÜBECK
KLINIK FÜR KINDER- UND JUGENDMEDIZIN

From the Department of Pediatrics, University of Lübeck

Director: Prof. Dr. med. Egbert Herting

# Immune responses of preterm macrophages and their role for the development of bronchopulmonary dysplasia

**Dissertation**

for Fulfillment of Requirements

for the Doctoral Degree

of the University of Lübeck

from the Department of Natural Sciences

Submitted by

Nele Twisselmann

from Kaltenkirchen

Lübeck 2019

First referee: Prof. Dr. med. Christoph Härtel
Second referee: Prof. Dr. rer. nat. Ulrich Schaible

Date of oral examination: 16th of January 2020

Approved for printing. Lübeck, 21st January 2020

## Table of content

## List of figures

## List of tables

## Abbreviations

| | |
|---|---|
| °C | degree Celsius |
| µg | microgram |
| µL | microliter |
| AM | alveolar macrophage |
| APC | allophycocyanin |
| BPD | bronchopulmonary dysplasia |
| BSA | bovine serum albumin |
| BV | brilliant violet |
| CD | cluster of differentiation |
| cDNA | complementary DNA |
| COX | cyclooxygenase |
| CXCL | chemokine (C-X-C motif) ligand |
| DC | dendritic cell |
| DNA | deoxyribonucleic acid |
| dNTP | deoxyribonucleoside triphosphate |
| EDTA | ethylenediaminetetraacetic acid |
| *et al.* | *et alii*, and others |
| ETC | electron transport chain |
| FBS | fetal bovine serum |
| FcR | Fc receptor |
| FGF | fibroblast growth factor |
| FITC | fluorescein isothiocyanate |
| FOXP3 | forkhead box P3 |
| GM-CSF | granulocyte-macrophage colony-stimulating factor |
| GNN | German Neonatal Network |
| h | hour |
| HEPES | 4-(2-hydroxyethyl)-1-piperazineethanesulfonic acid |
| HIF-1 | hypoxia-inducible factor 1 |
| HLA-DR | human leukocyte antigen - DR isotype |
| IgG | immunoglobulin G |
| IFN | interferon |
| IL | interleukin |
| ILC | innate lymphoid cell |
| LPS | lipopolysaccharide |
| MΦ | macrophages |

| | |
|---|---|
| MCP | monocyte chemoattractant protein |
| M-CSF | macrophage colony-stimulating factor |
| MDM | monocyte-derived macrophages |
| MIF | macrophage migration inhibitory factor |
| min | minute |
| mL | milliliter |
| mRNA | messenger RNA |
| NEC | necrotizing enterocolitis |
| NF-κB | nuclear factor kappa-light-chain-enhancer of activated B cells |
| ng | nanogram |
| NK cell | natural killer cell |
| nm | nanometer |
| NO | nitric oxide |
| Nrf2 | nuclear factor-like 2 |
| $O_2$ | oxygen |
| OXPHOS | oxidative phosphorylation |
| PBS | phosphate buffered saline |
| PCR | polymerase chain reaction |
| PD-L 1 | programmed cell-death ligand 1 |
| PE | R-phycoerythrin |
| PerCP | peridinin chlorophyll |
| pg | picogram |
| PRR | pattern recognition receptor |
| RDS | respiratory distress syndrome |
| RNA | ribonucleic acid |
| RORC | RAR-related orphan receptor C |
| ROS | reactive oxygen species |
| rpm | rounds per minute |
| RPMI medium | Roswell Park Memorial Institute medium |
| RSV | respiratory syncytial virus |
| RT | room temperature |
| RT-PCR | reverse transcription PCR |
| sec | seconds |
| SP-A | surfactant protein A |
| TBX21 | T-box transcription factor 21 |
| TCA | tricarboxylic acid |

| | |
|---|---|
| TGF | transforming growth factor |
| Th | T helper cell |
| TLR | toll-like receptor |
| TNF | tumor necrosis factor |
| Treg | regulatory T cell |
| VLBW | very low birth weight |

## Abstract

Preterm infants are highly susceptible to sustained lung inflammation, which may be triggered by exposure to multiple environmental cues such as supplemental $O_2$ and infections. The underlying mechanisms are still poorly understood. The hypothesis of this study is that dysregulated macrophage (MΦ) activation is a key feature leading to inflammation-mediated development of bronchopulmonary dysplasia (BPD) in preterm infants.

To address this hypothesis, age-dependent differences in immune responses of monocyte-derived macrophages from preterm infants were characterized and compared to term infants and adults. To better understand lung immunity, an *ex-vivo* double-hit model was developed to mimic key lung exposure factors. Therefore, cord blood samples of preterm infants (n=14) and term infants (n=19) as well as peripheral blood from healthy adults (n=17) were collected. Surface markers, cytokine release, transcriptome pathway profiles and T cell polarization of preterm MΦ were compared to those of term and adult MΦ after double-hit exposure to different $O_2$ concentrations and subsequent lipopolysaccharide (LPS) stimulation.

After LPS stimulation, preterm MΦ demonstrated increased interleukin and chemokine signaling as well as decreased respiratory electron transport chain gene expression determined by transcriptome pathway profiling compared to term MΦ. Additionally, increased basal toll-like receptor 4 surface expression and sustained cytokine release of tumor necrosis factor (TNF)α, interleukin (IL)-6, IL-10, IL-23 and chemokine CXCL10 were detected in preterm MΦ. The supernatant of preterm MΦ led to a T helper (Th)17 rather than a Th1 polarization in neonatal naïve T cells as compared to supernatants of term and adult MΦ. There were no differences in immune responses of term and adult MΦ.

After exposure to 65% $O_2$ and subsequent LPS stimulation, preterm MΦ showed increased surface expression of human leukocyte antigen - DR isotype (HLA-DR) and exaggerated cytokine release of TNFα, IL-6 and IL-1β compared to LPS stimulation alone. The released cytokine pattern of preterm infants led to a decrease of regulatory T cell (Treg) polarization after the double-hit stimulation compared to the responses of adult MΦ. Furthermore, chemokine signaling pathways were upregulated, while the respiratory electron transport chain was downregulated after the double-hit with 65% $O_2$ and LPS compared to LPS stimulation alone.

Preterm MΦ responses to key lung exposure factors suggest their involvement in excessive inflammation due to age-dependent differences, potentially associated with a Th17/Treg imbalance in the developing lung.

## Zusammenfassung

Frühgeborene haben ein hohes Risiko, eine chronische Lungenerkrankung zu entwickeln, die durch mehrere Einflussfaktoren wie zum Beispiel Sauerstoffbedarf und Infektionen ausgelöst werden kann. Wie genau diese Einflussfaktoren zu einer anhaltenden Entzündung führen, ist noch nicht im Detail verstanden. Die Hypothese dieser Arbeit ist, dass fehlregulierte Makrophagenaktivierung eine zentrale Rolle spielt und zu einer chronischen Entzündung in der Lunge von Frühgeborenen führt.

Um diese Hypothese zu beweisen, wurden Gestationsalter-abhängige Unterschiede in der Immunantwort von monozyten-abstammenden Makrophagen (MDMs) von Frühgeborenen im Vergleich zu Reifgeborenen und Erwachsenen charakterisiert. Außerdem wurde ein *ex-vivo* Doppel-Hit Modell entwickelt, welches die Haupteinflussfaktoren der chronischen Lungenerkrankung nachahmt, um die Immunität der Lunge besser beschreiben zu können. Daher wurde Nabelschnurblut von Frühgeborenen (n=14) und Reifgeborenen (n=19) sowie peripheres Blut von gesunden Erwachsenen (n=17) gesammelt. Oberflächenmarker, Zytokinausschüttung, Signalwegprofile auf Transkriptomebene und T Zellpolarisation wurden von Frühgeborenen MDMs charakterisiert und mit MDMs von Reifgeborenen und Erwachsenen nach einem Doppel-Hit mit verschiedenen $O_2$ Konzentrationen und anschließender Lipopolysaccharid (LPS) Stimulation verglichen.

Interleukin- und Chemokin-Signalwege waren bei Frühgeborenen MDMs im Vergleich zu Reifgeborenen MDMs hochreguliert, während Signalwege des respiratorischen Elektronentransports nach LPS Stimulation bei Frühgeborenen herunterreguliert waren. Außerdem konnte eine erhöhte basale Toll-like-Rezeptor 4 Oberflächenexpression auf Frühgeborenen MDMs und eine anhaltende Zytokinausschüttung von Tumornekrosefaktor (TNF)α, Interleukin (IL)-6, IL-10, IL-23 und Chemokin CXCL10 von Frühgeborenen MDMs nach LPS Stimulation nachgewiesen werden. Die Mediumüberstände von Frühgeborenen MDMs nach LPS Stimulation führten zu einer T Helfer (Th)17 Polarisation in neonatalen naiven T Zellen, welche nicht bei Reifgeborenen nachweisbar war.

Nach einem Doppel-Hit mit 65% $O_2$ und anschließender LPS Stimulation wiesen Frühgeborene MDMs eine verstärkte Oberflächenexpression von humanem Leukozytenantigen - DR (HLA-DR) auf und die Zytokinausschüttung von TNFα, IL-6 und IL-1β im Vergleich zur LPS Stimulation unter atmosphärischem $O_2$ war verstärkt. Die Herunterregulierung der Polarisierung zu regulatorischen T Zellen (Treg) war nach dem Doppel-Hit von Frühgeborenen MDMs im Vergleich zu Erwachsenen MDMs ausgeprägter. Des Weiteren war nach dem Doppel-Hit der Chemokin-Signalweg intensiver hochreguliert und der respiratorische Elektronentransport zusätzlich herunterreguliert in Frühgeborenen MDMs im Vergleich zur einfachen LPS Stimulation.

Nach Stimulation mit den Haupteinflussfaktoren der chronischen Lungenerkrankung, erhöhter $O_2$ Bedarf und Infektion, vermitteln Frühgeborenen Makrophagen eine verstärkte inflammatorische Immunantwort aufgrund von gestationsalter-abhängigen Unterschieden, die möglicherweise mit einem Th17/Treg Ungleichgewicht in der sich noch entwickelnden Lunge assoziiert ist.

# 1. Introduction

## 1.1 Bronchopulmonary dysplasia

Bronchopulmonary dysplasia (BPD) is a chronic lung disease of preterm infants leading to persistent pulmonary problems (Thorkelsson and Sigfusson 2014). To understand the disease, several aspects of BPD are important, including epidemiological data, risk profiles and multiple factors contributing to pathophysiology (Thorkelsson and Sigfusson 2014). Hence, it is a major challenge to find specific BPD markers, which would help to guide individualized strategies of prevention and therapy in the future.

### 1.1.1 Susceptibility of preterm infants

More than 1 in 10 babies are born preterm, accounting for approximately 10% of all births even in developed countries (Beck et al. 2010). Preterm birth is defined as delivery of a baby before 37 weeks of gestation (Figure 1-1, Tucker and Mcguire 2004). Furthermore, over 1% of all newborns are born before 32 weeks of gestation with a very low birth weight (VLBW) below 1500 g (Howson, Kinney, and Lawn 2012). Preterm infants have an increased mortality as well as short- and long-term morbidities due to their prematurity (Howson, Kinney, and Lawn 2012).

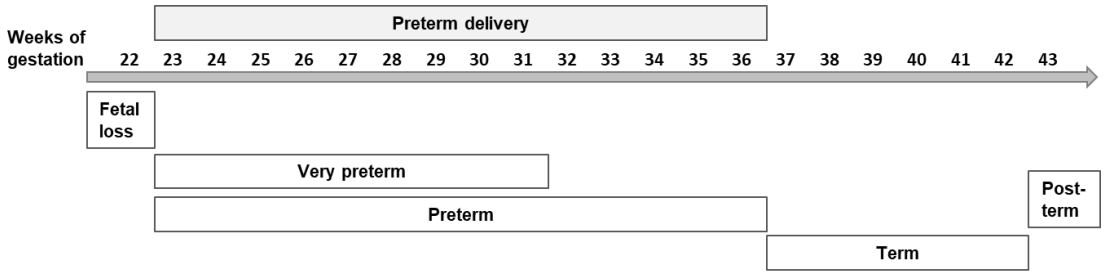


**Figure 1-1: Definitions of preterm birth by completed weeks of gestation** (Tucker and Mcguire 2004).

The German Neonatal Network (GNN), initiated and implemented at the Department of Pediatrics at the University of Lübeck in 2009 (Prof. Dr. Göpel, Prof. Dr. Herting), contains demographic information, details of hospitalization and discharge, and an established biobank including DNA samples of all preterm infants in 60 neonatal centers across Germany. According to data of the GNN, leading causes of mortality and morbidity in preterm infants are respiratory failure, infections, necrotizing enterocolitis and chronic lung diseases such as BPD. Antenatal glucocorticoid therapy accelerating lung maturation (Roberts et al. 2017), and surfactant therapy reducing surface tension at the air-liquid

interface of the alveolus (Nkadi, Merritt, and Pillers 2009), as well as gentler respiratory support have led to a decrease in mortality due to respiratory problems in preterm infants (Jobe and Bancalari 2001). However, the number of surviving preterm infants developing BPD has not changed over the last few decades (Gortner et al. 2011; Klinger et al. 2013; Tröger et al. 2014). Epidemiological data of GNN show that BPD affects 14% of VLBW infants born with a gestational age before 32 weeks (Figure 1-2).

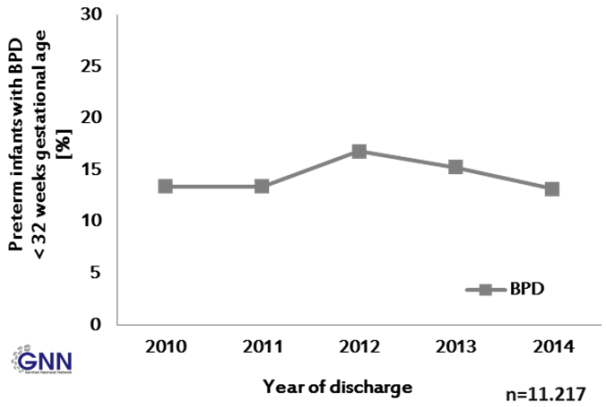


**Figure 1-2: Rate of bronchopulmonary dysplasia (BPD) in very low birth weight infants born below 32 weeks of gestation in Germany between 2010 and 2014** (Data from GNN).

Therefore, BPD remains one of the most common serious pulmonary morbidities in preterm infants. BPD can lead to long-term problems, such as reduced lung function, recurrent respiratory tract infections, and the development of asthma, as well as neurodevelopmental impairments (Doyle and Anderson 2009; Landry et al. 2011; Islam et al. 2015; Goedicke-Fritz et al. 2017; Näsänen-Gilmore et al. 2018).
A better understanding of BPD in preterm infants and development of new preventive and therapeutic strategies can improve the quality of life in those patients and can reduce long-term health care costs.

### 1.1.2 History and clinical definitions of bronchopulmonary dysplasia

BPD has first been described by Northway *et al*. in 1967 as a lung injury in preterm infants, resulting from supplemental $O_2$ and mechanical ventilation. Airway injury, inflammation and severe fibrosis have been the main findings in BPD at that time (Northway Jr, Rosan, and Porter 1967). The described study population has consisted of preterm infants with a mean gestational age of 34 weeks. Those infants rarely develop BPD today due to improved clinical practices (Abman, Bancalari, and Jobe 2017). Nowadays, very preterm infants born below 32 weeks of gestation have increased survival

rates (Stoll et al. 2015), but their survival is accompanied by an increased risk of developing BPD (Tröger et al. 2014). With current progress in neonatal intensive care, including surfactant therapy to spontaneously breathing infants and less invasive ventilation, lungs of very premature infants developing BPD are characterized less by fibrosis and airway obstruction, but instead show larger and fewer alveoli, reduced vascularization and increased elastic tissue, indicating an interference with lung development (Jobe and Bancalari 2001). Compared with the pathology described by Northway *et al*., the common BPD phenotype today is changed and is now characterized by an arrest of lung development (Day and Ryan 2017).

Since there is no specific maker for the diagnosis of BPD due to the complexity of this multifactorial disease (Trembath and Laughon 2012), the diagnosis relies on clinical parameters only (Jobe and Bancalari 2001). The original definition has been the use of $O_2$ therapy for at least 28 days, which in fact does not take into account the developmental differences in infants born across various gestational ages (Jobe and Bancalari 2001). The $O_2$ requirement at 36 weeks of corrected gestational age (equivalent to 32 weeks gestational age at birth plus 4 weeks postnatal age) is a better predictor of long-term adverse respiratory outcomes (Shennan et al. 1988). A workshop in 2000 has attempted to clarify the definition with the introduction of a severity scale, classifying the disease as mild, moderate, and severe BPD (Table 1-1, Jobe and Bancalari 2001). The diagnosis time point depends on the gestational age at birth being below or above 32 weeks. Infants born below 32 weeks of gestation are diagnosed at 36 weeks of corrected gestational age or discharge from the hospital. Infants born above 32 weeks of gestation are diagnosed at 56 days postnatal age or discharge. All infants, who are treated with supplemental $O_2$ over 21% for at least 28 days, but not at diagnosis time point are defined as having a mild BPD. If an infant needs supplemental $O_2$ below 30% at diagnosis time point, moderate BPD is diagnosed. Infants requiring supplemental $O_2$ above 30% or other respiratory support at diagnosis time point are diagnosed with severe BPD. The risk for long-term morbidities increases with BPD severity (Jobe and Bancalari 2001). A physiological definition developed by Walsh *et al*. defines BPD as a failure to maintain an $O_2$ saturation value above 90% when challenged with 21% $O_2$ at 36 weeks corrected gestational age (Walsh et al. 2004). This definition has reduced the between-center variability in diagnosing infants with BPD.

Regardless of which BPD definition is used, the diagnosis is made at a time point when the disease is already present, making the identification of preventive therapies for preterm infants at risk for BPD challenging. Additionally, the clinical definitions of BPD have only a moderate sensitivity and specificity in diagnosing the disease and predicting

long-term problems (Jobe 2011). Understanding risk factors leading to the development of BPD is therefore critical for better characterizing the disease and improving outcomes in patients.

**Table 1-1: Definition of bronchopulmonary dysplasia (BPD): Diagnostic criteria** (Jobe and Bancalari 2001).

| **Gestational age at birth** | < 32 weeks | > 32 weeks |
|---|---|---|
| **Diagnosis time point** | 36 weeks corrected gestational age or discharge | 56 days postnatal age or discharge |
| | **Treatment with $O_2$ > 21% for at least 28 days PLUS** | |
| **Mild BPD** | Breathing room air at time point of diagnosis | |
| **Moderate BPD** | Need for < 30% $O_2$ at time point of diagnosis | |
| **Severe BPD** | Need for > 30% $O_2$ and/or other respiratory support at time point of diagnosis | |

### 1.1.3 Risk factors for bronchopulmonary dysplasia

Researchers have identified risk factors for BPD by categorizing preterm infants as having or not having the disease based on one of the definitions mentioned above (1.1.2), and retrospectively analyzing factors that influenced the risk up to the time point of BPD diagnosis. Figure 1-3 shows the most important risk factors of BPD development in preterm infants categorized into endogenous and exogenous factors (Trembath and Laughon 2012). The degree of prematurity, genetic susceptibility, and male gender are endogenous risk factors that have been associated with disease development (Gortner et al. 2011; Trembath and Laughon 2012; Klinger et al. 2013; Lal and Ambalavanan 2015b). A negative correlation of BPD development with gestational age and birth weight has been shown in several studies (Data from GNN, Klinger et al. 2013; Tröger et al. 2014). Antenatal exposures, including fetal growth restriction and intra-amniotic infection, are also connected to an adverse BPD outcome, although some epidemiological studies have not found an association with intra-amniotic infection (Trembath and Laughon 2012). The main exogenous risk factors after birth include respiratory distress syndrome (RDS) accompanied by prolonged need for supplemental $O_2$ and mechanical ventilation, as well as sepsis development and inflammation (Data from GNN, Speer 2006; Trembath and Laughon 2012; Klinger et al. 2013).

Exogenous BPD risk factors, such as need for respiratory support and infections, also shape the developing immune system of preterm infants, suggesting a tight interaction of immune development and BPD (Speer 2006; Popova 2013; Hilgendorff et al. 2014; Niedermaier and Hilgendorff 2015; Jobe 2015; Balany and Bhandari 2015). Identifying risk

factors has led to a better understanding of the disease and has improved health care of preterm infants (e.g. less invasive respiratory support) (Jobe and Bancalari 2001). However, prediction models developed based on clinical risk factors for BPD have at best only moderate predictive accuracy (Onland et al. 2013), which highlights the importance to understand pathological changes in lung development and underlying immune mechanisms for the development of this multifactorial disease.

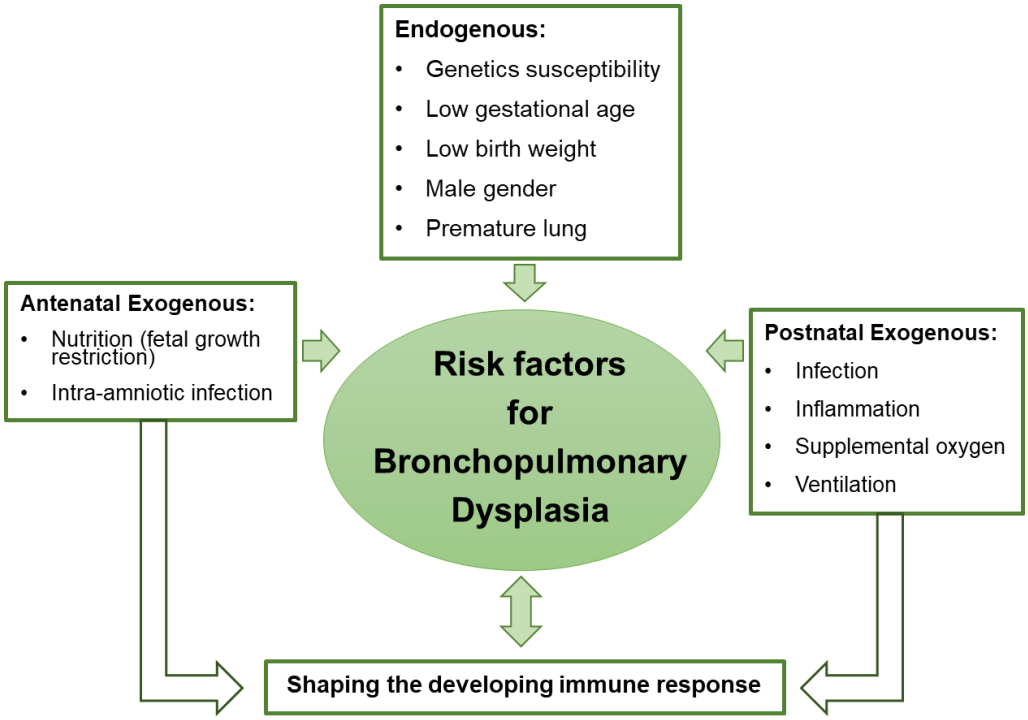


**Figure 1-3: Endogenous and exogenous risk factors shaping the developing immune system leading to an increased risk of BPD development in preterm infants** (Trembath and Laughon 2012)**.**

## 1.2 The developing lung and its immunity in infants

### 1.2.1 Lung development

The organogenesis of the lung is divided into 5 fetal developmental stages that are chronological but overlapping: embryonic (3-7 weeks of gestation), pseudoglandular (5-17 weeks), canalicular (16-26 weeks), saccular (21-38 weeks) and alveolar (starting at 36 weeks of gestation to at least 2 years postnatally) (Figure 1-4; Buczynski, Maduekwe, and O'Reilly 2013; Thorkelsson and Sigfusson 2014). Within this study, the focus is on the last three stages of lung development, since those are the most relevant to the pathogenesis of BPD.

During the canalicular stage (Figure 1-4), the distal airway branching extends further, resulting in the formation of future acini, the gas-exchanging units of the lung. The distal airway is lined by cuboidal cells, which differentiate into type I and II alveolar epithelial cells. Around 24 weeks of gestation, surfactant-containing lamellar bodies are found in type II alveolar cells. In order to form the blood gas barrier, the epithelium starts thinning and becomes surrounded by a network of capillaries. At the end of the canalicular stage, the air blood barrier is thin enough and a large enough surfactant area exists to allow adequate gas exchange, which is necessary for the survival of extremely preterm infants. Infants who are born during the late canalicular and early saccular stage of normal lung development are likely to develop pathologies due to the premature lung developmental stage that exists independent of treatment modalities, making them susceptible for BPD (Thorkelsson and Sigfusson 2014; Rivera et al. 2016).

In the saccular stage (Figure 1-4), surfactant maturation continues and the most distal airways form sac-like structures. Secondary crests divide each saccule into primitive alveoli with flattened epithelium and a double capillary network. This primary septation results in an increase of the inner surface area in the lung and completes the organization pattern of the gas-exchanging unit. Most of the preterm infants are born at some point during the saccular stage of lung development (Thorkelsson and Sigfusson 2014; Rivera et al. 2016).

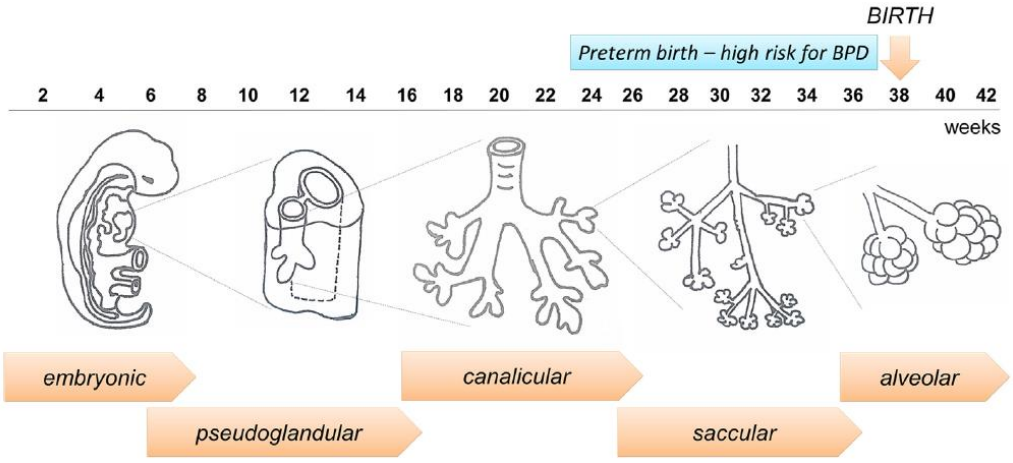


**Figure 1-4: Fetal lung developmental stages during pregnancy.** At preterm birth the fetal lung is in the late canalicular or the saccular stage and can be affected by postnatal risk factors, resulting in increased susceptibility to develop BPD © 2016 Rivera, Siddaiah, Oji-Mmuo, Silveyra and Silveyra (Modified from Rivera et al. 2016).

Finally, the alveolar stage is characterized by the formation of secondary alveolar septa dividing the saccules into alveoli (Figure 1-4). The maturation of the alveolar-capillary

membrane continues by further lengthening and thinning of secondary septa and fusion of the two capillary networks, increasing the surface area available for gas exchange. At term gestation, around 50 million alveoli are present, continuing to increase over the first years of life to reach approximately 300 million alveoli (Thorkelsson and Sigfusson 2014; Rivera et al. 2016).

A careful orchestration of transcription and growth factors, morphogens, and extracellular matrix molecules is required in each of these developmental stages in order to ensure the formation of a lung capable of performing gas exchange upon the transition from intra- to extrauterine life (Buczynski, Maduekwe, and O'Reilly 2013). In case of insufficient functioning of any factor, triggered by a stimulus during preterm birth for example, respiratory disease can occur postnatally (Buczynski, Maduekwe, and O'Reilly 2013). However, preterm infants` lungs are capable to fully develop after birth (Rivera et al. 2016). The main risk factors for BPD, namely respiratory support and infections, can interfere with lung development leading to an arrest in the saccular stage (Rivera et al. 2016). The factors important for lung development and lung immunity are critically intertwined, and therefore the next chapter outlines development and function of lung immunity in early life.

### 1.2.2 Immunity of the lung

At birth, infants undergo a transition from a sheltered intrauterine environment to the extrauterine environment, in which they are challenged by antigens from pathogens, commensals, and their surroundings. Therefore, neonatal immunity is more attenuated in general compared to adults (Levy 2007; Kollmann et al. 2012; Dowling and Levy 2014). Differences include fewer leukocytes in the tissues, a hypo-responsiveness of pro-inflammation and immunoregulatory mechanisms such as increased numbers of regulatory T cells (Treg) and high adenosine levels in extracellular fluids inhibiting pro-inflammatory immune cell functions (Levy et al. 2006; Debock and Flamand 2014; Pettengill, van Haren, and Levy 2014; Pagel et al. 2016). In addition, infants produce less antibodies and have a blunted protective T helper (Th)1 response in early life, with a bias towards Th2 and Th17 responses, as well as dysregulated inflammation (Kollmann et al. 2012; Debock and Flamand 2014; Pang et al. 2018; Jia et al. 2018; Twisselmann et al. 2019). Toll-like receptor (TLR) stimulated cord blood leukocytes produce less Th1-associated cytokines such as interleukin (IL)12p70, interferon (IFN)γ and tumor necrosis factor (TNF)α, but produce greater amounts of IL-10 and Th-17-promoting IL-6 and IL-23 compared to adult leukocytes, even so equivalent cytokine level as in adults occur (Figure 1-5; Kollmann et al. 2009; Belderbos et al. 2009; Corbett et al. 2010; Sharma et al. 2014).

To compensate for the immature adaptive immune reponse, the diaplacentar transfer of immunoglobulins (Ig) from the mother plays an important role for immunity of the offspring ("Nestschutz"). Gestational age-based differences have recently been characterized in glycosylation patterns of IgGs, which may determine pro- and anti-inflammatory profiles of IgGs (Twisselmann et al. 2019). A rather pro-inflammatory profile has been associated with BPD development of preterm infants (Twisselmann et al. 2019). Because of a less-trained adaptive immune response, innate immunity is likely to play a major role in protection against early-life infections and other insults.

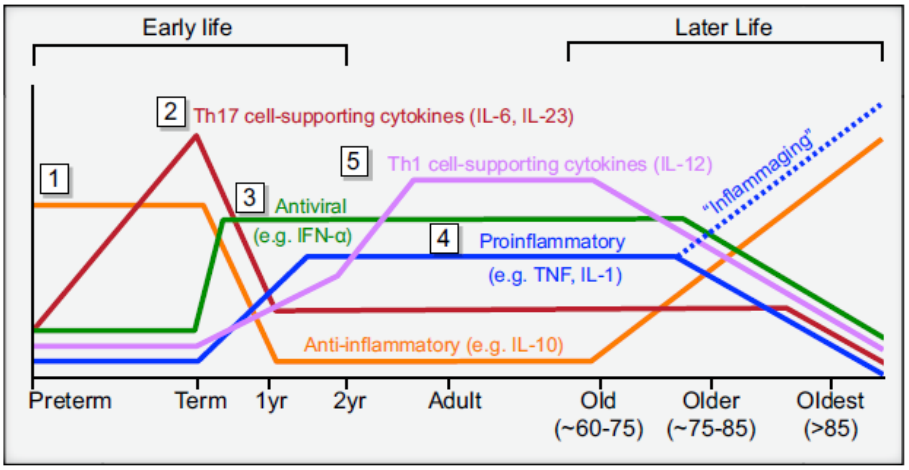


**Figure 1-5: Age-dependent immune development of cytokines and T helper response.** Abbreviations: T helper cells (Th); interleukin (IL); tumor necrosis factor (TNF); interferon (IFN) © 2012 Elsevier Inc., licensee Elsevier Inc. (Reprinted from Kollmann et al. 2012).

Immune cells in the neonatal lung differ in quantity and quality compared to adult lungs and, therefore, respond differently to environmental and microbial exposures (Torow et al. 2017; Lambert and Culley 2017). Not only adequate postnatal lung development, which involves immune cells for tissue remodeling, but also proper immune cell education have to be balanced by the infant in the context of facing massive amounts of antigens (Torow et al. 2017).

Immune cells start populating the lung already in the early pseudoglandular stage, in which low numbers of embryonic macrophages (MΦ), fetal dendritic cells (DCs) and natural killer (NK) cells are found in the primitive respiratory structure (Figure 1-6, Torow et al. 2017). Embryonic MΦ play an important role in orchestrating lung morphogenesis by the release of mediators involved in tissue remodeling, vascularization, and airway branching (Blackwell et al. 2011). Activation of these MΦ by pro-inflammatory stimuli can lead to disruption of normal lung morphogenesis (Blackwell et al. 2011). At the transition to the canalicular phase of lung development, in which epithelium differentiates and

angiogenesis begins (Figure 1-6), embryonic MΦ and DCs are outnumbered by fetal liver-derived monocytes (De Kleer et al. 2014). Under physiological conditions, these monocytes show an immature phenotype at this stage, and they differentiate to alveolar macrophages (AMs) directly after birth due to an increase of granulocyte-macrophage colony-stimulating factor (GM-CSF) in the tissue (Guilliams et al. 2013; De Kleer et al. 2014).

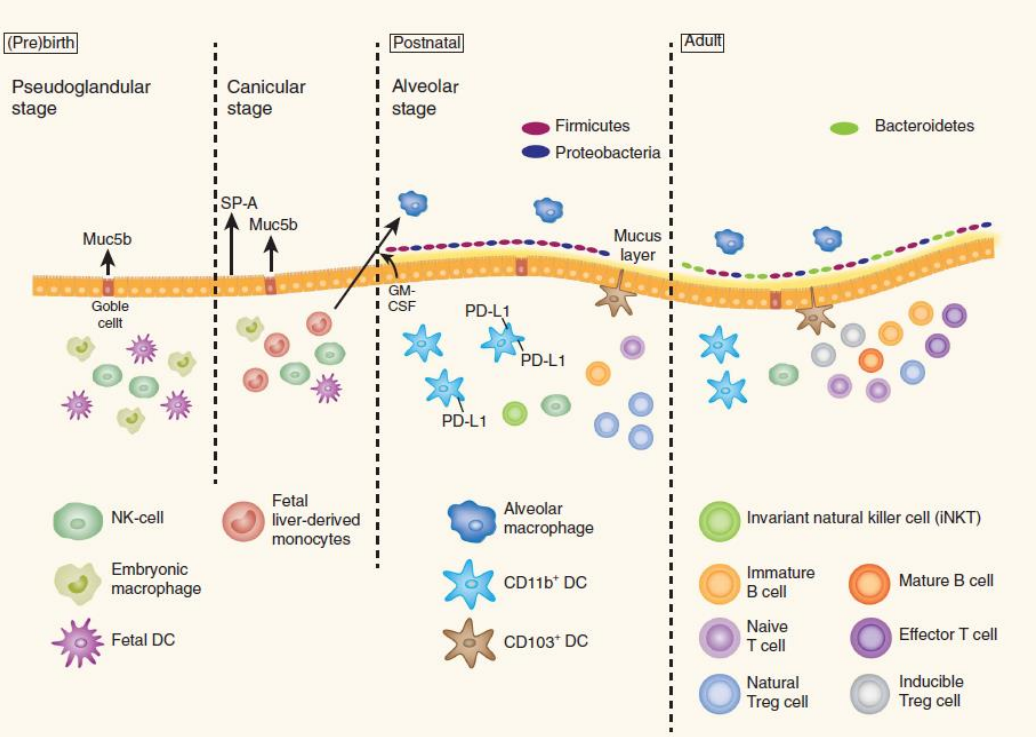


**Figure 1-6: Developing immunity in the lung mucosal tissue during fetal and postnatal lung developmental stages compared to adults.** Embryonic macrophages (MΦ), fetal dendritic cells (DCs), and natural killer (NK) cells are the first cell types that infiltrate the fetal lung during the pseudoglandular stage development. Additionally, goblet cells start to produce mucus (Muc5b). During the canicular phase, fetal liver-derived monocytes begin to replace the embryonic MΦ and surfactant proteins (SP), especially SP-A, are produced. After birth, these fetal liver-derived monocytes differentiate into alveolar macrophages (AM). Other innate and adaptive immune cell types (including invariant natural killer T (iNKT) cells, B and T cells, natural T-regulatory (nTreg) cells) slowly start to infiltrate the lung. nTregs have a high frequency whereas B and T cells are abundant in low numbers with a naïve phenotype. CD11b+ DCs also populate the lung after birth, expressing highest levels of programmed cell death ligand (PD-L) 1, an inhibitory marker induced by the microbiota which starts to establish. Adaptive immune cells increase steadily during postnatal development and display a more mature phenotype with age  (Reprinted from Torow et al. 2017).

CD11b+ DCs process antigens that are biased to induce a Th2 response. Colonizing lung microbes such as Firmicutes and Proteobateria induce transient expression of programmed cell-death ligand 1 (PD-L1) on DCs. PD-L1 facilitates DCs to induce Tregs that are considered important for tolerance during colonization (Figure 1-6; Torow et al. 2017; Lambert and Culley 2017). Resident T and B cells are only detected in low numbers in the postnatal alveolar stage of development and have a naïve phenotype (Figure 1-6; Torow et al. 2017; Lambert and Culley 2017). Naïve neonatal T cells have an intrinsic bias towards a Th2 and Th17 response (Kollmann et al. 2012; Debock and Flamand 2014). However, Tregs accumulate in substantial numbers in the lung (Thome et al. 2016). Tregs are likely to facilitate establishment of a lung microbiome after birth because the microbiome increases in load and diversity over the first weeks of life (Torow et al. 2017).

Immune cells in the neonatal lung have an important dual role. On one hand they are important for remodeling and repairment of the tissue, especially during the alveolar stage of development (Torow et al. 2017; Lambert and Culley 2017; Loering et al. 2019). On the other hand, neonatal lung immune cells need to be properly educated in order to balance tolerance to colonizing bacteria and to mount a pro-inflammatory response against pathogens (Torow et al. 2017; Lambert and Culley 2017; Loering et al. 2019). This is a critical task that can be complicated by preceding intra-amniotic infection *in utero*. Fetal lung inflammation activates immune cells within the tissue, which can lead to accelerated lung maturation (Kramer, Kallapur, Newnham, et al. 2009). A failure of immunoregulatory mechanisms can lead to excessive inflammation upon lung infection or other insults (Lambert and Culley 2017). Recruitment of innate leukocytes is likely to play an important role in the innate response to infection in the neonatal lung following microbial recognition, since the adaptive immune response is still naïve. In support of that concept, TLR4 expression is already present in the fetal murine lung and increases after birth (Jia et al. 2018; Lambert and Culley 2017). The general bias towards a type 2 immune response in neonates is associated with increased vulnerability of the lung and exaggerated inflammation along with impaired IFN-γ production during infection with respiratory syncytial virus (RSV) (Torow et al. 2017).

Understanding the mechanisms leading to a disruption in the balance of immune responses in the neonatal lung is a very important step towards preventive and therapeutic strategies for BPD in preterm infants.

## 1.3 Development of bronchopulmonary dysplasia

BPD is a surrogate marker of the persistent pulmonary insufficiency after birth in vulnerable infants such as preterm babies or infants with severe pulmonary distress (see

1.1; Niedermaier and Hilgendorff 2015). The current concepts of how BPD develops is depicted in Figure 1-7. The main postnatal exogenous risk factors that trigger BPD development include $O_2$ toxicity due to the need for supplemental $O_2$ and hypoxic episodes that are features of RDS and can lead to mechanical ventilation as well as infection (Niedermaier and Hilgendorff 2015; Martin, Di Fiore, and Walsh 2015). These risk factors act on a structural and functional immature lung that is in the saccular stage when preterm birth occurs (Rivera et al. 2016). Preterm infants are usually exposed to several of these challenges in the first weeks of life, which in combination aggravate the pro-inflammatory immune response that may impact on lung development (Figure 1-7). The pro-inflammatory response includes factors such as infiltrating immune cells, increased inflammatory cytokine release (e.g. IL-1β), active pro-inflammatory gene transcription factors (e.g. NF-κB), and dysregulated growth factors (e.g. Fibroblast growth factor (FGF)-10) (Speer 2006; Popova 2013; Hilgendorff et al. 2014; Niedermaier and Hilgendorff 2015; Balany and Bhandari 2015; Jobe 2015; Pryhuber 2015).

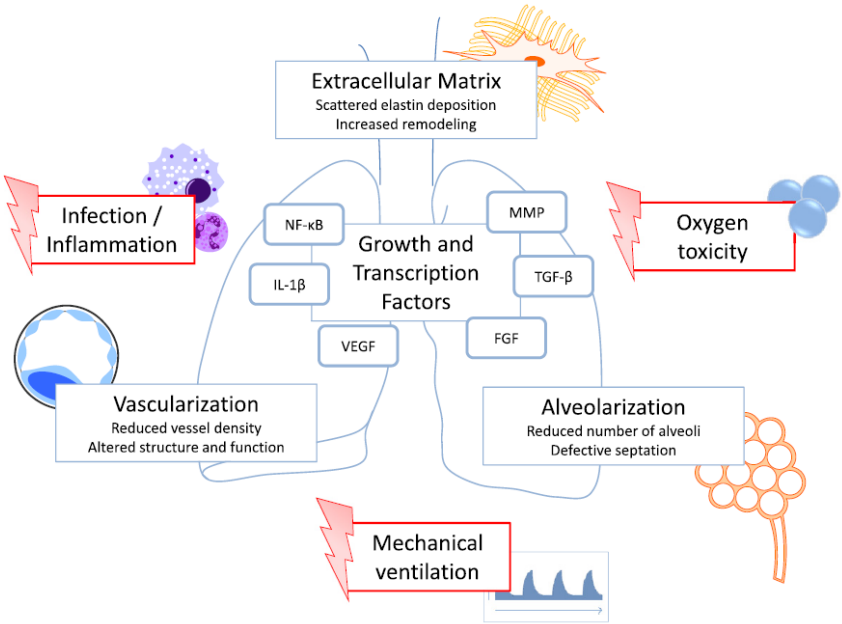


**Figure 1-7: Overview of BPD development**. The risk factors for BPD (V) resulting in a pro-inflammatory response in the lung with immune cell influx and changes in patterns of cytokines, transcription factors and growth factors. These prolonged changes lead to reduced vascularization, alveolarization and increased matrix remodeling © 2015 Niedermaier and Hilgendorff; licensee Springer (Reprinted from Niedermaier and Hilgendorff 2015).

Over time, the preterm infant with BPD has a sustained low-level inflammatory response and impaired lung development characterized by abnormal alveolar and vascular growth and increased matrix remodeling (Niedermaier and Hilgendorff 2015). This leads to

decreased numbers of alveoli and an enlargement of airspaces, which causes reduction in the total lung internal surface (Nold et al. 2013).

### 1.3.1 Pulmonary inflammation in the developing lung

Clinical data and animal studies highlight a central role of pulmonary inflammation in BPD development (Speer 2006; Ryan, Ahmed, and Lakshminrusimha 2008; Popova 2013; Pryhuber 2015; Lal and Ambalavanan 2015a; Niedermaier and Hilgendorff 2015). Since there is only limited access to lung tissue of preterm infants, several studies using human samples focus mainly on blood and tracheal aspirate to characterize inflammatory markers (Jobe 2011; A. Bhandari and Bhandari 2013; Lal and Ambalavanan 2015a). Therefore, most studies of lung tissues are performed in neonatal animal models. Clinical studies have suggested that chronic exposure to high $O_2$ saturations can injure the lungs of preterm infants (Trembath and Laughon 2012; Klinger et al. 2013). This can be modeled in animals by altering the amount of inspired $O_2$. Lung injury, followed by a chronic repair phase, is well established using 60-100% $O_2$ exposure of neonatal mice and other animals such as rats, sheep or baboons (Bonikos et al. 1975; Randell, Mercer, and Young 1990; Warner et al. 1998; Nold et al. 2013; Jobe 2015). Those animals when exposed to high $O_2$ concentrations have also shown disrupted lung structure with reduced alveolarization and vascularization and enlarged airspace. Additionally, a dysregulated growth factor expression and lung cell proliferation have been reported (Warner et al. 1998; V. Bhandari 2010). Increased $O_2$ has also been shown to be a powerful pro-inflammatory stimulus, as described in more detail below. Other important risk factors contributing to the pathogenesis of BPD in humans are pre- and postnatal infections (Trembath and Laughon 2012; Klinger et al. 2013). Not only increase $O_2$ exposure, but also administration of antenatal or postnatal LPS to neonatal animals induces lung inflammation and a BPD-like phenotype (Kramer et al. 2009; Hou et al. 2015).

Pulmonary inflammation, which can subsequently lead to a BPD-like lung phenotype, is characterized by enhanced cytokine and chemokine release (Ryan, Ahmed, and Lakshminrusimha 2008). In addition, infiltrating immune cells, such as neutrophils, MΦ, and potentially also lymphocytes, are thought to play central roles (Ryan, Ahmed, and Lakshminrusimha 2008). An imbalance of pro- and anti-inflammatory cytokines is suggested to be important in BPD development (Speer 2006). Increased levels of IL-1β, TNF-α, IL-6 and IL-8 have been present in blood, bronchoalveolar lavage, and tracheal aspirates of infants who subsequently developed BPD (Kotecha et al. 1996; Jonsson et al. 1997; Patterson et al. 1998; Ambalavanan et al. 2009). The lungs of neonatal animals exposed to increased $O_2$ have shown a similar cytokine release with enhanced IL-1β,

TNF-α, IL-6 and IL-8 levels that has occurred before the onset of impaired lung development (Johnston et al. 1997; Coalson et al. 1999; Deng, Mason, and Auten 2000; Choo-Wing et al. 2007; Johnson et al. 2009; Nold et al. 2013). Chemokines other than IL-8 have also been upregulated. For example, monocyte chemoattractant protein (MCP)-1, -2, and -3 have been increased in tracheal aspirates of infants developing BPD (Baier et al. 2004). In neonatal animals exposed to increased $O_2$, MCP-1 and other chemokines such as MCP-5 and CXCL13 have been upregulated (Vozzelli et al. 2004; Weichelt et al. 2013; Nold et al. 2013). Those soluble factors create a strong pro-inflammatory milieu capable of activating tissue resident cells and recruiting other immune cells from the circulation to the lung (Ryan, Ahmed, and Lakshminrusimha 2008). The role of IL-10, which is capable of suppressing immune cell activation, is less clear in the context of BPD development. In one study, serum and tracheal aspirate IL-10 levels have been decreased in infants that develop BPD (V. Bhandari 2010). However, another study has demonstrated increased IL-10 levels in blood of infants developing BPD (Ambalavanan et al. 2009). Neonatal mice exposed to increased $O_2$ have not demonstrated any changes in lung IL-10 levels (Johnston et al. 1997; Nold et al. 2013), and no significant differences have been observed in IL-10 levels of tracheal aspirates in a baboon model of BPD (Coalson et al. 1999).

The early cellular immune response is characterized by the influx of neutrophils and MΦ that are attracted by inflammatory mediators such as those discussed above. Neutrophils and MΦ have been increased in bronchoalveolar lavage fluid of infants who later developed BPD (Kotecha et al. 1995; C. A. Jones et al. 1996). Another study, however, has demonstrated fewer mature airway MΦ characterized by less CD36+ surface protein expression in the immediate postnatal period of infants later developing BPD (Prince et al. 2014). Neonatal animals exposed to increased $O_2$ have shown infiltrating neutrophils shortly after exposure (Auten et al. 2001; Weichelt et al. 2013) alongside with influx and activation of MΦ (Jankov et al. 2001; Johnson et al. 2009; Weichelt et al. 2013; Nold et al. 2013) leading to lung developmental arrest. More recently, mast cell accumulation has been reported in lung connective tissue of patients who died from BPD (Bhattacharya et al. 2012). The infiltration of neutrophils and MΦ has led to increased NF-κB activation (A. Bhandari and Bhandari 2013) and production of reactive oxygen species (ROS) in tracheal aspirates of infants developing BPD (Contreras et al. 1996). NF-κB has caused arrest of airway branching in a mouse model using embryonic lung explants (Blackwell et al. 2011). Jankov *et al*. have also shown that increased ROS production has caused lung injury in a neonatal animal model exposed to increased $O_2$ (Jankov et al. 2001).

In the context of BPD, less data are available about lymphocytes, another important component of the cellular immune response. Jackson *et al.* have analyzed blood from preterm infants over the first weeks of life and examined mRNA expression of RORC, TBET, GATA3, and FOXP3, which are characteristic for Th17, Th1, Th2 and Treg polarization of T cells, respectively. The TBET/FOXP3 ratio has been shown to increase in the first week of life in infants who subsequently developed BPD (Jackson et al. 2017). An upregulation of IL-4 has been reported in stimulated blood of preterm infants developing BPD (Jackson et al. 2017). However, T cell characteristics of peripheral blood might not reflect the situation in the lung. Other studies have found decreased T cell frequencies along with decreased Tregs in cord blood of preterm infants developing BPD (Turunen et al. 2009; Misra et al. 2015). This might suggest a recruitment of lymphocytes to the lung in BPD patients. T cells in the circulation have not only been decreased but have also been more activated (Turunen et al. 2009). In a baboon model using increased $O_2$ to induce BPD, $CD4^+$ T cells have been abundant in the lung, suggesting that autoreactive T cells might be important in BPD (Rosen et al. 2006). In a different model, investigators have studied lung injury and subsequent lymphocyte response induced through necrotizing enterocolitis in the gut of neonatal mice, which leads to systemic inflammation (Jia et al. 2018). In that model, TLR4-dependent activation of lung epithelial cells has led to an increase in pro-inflammatory Th17 cells and a reduction of Tregs, which have been required for the development of lung injury (Jia et al. 2018).

In order to understand the interaction between pulmonary inflammation and impaired pulmonary development, it is important to consider multiple factors that play roles in both immunity and lung development, e.g. the transcription factors Nuclear factor-like (Nrf)2, Hypoxia-inducible factor (HIF)-1α and NF-κB (Reddy et al. 2009; Nizet and Johnson 2009; Alvira 2014; Elberson et al. 2015; Cho et al. 2016). Activated Nrf2 leads to transcription of genes important for the antioxidant response to increased $O_2$ (Reddy et al. 2009) and furthermore is a key modulator of the signalling in the saccular to alveolar transition (Cho et al. 2016). NF-κB has a dual role in the developing lung as well. It is constantly active during the alveolar stage of lung development (Alvira 2014), but its activation through LPS during the late canalicular and early saccular stage disrupts lung development (Blackwell et al. 2011). In addition, NF-κB is a major transcription factor involved in the induction of pro-inflammatory responses in adults (Alvira 2014). However, its activation in the neonatal lung appears to have an opposite, anti-inflammatory effect, protecting against LPS-mediated lung inflammation by repressing the expression of inflammatory genes on an epigenetic level (Alvira et al. 2007; Hou et al. 2015). Increased NF-κB activation in infants developing BPD mentioned above suggests that its activation can also trigger pro-

inflammatory responses in neonates (A. Bhandari and Bhandari 2013), probably depending on the intensity of insult and stage of lung development. HIF-1α is also involved in lung development and immunity. HIF-1α supports alveolarization and vascularization and has been downregulated in a mouse model of intermittent treatment with increased and reduced $O_2$ concentration (Elberson et al. 2015). In addition, HIF-1α is upregulated under inflammatory conditions (Nizet and Johnson 2009). Growth factors also play a vital role in lung development and are partly regulated by inflammation. FGF-10 is required for saccular development and has been reduced in lung tissue of BPD infants (Benjamin et al. 2007). In mice, activation of TLR2 and TLR4 has inhibited FGF-10 expression, leading to abnormal saccular airways (Benjamin et al. 2007).

These data show that pulmonary inflammation and lung development are tightly intertwined, and a dysregulation of factors involved in such an important organ can have detrimental consequences. Epidemiological data suggest that BPD is a multifactorial disease, and its development and severity depend on the type and frequency of the insult.

### 1.3.2 Pulmonary immune response after repeated challenge

The nature of pulmonary immune responses develops with the different types of insult as well as their frequency and intensity, influencing the severity of BPD in preterm infants (Jobe 2011, 2012; Buczynski, Maduekwe, and O'Reilly 2013; Nold et al. 2013). Repeated intranasal priming of newborn mice with microbial extracts has increased opsonic factors and the amount of mature $CD11c^+$ DCs cells in the airway. These factors may contribute to airway resistance after infection and to the regulation of acute inflammatory responses in the lung (Kasahara et al. 2012). This study supports the potential for low-level but frequent insults to modulate lung immunity. Most of the commonly used animal models for BPD have induced lung injury by altering the amount of inspired $O_2$ or by inducing pre- or postnatal inflammation. Few studies have used a combination of exposures. Two studies using intra-amniotic LPS injection of dams followed by pup exposure to increased $O_2$ have demonstrated an exaggerated immune response in the lungs, with a more severe BPD phenotype after the double-hit (Velten et al. 2010; Nold et al. 2013). That response has been characterized by increased MΦ influx and associated with a diffuse fibrotic response and increased airway resistance, which has only persisted in animals exposed to both LPS and increased $O_2$. (Velten et al. 2010). Exaggerated cytokine and chemokine release (e.g. IL-1β, MCP-5, CXCL13) and increased MΦ activation have also been reported (Nold et al. 2013). Furthermore, even a mild antenatal inflammatory exposure has been shown to bias the programming of T cells toward pro-inflammatory phenotypes (Gleditsch et al. 2014). This, in combination with augmented innate immune responses, could enable

persistent inflammation in the lungs or other organs that lead to chronic morbidity (Gleditsch et al. 2014). Another experimental approach, that has been used to model lung injury induced by multiple challenges, has involved exposure of newborn mice to increased $O_2$ and either simultaneous intranasal LPS priming or subsequent RSV infection (Syed and Bhandari 2013; Cui et al. 2016). The double-hit with LPS has led to an amplified immune response characterized by increased IL-6 and IL-1β, enhanced cell influx to the lung, and a more simplified lung structure compared to LPS stimulation alone (Syed and Bhandari 2013). High $O_2$ and subsequent RSV has led to an exaggerated immune response compared to RSV alone characterized by more IL-12-procuding $CD103^+$ DCs in the lung. $CD103^+$ DCs have mediated an increased and sustained inflammation with activated IFNγ-producing T cells and airway hyper-responsiveness (Cui et al. 2016). Therefore, a more aggressive inflammatory response stimulated by multiple challenges may lead to a more severe BPD phenotype. However, other data have indicated that repetitive LPS exposure can lead to immune tolerance and a dampened inflammatory response in monocytes from sheep, which in turn has shown a low impact on lung development in experimental BPD animals (Kramer et al. 2009).

In addition to effects of multiple types of exposures, the intensity of an exposure can result in a different outcome. For example, preterm ventilated baboons have been exposed to either only enough $O_2$ to maintain normal arterial concentrations for 21 days, or 100% $O_2$ for 7 days followed by 80% $O_2$ for 14 more days (Buczynski, Maduekwe, and O'Reilly 2013). Eight month later, the lungs of animals in the low $O_2$ exposure group have had minimal inflammation and normal alveolarization, whereas animals in the high $O_2$ exposure group have shown signs of ongoing inflammation and have had larger alveoli and reduced alveolar numbers (Buczynski, Maduekwe, and O'Reilly 2013). In a different model, neonatal mice have been exposed to 65% or 85% $O_2$ for 28 days (Nold et al. 2013). Lung pathology of animals exposed to 85% $O_2$ has been characterized by a 60% reduction in alveolar number, and 4-fold increase in alveolar size. The damage induced by 65% $O_2$ has been milder, i.e. reduction in alveolar number by 44%, and the alveolar size increased 2.3-fold (Nold et al. 2013). After treatment of neonatal mice with interleukin-1 receptor antagonist (IL-1RA), the lung pathology has been reversed in animals exposed to 65% $O_2$, but not in those exposed to 85% $O_2$ (Nold et al. 2013).

In conclusion, the type of insult, its frequency and intensity are all capable of modulating the pulmonary immune response and subsequent lung pathology. The studies discussed above also suggest that increased frequency and higher intensity of insults are associated with hyperinflammation and with increasing severity and persistence of lung pathology.

### 1.3.3 Treatment strategies for bronchopulmonary dysplasia

Currently, there is no cure or standardized treatment for BPD. Because sustained inflammation is one of the major characteristics of BPD, mammalian models of BPD and primary cell models focus on several candidates that may decrease inflammation in the preterm lung.

In the past, dexamethasone, a glucocorticoid, has been used in BPD patients. However, due to severe side effects such as neurodevelopmental impairments, it is currently only used in very severe BPD cases (Principi, Di Pietro, and Esposito 2018). Its full mechanism of action is unknown, although it has been shown to exert anti-inflammatory effects by suppressing NF-κB and polarizing MΦ to an anti-inflammatory phenotype that has supported Treg responses (Aghai et al. 2007; Tu et al. 2017). Caffeine and vitamin A are also given to preterm infants and are associated with a slightly reduced risk for BPD development (Principi, Di Pietro, and Esposito 2018). They are also thought to play a role in reducing the pathogenic mechanisms of BPD due to their anti-inflammatory properties (Weichelt et al. 2013; Principi, Di Pietro, and Esposito 2018). Nitric oxide (NO), inhibiting NF-kB activation, has also been a promising candidate for BPD treatment (Wright et al. 2010). However, the use of NO has not turned out to reduce the risk for BPD development (Principi, Di Pietro, and Esposito 2018).

A new promising candidate for BPD treatment is IL-1RA, which has resulted in recovery of the lung morphology and partial reversal of immune cell numbers and MΦ hyperactivation in a double-hit BPD mouse model (Nold et al. 2013). Additionally, pulmonary cyclooxygenase (COX)-2 inhibitors such as aspirin and celecoxib have reduced MΦ numbers in the alveolar walls and airspaces and decreased COX activity in a mouse model of BPD. However, COX-2 inhibition has not prevented hyperoxia-induced lung developmental deficits (Britt et al. 2013). IL-10 treatment of LPS-treated monocyte-derived macrophages (MDMs) from cord blood of term infants has reduced pro-inflammatory cytokines without an impact on MΦ function (Kasat et al. 2014). In adult mice, exogenous IL-10 has attenuated lung injury induced by increased $O_2$ exposure (H. D. Li et al. 2015). Furthermore, neutralization of chemokines to reduce immune cell infiltration into the lung has also reduced pulmonary inflammation in rats (Auten et al. 2001; Vozzelli et al. 2004; Drummond et al. 2015). CXC receptor 4 and cytokine-induced neutrophil chemoattractant-1, an analogue of human IL-8, have even restored alveolarization (Auten et al. 2001; Drummond et al. 2015). In addition to direct anti-inflammatory treatment, targeting lung cell metabolism could be another therapeutic option, since decreased alveolarization has correlated with decreased oxidative phosphorylation (OXPHOS) in the mitochondria in a BPD mouse model (Ratner et al. 2009).

All of these treatment strategies seem to reduce the inflammatory response in the lung, and some reduce the pathophysiology of the BPD lung, which indicates therapeutic potential. However, most of these studies are based on animal models, and very few studies have targeted MΦ.

## 1.4 Importance of macrophages in the lung, its development, and in BPD

MΦ are the most abundant immune cells in the lung, including infant lung tissue (Dos Santos et al. 2013). They are the main effector cells of immune responses in the lung and have a high plasticity, changing their phenotype depending on signals from the environment (Biswas and Mantovani 2010). They also play a major role in maintaining tissue homeostasis (Zhang et al. 2018).

In infants, the role of lung MΦ is even more complex, since they are also thought to support remodeling and repair during lung development even after birth, when they rapidly increase in number and mature in the lung (for more detail see 1.2.2; Guilliams et al. 2013; Loering et al. 2019). As a result, MΦ in the developing lung maintain the balance between an appropriate inflammatory response to harmful insults and continued tissue remodeling and maintenance of homeostasis during development. In order to maintain the balance, the characteristic high plasticity of MΦ is essential. Upon activation, MΦ can develop a variety of phenotypes rather than discrete stable subpopulations, adapting to multifactorial stimuli of the surrounding microenvironment (Galli, Borregaard, and Wynn 2011). This process can also be reproduced *in vitro*. In a physiological setting, tissue MΦ are mainly anti-inflammatory, existing in a stage of reduced responsiveness mediated by several surrounding factors, such as TGF-β, IL-10 and CD200R interaction with alveolar epithelial cells (Kaur et al. 2015). Anti-inflammatory MΦ are also prone to cell metabolism characterized by fatty acid oxidation and OXPHOS (Mills and O'Neill 2016). In the setting of an inflammatory stimulus, the phenotype of MΦ switches to a pro-inflammatory one, altering metabolism to produce energy through glycolysis and flux through the pentose phosphate pathway (Mills and O'Neill 2016). Stouch *et al.* has also suggested that the development of fetal lung MΦ into mature MΦ includes features of both pro-inflammatory and alternative activation patterns that may be important for their plasticity (Stouch et al. 2014). In the event of a strong inflammatory insult, such as infection and exposure to increased $O_2$ as outlined in section 1.3.1, lung MΦ switch to a pro-inflammatory phenotype, which directly mediates an arrest of lung development characterized by reduced airway branching (Blackwell et al. 2011). Additionally, monocytes are recruited to the developing lung, differentiate into MΦ and are activated under these pathological conditions (Vozzelli et al. 2004; Velten et al. 2010; Nold et al. 2013). Several studies have

shown that blocking neutrophil and MΦ recruitment has improved lung structure after exposure to increased $O_2$ (Vozzelli et al. 2004; Drummond et al. 2015). These studies suggest that persistent pro-inflammatory responses associated with MΦ recruitment lead to arrest of lung development. In addition, increased $O_2$ exposure has been shown to direct MΦ polarization towards pro-inflammation, because *in vitro* increased $O_2$ has enhanced LPS-induced pro-inflammatory phenotypes and inhibited IL-4-induced anti-inflammatory phenotypes (Syed and Bhandari 2013). However, other studies have determined that only resident, but not recruited lung MΦ have contributed to dysregulated lung development, and that ROS-mediated injury may be enhanced by recruited MΦ (Jankov et al. 2001; C. V. Jones et al. 2014; Kalymbetova et al. 2018).

It is notable that most studies have been performed in the acute phase of lung injury due to cost and labor intensity of long-term studies. As a consequence, those studies may have been unable to adequately address important mechanisms underlying chronic inflammation, subsequent developmental arrest, and long-term alterations in lung immune response. One of the most important candidates linked to structural changes in the developing lung is TGF-β. Increased amounts of TGF-β produced by persistent MΦ have been detected in tracheal aspirates and bronchoalveolar lavage fluids of infants developing BPD (Kotecha et al. 1996; Ryan, Ahmed, and Lakshminrusimha 2008). Sime *et al.* have demonstrated that local overexpression of active TGF-β has resulted in significant fibrosis, with extensive deposition of extracellular matrix proteins such as collagen, fibronectin, and elastin in the lungs of rats (Sime et al. 1997). Another MΦ-mediated feature during chronic phase of BPD, that is not well characterized, is the lymphocyte response. In neonatal rabbits, there has been a lymphocytic infiltrate after three and five weeks of chronic hyperoxia (Ryan, Ahmed, and Lakshminrusimha 2008). However, the nature of lymphocyte responses in the lung in this context is unknown. Another mouse study has reported downregulation of adaptive immune responses three months after neonatal $O_2$ exposure (Kumar, Wang, and Nielsen 2018). After induction of acute lung injury in adult mice, the pro-inflammatory MΦ response has induced a Th17 polarization (Tu et al. 2017). In that report, steroid treatment has led to an anti-inflammatory MΦ phenotype with increasing Treg responses, which partially reversed lung injury (Tu et al. 2017).

In summary, MΦ are likely to play a key role in the neonatal lung, with important contributions to appropriate immune response and lung development. In animal models, a dysregulated MΦ response due to strong pro-inflammatory insults contributes to BPD. However, the role of MΦ-mediated lymphocyte responses in that context is not well characterized.

### 1.4.1 *Ex-vivo* model for lung immunity using human monocyte-derived macrophages from preterm infants

MΦ are the most abundant immune cell population in the lung and can not only influence lung development but also immune responses due to their plastic phenotype (Dos Santos et al. 2013; Blackwell et al. 2011). Additionally, they are increased in number through recruitment to the lung following exposure to increased $O_2$ and infection, thereby contributing further to lung injury (Jankov et al. 2001; Velten et al. 2010). Therefore, MΦ are likely to have a key role in the immature lung immunity of preterm infants.

So far, there have been very few studies investigating human neonatal MΦ and their immunological response and function. Existing studies have described human MDMs from term infants. They have exhibited decreased responsiveness to IFNγ (Maródi et al. 2001) and similar immune responses after TLR2 and TLR4 stimulation regarding cytokine release, changes in costimulatory activation marker expression, and antigen presentation compared to adult MDMs (Wisgrill et al. 2018). Phagosome activity has either been similar or enhanced in term MDMs compared to adults depending on the study design (Lawrence and Koenig 2012; Wisgrill et al. 2018).

There are a limited number of studies that describe a gestational age-dependent difference in immune function of infant monocytes (Figure 1-8; de Jong et al. 2017). Human cord blood mononuclear cells of term infants have been shown to produce less IFNγ, TNFα and IL-12p70 but equal or greater amounts of IL-1β, IL-6 IL-23, IL-12p40 and IL-10 as compared to adult cells (Kollmann et al. 2009). Those patterns of cytokine expression suggest a robust if not enhanced capacity of the neonatal mononuclear cell TLR-mediated response in a manner that supports Th17- and Th2-type immunity, but a reduced capacity to support Th1-type responses at term (Kollmann et al. 2009). Preterm monocytes have shown functional differences, especially in pattern recognition receptor expression (e.g. TLR4 and CD14), cytokine production (e.g. IL-6 and TNFα), phagosome acidification, and antigen presentation (e.g. HLA-DR), which have tended to increase in a gestational age-dependent manner (Prosser et al. 2013; Wisgrill et al. 2016; de Jong et al. 2017). Two recent studies have investigated monocytes of preterm infants in the context of intra-amniotic infection and necrotizing enterocolitis (de Jong et al. 2018; Pang et al. 2018). Jong *et al.* have reported an association between intra-amniotic infection and a hypo-responsive transcriptional phenotype of monocytes after *Staphylococcus epidermidis* exposure, with regard to a subset of genes involved in antigen presentation and adaptive immunity (de Jong et al. 2018). This suggests that exposure to early inflammation reduces the responsiveness of monocytes towards pro-inflammatory stimuli. Pang *et al.* have demonstrated an activated monocyte phenotype that exacerbates

Treg/Th17 imbalance in preterm infants with necrotizing enterocolitis (NEC) compared to age- and weight-matched controls (Pang et al. 2018). Here, systemic inflammation due to NEC has led to activated monocytes which has induced a pro-inflammatory Th17 response.

Monocytes show a gestational age-dependent difference in immune function that increases with gestational age towards term infant levels and can be influenced by exposure to infection. However, there is a paucity of data regarding neonatal MΦ function, especially in the context of prematurity, probably due to challenges with sample collection and limited amounts of available biomaterial from infants. However, preterm infants are the main risk group to develop BPD, which seems to be influenced by MΦ. It is therefore important to characterize age-dependent differences in human MΦ and determine their role in BPD.

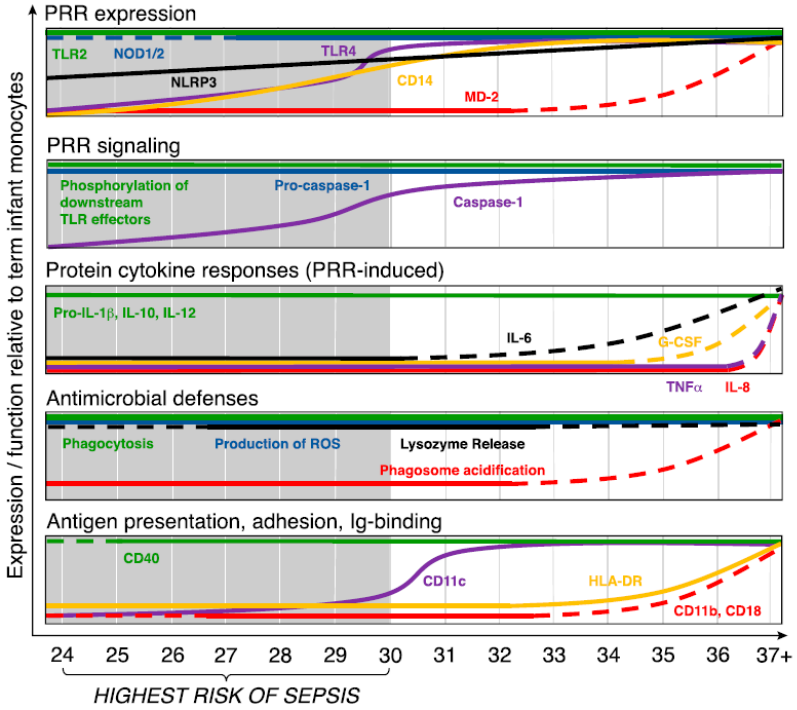


**Figure 1-8: Gestational age-dependent differences in immune functions of preterm monocytes relative to term infant monocytes.** PRR: pattern recognition receptor © 2017 Society for Leukocyte Biology, licensee John Wiley & Sons, Inc. (Reprinted from de Jong et al. 2017).

## 2. Objectives

BPD is a leading cause of long-term morbidity in preterm infants. Existing options for treatment are limited, and they are not sufficiently effective. An improved understanding of the mechanisms leading to BPD development is needed to facilitate the development of new preventive and therapeutic strategies. One central pathology of BPD is sustained pulmonary inflammation due to several pro-inflammatory insults (e.g. supplemental $O_2$ and infection) in the first weeks of life, which lead to an arrest of lung development. MΦ are likely to play a key role in mediating disease development. But there is a paucity of data regarding immune responses of human preterm infant MΦ.

The central hypothesis of this study is that human MΦ show a gestational age-dependent difference in their immune response, which can lead to detrimental lung inflammation in preterm infants. As compared to term infant and adult MΦ, an enhanced pro-inflammatory signature of preterm MΦ has been speculated at different levels: signaling pathways, cytokine release and surface marker expression. Two specific aims have been pursued:

1) To characterize immune responses in cord blood-derived MΦ from term and preterm infants born at different weeks of gestation as compared to adults

2) To determine the role of MΦ for lung immunity of preterm infants using an *ex-vivo* double-hit ($O_2$, LPS) model

# 3. Material and methods

## 3.1 Material

### 3.1.1 Devices

**Table 3-1: Devices**

| Device | Version | Supplier |
|---|---|---|
| Air-tight sealed chamber | Hypoxia Incubator Chamber | Stemcell Technologies, Vancouver, Canada |
| Centrifuge | 2-16PK | Sigma Laborzentrifugen GmbH, Osterode, Germany |
| | 4-15C | Sigma Laborzentrifugen GmbH, Osterode, Germany |
| | 5417R | Eppendorf, Hamburg, Germany |
| | Biofuge fresco | Heraeus Instruments GmbH, Hanau, Germany |
| | Biofuge pico | Heraeus Instruments GmbH, Hanau, Germany |
| | Megafuge 2.0 R | Heraeus Instruments GmbH, Hanau, Germany |
| | Multifuge 3 S-R | Heraeus Instruments GmbH, Hanau, Germany |
| | Sprout | Heathrow Scientific,Vernon Hills, IL, USA |
| Clean bench | EN 12469 | Clean Air Techniek B.V. Woerden, Netherlands |
| | Z195™ | Schulz Lufttechnik GmbH, Sprockhövel, Germany |
| | PCR Workstation Pro | Peqlab, Darmstadt, Germany |
| Flow cytometer | BD FACSCanto™ II | BD Biosciences, San Jose, USA |
| Flow meter | Single | Stemcell Technologies, Vancouver, Canada |
| Fluorescence microscope | BZ-9000 | Keyence, Osaka, Japan |
| Fluorometer | Qubit 2.0 | Invitrogen, Carlsbad, California, USA |
| Freezer | MDF-U7386S; Ultra-low -80°C | Sanyo, Leicestershire, UK |
| | RevcoUxF, Ultra-low -80°C | Thermo Fischer Scientific, Waltham, MA, USA |
| | Comfort -20°C | Liebherr, Biberach an der Riß, Germany |
| | GS368T; Luxus -20°C | Bosch, Munich, Germany |

| | | |
|---|---|---|
| Fridge | Profi line | Liebherr, Biberach an der Riß, Germany |
| Heating block | PCH-2 | Grands-Instruments Ltd, Shepreth, UK |
| Hood | 2-410H | Köttermann, Uetze-Hänigsen, Germany |
| Incubator (37°C, 5% $CO_2$) | CB series | Binder GmbH, Tuftlingen, Germany |
| | Forma Series II 3131 | Thermo Fisher Scientific, Waltham, USA |
| Incubator (37°C, 5% $CO_2$, N2-regulation, $O_2$-sensor) | Forma Series II 3141 | Thermo Fisher Scientific, Waltham, USA |
| Incubator (37°C) | B6060 | Heraeus Instruments GmbH, Hanau, Germany |
| | INCU-line | VWR, Radnor, PA, USA |
| Lightcycler | 480 Instrument II | Roche Diagnostics GmbH, Mannheim, Germany |
| Magnet | BigEasy EasySep™ | Stemcell Technologies, Vancouver, Canada |
| | EasyEights EasySep™ | Stemcell Technologies, Vancouver, Canada |
| Magnetic stirrer | RET basic | IKA®-Labortechnik, Staufen, Germany |
| Microscope | Axiovert 25 | Carl Zeiss Microscopy GmbH, Jena, Germany |
| Multichannel pipette | Transferpette-8 (20-200µl) | Brand GmbH, Weimheim, Germany |
| pH meter | MP220 | Mettler Toledo, Gießen, Germany |
| Pipette | Reasearch plus (10, 100, 1000 µl) | Eppendorf AG, Hamburg, Germany |
| Pipette controller | accu-jet pro | Brand GmbH, Weimheim, Germany |
| Scale | KB 600-2 | Kern & Sohn GmbH, Ballingen-Frommen, Germany |
| Sequencer | Hiseq4000 | Illumina®, San Diego, California, USA |
| Thermocycler | C1000 | Bio-Rad, Munich, Germany |
| Thermomixer | Comfort | Eppendorf AG, Hamburg, Germany |
| Vortex device | REAX 2000 | Heidolph Instruments GmbH, Schwalbach, Germany |
| Waterbath | WNB | MemmertGmbH & Co. KG, Schwabach, Germany |

### 3.1.2 Consumable supplies

**Table 3-2: Consumable supplies**

| Consumables | Supplier |
|---|---|
| Cell scraper (28 cm lenght) | Greiner Bio-One GmbH, Frickenhausen, Germany |
| Chamber slides, 8-wells | Corning Incorporated, Corning, New York, USA |
| Coverslides, 24x60mm | Thermo Fisher Scientific, Waltham, MA, USA |
| Disposable bag | Labsolute Th. Geyer GmbH, Renningen, Germany |
| Facial tissues | Abena A/S, Aabenraa, Denmark |
| FACS tube | Sarstedt AG&Co, Nürnbrecht, Germany |
| FACS tubes with snap cap, sterile (5ml) | Corning Incorporated, Corning, New York, USA |
| Falcon tubes (12, 15, 50 ml) | Sarstedt AG &Co, Nürnbrecht |
| Gloves, Vinyl 2000PF (M) | Meditrade GmbH, Kiefersfelden, Germany |
| Lightcycler 480 multiwell plate 96, white | Roche Diagnostics GmbH, Mannheim, Germany |
| Neubauer counting chamber | Haasa, Laborbedarf, Lübeck, Germany |
| Parafilm | Bemis, Neenah, WI, USA |
| PCR reaction tube strips (8, 0.2 ml) | Sarstedt AG&Co, Nürnbrecht, Germany |
| Pipette tips | Sarstedt AG &Co, Nürnbrecht, Germany |
| Polystyrene round-bottom Tubes (14ml) | Corning Incorporated, Corning, New York, USA |
| Qubit assay tubes | Thermo Fisher Scientific, Waltham, MA, USA |
| Reaction tubes (0.5, 1.5, 2 ml) | Sarstedt AG &Co, Nürnbrecht, Germany |
| Serologic pipette (5, 10, 25 mL) | Greiner Bio-One GmbH, Frickenhausen, Germany |
| S-Monovette, 9ml, K3E | Sarstedt AG &Co, Nürnbrecht, Germany |
| Tissue culture dish (60x15 mm) | BD Bioscience, San Jose, USA |
| Tissue culture flasks (25, 75, 175 $cm^2$) | Greiner Bio-One GmbH, Frickenhausen, Germany |
| Tissue culture plate (96-well, U-bottom) | Greiner Bio-One, Frickenhausen, Germany |
| Tissue culture plates (6-well, 24-well, 96-well, F-bottom) | Greiner Bio-One, Frickenhausen, Germany |

### 3.1.3 Reagents

Used chemicals, kits, stimulants and enzymes are listed in the tables below.

**Table 3-3: Chemicals**

| Chemicals | Supplier |
|---|---|
| 4-(2-hydroxyethyl)-1-piperazineethanesulfonic acid (HEPES) buffer solution (1M) | PAN-Biotech, Aidenbach, Germany |
| 4′,6-Diamidin-2-phenylindol (DAPI) | Life Technologies, Thermo Fisher Scientific, Waltham, MA, USA |
| Accutase | Gibco®, Thermo Fisher Scientific, Waltham, MA, USA |
| Bovine serum albumin (BSA) | Sigma-Aldrich Corporation, St. Louis, USA |
| Cell-Tak - Cell and tissue adhesive | Corning Incorporated, Corning, New York, USA |
| $ddH_2O$ | Roth GmbH & Co. KG, Karlsruhe, Germany |
| dNTP (PCR nucleotide mix) | Roche Diagnostics GmbH, Mannheim, Germany |
| Ethylenediaminetetraacetic acid (EDTA, Tritriplex III) | Merck KgaA, Darmstadt, Germany |
| EDTA solution (0.5M) | Sigma-Aldrich Corporation, St. Louis, USA |
| Ethanol, absolute | Merck KGaA, Darmstadt, Germany |
| Flow Cytometry Staining Buffer | eBioscience, Thermo Fisher Scientific, Waltham, MA, USA |
| FACSFlow Solution | BD Biosciences, San Jose, USA |
| FACSShutdown Solution | BD Biosciences, San Jose, USA |
| FACSClean Solution | BD Biosciences, San Jose, USA |
| Fetal bovine serum (FBS) | PAN-Biotech, Aidenbach, Germany |
| Gas mixture (65% $O_2$, 5% $CO_2$, rest $N_2$) | Airliquide Medical GmbH, Düsseldorf, Germany |
| Glycine | AppliChem GmbH, Darmstadt, Germany |
| Isopropanol | Carl Roth GmbH, Karlsruhe, Germany |
| L-glutamine | Lonza, Veriers, Belgium |
| Mounting solution | Oxoid, Hampshire, United Kingdom |
| Paraformaldehyde (PFA) | Sigma-Aldrich Corporation, St. Louis, USA |
| Penicillin (10000U)/Streptomycin (10mg/ml) (P/S) | Sigma-Aldrich Corporation, St. Louis, USA |

| | |
|---|---|
| pH 6.865 calibration buffer | WTW Inc. College Station, Texas, USA |
| pH 9.180 calibration buffer | WTW Inc. College Station, Texas, USA |
| Potassium chloride (KCl) | Merck KGaA, Darmstadt, Germany |
| Potassium dihydrogen phosphate ($KH_2PO_4$) | Merck KGaA, Darmstadt, Germany |
| RPMI-1640 medium (without glutamine) | Gibco®, Thermo Fisher Scientific, Waltham, MA, USA |
| Sodium azide ($NaN_3$) | Merck KGaA, Darmstadt, Germany |
| Sodium bicarbonate ($NaHCO_3$) | Merck KGaA, Darmstadt, Germany |
| Sodium chloride (NaCl) | Merck KGaA, Darmstadt, Germany |
| Sodium hydrogen phosphate monohydrate ($NaH_2PO_4xH_2O$) | Merck KGaA, Darmstadt, Germany |
| Triton-X 100 | Roche Diagnostics GmbH, Mannheim, Germany |
| Trypan blue (0.4%) | Sigma-Aldrich Corporation, St. Louis, USA |
| β-mercaptoethanol (β-ME) | AppliChem GmbH, Darmstadt, Germany |

**Table 3-4: Kits**

| Kit | Supplier |
|---|---|
| EasySep™ Direct Human CD4+ T Cell Isolation Kit | Stemcell Technologies, Vancouver, Canada |
| EasySep™ Direct Human Monocyte Isolation from whole blood | Stemcell Technologies, Vancouver, Canada |
| EasySep™ Human CD25 Positive Selection Kit | Stemcell Technologies, Vancouver, Canada |
| Foxp3/Transcription Factor Staining Buffer Set | eBioscience, Thermo Fisher Scientific, Waltham, MA, USA |
| LEGENDplex™ Human M1/M2 Macrophage Panel (10-plex) with V-bott | Biolegend, San Diego, CA, USA |
| LightCycler® 480 SYBR Green I Master | Roche, Penzberg, Germany |
| NucleoSpin® RNA Isolation | Macherey-Nagel, Düren, Germany |
| Qubit RNA HS Assay Kit | Invitrogen GmbH, Darmstadt, Germany |

**Table 3-5: Stimulants**

| Stimulants | Supplier |
|---|---|
| Interleukin (IL)-2, human recombinant | eBioscience, Thermo Fisher Scientific, Waltham, MA, USA |
| Lipopolysaccharide (LPS) | Sigma-Aldrich Corporation, St. Louis, USA |
| Macrophage colony-stimulating factor (M-CSF), recombinant human | PeproTech, Rocky Hill, NJ, USA |
| Treg inspector beads | Miltenyi Biotec, Bergisch Gladbach, Germany |

**Table 3-6: Enzymes**

| Enzyme | Supplier |
|---|---|
| Maxima H minus reverse transcriptase | Thermo Fisher Scientific, Waltham, MA, USA |
| RiboLock Rnase Inhibitor | Thermo Fisher Scientific, Waltham, MA, USA |

### 3.1.4 Buffers and solutions

Used buffers and solutions as well as their ingredients are listed below.

**Table 3-7: Buffers and solutions**

| Buffers/ solutions | Ingredients |
|---|---|
| FACS buffer | 5 g BSA, 2mM EDTA, ad 1 L PBS |
| Fixing buffer | 4 g PFA (3%), ad 100 mL destilled water and 50 mL PBS |
| Immunostaining buffer | 5 g BSA (1%), 0.5 mL 10% NaN3 solution (0.01%), 5 g human serum (1%), ad 500 mL PBS |
| PBS buffer | 80 g NaCl, 2 g KCl, 11.5 g NaH2PO4x12H2O, 2 g KH2PO4, ad 1 L destilled water, pH 7.2 |
| Isolation buffer | 1 mL 0.5M EDTA, ad 500 mL PBS |
| Permeabilization buffer | 0.1 mL Triton-X 100 (0.1%), ad 100 mL PBS |
| Sodium bicarbonate buffer | 0,84 g sodium bicarbonate (0.1M), ab 50 mL destilled water |
| Washing solution | 75 mg glycine (10mM), ad 100 mL PBS |

### 3.1.5 Cultivation media

Table 3-8 comprises the used cultivation media for cell culture of primary isolated cells as well as their ingredients.

**Table 3-8: Cultivation media**

| Cultivation media | Ingredients |
|---|---|
| Differentiation medium | RPMI with 10% FBS, 1M HEPES, 10 mg/mL L-glutamine, 1x P/S, 25mM β-ME |
| Stimulation medium | RPMI with 10% FBS, 10 mg/mL L-glutamine |

### 3.1.6 Primers for quantitative RT-PCR

Self-designed primers from TIB MOLBIOL, Berlin were obtained as lyophilizate and diluted according to the supplier's protocol: 20 µM in RNase-free $H_2O$ (Table 3-9). Primers from Bio-Rad, Munich were ready to use (Table 3-10).
Random hexamer primer from Roche Diagnostics GmbH, Mannheim, Germany were used to generate complementary DNA (cDNA).

**Table 3-9: Primer from TIB MOLBIOL, Berlin, Germany**

| Primers | Species | Sequence (5´>3´) |
|---|---|---|
| ActB | Human | Forward CCT GGC ACC CAG CAC AAT<br>Reverse GGG CCG GAC TCG TCA TAC |

**Table 3-10: Primer from Bio-Rad, Munich, Germany**

| Primers | Species | Unique Assay ID |
|---|---|---|
| FOXP3 | Human | qHsaCID0007630 |
| GATA3 | Human | qHsaCED0043189 |
| RORC | Human | qHsaCID0008528 |
| STAT3 | Human | qHsaCID0010912 |
| TBX21 | Human | qHsaCED0042343 |

### 3.1.7 Antibodies

Antibodies used for flow cytometry analysis are listed in Table 3-11 and for immunostaining in Table 3-12.

**Table 3-11: Antibodies used for flow cytometry**

| Primary antibodies | Species | Clone | Dilution | Supplier |
|---|---|---|---|---|
| CD11b, APC conjugated | Human | ICRF44 | 1:25 | Biolegend, San Diego, CA, USA |
| CD14, PE conjugated | Human | M5E2 | 1:33 | Biolegend, San Diego, CA, USA |

| | | | | |
|---|---|---|---|---|
| CD45, APC conjugated | Human | HI30 | 1:33 | Biolegend, San Diego, CA, USA |
| CD68, FITC conjugated | Human | Y1/82A | 1:25 | Biolegend, San Diego, CA, USA |
| CD80, FITC conjugated | Human | 2D10.4 | 1:25 | eBioscience, Thermo Fisher Scientific, Waltham, MA, USA |
| CD200R, PE conjugated | Human | OX108 | 1:25 | eBioscience, Thermo Fisher Scientific, Waltham, MA, USA |
| CD206, APC conjugated | Human | 19.2 | 1:25 | eBioscience, Thermo Fisher Scientific, Waltham, MA, USA |
| CD284 (TLR4), BV421 conjugated | Human | HTA125 | 1:25 | Biolegend, San Diego, CA, USA |
| FcR Blocking Reagent | Human | | 1:5 | Miltenyi Biotec, Bergisch Gladbach, Germany |
| Fixable Viability Dye eFluor®780 conjugated | Human | | 1:2000 | eBioscience, Thermo Fisher Scientific, Waltham, MA, USA |
| HLA-DR, PerCP/Cy5.5 conjugated | Human | L243 | 1:25 | Biolegend, San Diego, CA, USA |

**Table 3-12: Antibodies used for immunostaining**

| Antibody | Category | Species | Dilution | Supplier |
|---|---|---|---|---|
| HIF-1α, rabbit [EPR16897] | primary | Human | 1:50 | Abcam, Cambridge, UK |
| Nrf2, rabbit [EP1808Y] | primary | Human | 1:100 | Abcam, Cambridge, UK |
| IgG, goat 594nm | secondary | Rabbit | 1:1000 | Cell Signaling Technology, Danvers, MA, USA |

## 3.2 Methods

### 3.2.1 Study population

#### 3.2.1.1 Study cohort

This study was performed in the Department of Pediatrics at the University Hospital of Lübeck, a level 1 perinatal center for the treatment of high-risk neonates. This study was integrated in the Immunoregulation of the Newborn (IRoN) study. Cord blood samples and clinical data were obtained from preterm infants with a gestational age between 30+0 and 34+4 weeks born between May 1st, 2017 and January 31st, 2019. The inclusion criteria were infants without lethal abnormalities, and written informed consent provided by parents or a legal representative. Cord blood samples from late preterm and term infants born with a gestational age above 36+0 weeks and peripheral blood samples from healthy adult donors above 18 years served as controls.

#### 3.2.1.2 Ethics

Written informed consent was obtained from parents on behalf of the infants enrolled in the study. The study was approved by the local committee on research in human subjects at the University of Lübeck (IRON AZ 15-304). All blood samples were obtained in line with current guidelines of the European Medical Agency on the investigation of medicinal products in term and preterm infants; Committee for Medicinal Products for Human Use and Pediatric Committee (PDCO, 2006).

#### 3.2.1.3 Clinical definitions

Gestational age was calculated from the best obstetric estimate based on early prenatal ultrasound and obstetric examination.

### 3.2.2 Sample collection

All blood samples analyzed in this study were collected using EDTA as an anticoagulant (S-monovettes K3E). Cord blood was collected by the attending physician or midwife directly after the infant was born from the umbilical cord vein attached to the placenta. Adult blood samples were collected by peripheral vein puncture. All samples were processed within 24 h.

### 3.2.3 Cell isolation

All procedures described in this section were performed under sterile conditions.

#### 3.2.3.1 Monocyte isolation from whole blood

Monocytes were isolated directly from whole blood by immunomagnetic negative selection using the EasySep™ Direct Human Monocyte Isolation Kit. The whole procedure was performed according to the manufacturer's instructions. In brief, 1-4 mL of human whole blood were incubated with 50 µL/mL Isolation Cocktail and 50 µL/mL RapidSpheres™ for 5 min. In this step, non-monocytes and CD16+ monocytes were labeled with antibodies from the Isolation Cocktail recognizing specific surface markers and RapidSpheres™ for removal of unwanted cells. Next, isolation buffer was added to the sample before it was placed in a magnet (BigEasy or EasyEights) for 5 min for magnetic separation. The clear enriched cell suspension was then transferred into a new tube. Subsequently, the same amount of RapidSpheres™ used the first time was added to the sample, which was again mixed and incubated. Afterwards the magnetic separation was repeated twice, only transferring the clear fraction of the enriched cell suspension into a new tube.

#### 3.2.3.2 CD4+ CD25- T cell isolation from whole blood

CD4+ T cells were isolated directly from cord blood of term infants by immunomagnetic negative selection using the EasySep™ Direct Human CD4+ T Cell Isolation Kit. The procedure was performed according to the manufacturer's instructions. In brief, 7 mL of human whole blood were incubated with 50 µL/mL Isolation Cocktail and 50 µL/mL RapidSpheres™ for 5 min. In this step, non-CD4+ T cells were labeled with antibodies from the Isolation Cocktail, recognizing specific surface markers and RapidSpheres™ for removal of unwanted cells. Next, PBS buffer was added to the sample before it was placed into the EasyEights magnet for 5 min for magnetic separation. The clear enriched cell suspension was then transferred into a new tube. Subsequently, the same amount of RapidSpheres™ used the first time was added to the sample, which was again mixed and incubated for 5 min. Afterwards, the magnetic separation was repeated twice only transferring the clear fraction of the enriched cell suspension into a new tube. The isolated CD4+ cells were centrifuged at 300x g for 8 min.

CD25- selection was performed using the EasySep™ Human CD25 Positive Selection Kit, which, according to the manufacturer's instructions, can also be used for CD25 depletion. This kit targeted CD25+ cells for positive selection with an antibody recognizing the CD25 surface marker. After centrifugation of CD4+ cells, supernatant was discarded and the cell pellet was resuspended in 1mL isolation buffer containing 2% FBS. 50 µL/mL Selection Cocktail was added, cells were mixed and incubated for 15 min. Following the 15 min incubation period, 50 µL/mL mixed magnetic particles were added, cells were mixed and incubated for 10 min. Subsequently, 4 mL isolation buffer containing 2% FBS were added to the sample. The sample was gently mixed 2 to 3 times and placed into the BigEasy magnet for 5 min for magnetic separation. The supernatant containing the enriched CD25- cells was transferred into a new tube, centrifuged at 300x g for 8 min, and resuspended in 500 µl isolation buffer containing 2% FBS. Subsequently, the CD25- selection was repeated as described above only using 50 µl Selection Cocktail and magnetic particles, respectively. Next, isolation buffer containing 2% FBS was added to bring the total sample volume to 2.5 mL. Magnetic separation was repeated twice for 10 min, transferring the CD25 depleted cell suspension into a new tube.

### 3.2.4 Cell culture

#### 3.2.4.1 Counting

Following isolation, cells were centrifuged at 300x g for 8 min at room temperature. After discarding the supernatant, the cell pellet was resuspended in 1-4 mL differentiation medium. Cell counting was performed with 10 µL of cell suspension, which was mixed

with 10 µL or 80 µL PBS buffer and 10 µL trypan blue (0.4%) for a final dilution of 1:3 for monocyte count or 1:10 for T cells count, respectively. From this final dilution, 10 µL were pipetted into a Neubauer counting chamber (depth 0.1 mm). Living cells were counted in four squares with a 10x magnification. Cells that appeared blue were considered dead, because live cells prevent trypan blue from diffusing through the cell membrane. Cell number was determined using the formula:

$$cells/mL = \frac{sum\ up\ number\ of\ cells\ counted\ per\ square}{number\ of\ counted\ squares} * dilution\ factor * 10^4$$

The result was multiplied by the volume of the cell suspension to achieve the total monocyte cell number.

#### 3.2.4.2 Differentiation into monocyte-derived macrophages

Following monocyte isolation, $5x10^5$ to $7.5x10^5$ cells per $cm^2$ were seeded in tissue culture flasks or plates. Differentiation medium was added to achieve a total volume of 1 mL medium per $cm^2$. After a 1 to 2 h resting and adherence phase in an incubator containing an atmosphere of 5% $CO_2$ and 21% $O_2$ at a temperature of 37 °C, differentiation medium was replaced with media containing 10 ng/mL M-CSF and cells were placed back in the incubator. Following 3 days of differentiation, the medium was replaced with fresh media containing 10 ng/mL of M-CSF, and cells were incubated for another 3 days.

#### 3.2.4.3 Double-hit stimulation model

To detach MDMs after 6 days of differentiation, differentiation medium was carefully removed, and cells were washed once with PBS buffer. Accutase was added to adherent cells according to the manufacturer's instructions and incubated for 8 min in an incubator (5% $CO_2$ and 21% $O_2$) at 37 °C. Afterwards, the surface was flushed, and the cell suspension was mixed carefully multiple times to obtain a single cell suspension, which was transferred to a 15 mL tube. Next, stimulation medium was added to the flask, remaining cells were carefully scraped off the surface, and it was flushed again before transferring the cells to the same 15 mL tube. Following a centrifugation step at 300x g for 8 min at room temperature, supernatant was discarded, and the cell pellet was resuspended in stimulation medium. Cells were counted as described in section 3.2.4.1 using a 1:3 dilution. 4.5 to $5.0x10^5$ cells/mL were seeded in 200 µL per well in a flat-bottom 96-well plate for RNA isolation (see 3.2.7.1) or in 400 µL per FACS tube for flow cytometry (see 3.2.6). After a 1 to 2 h resting and adherence phase in an incubator

containing an atmosphere of 5% $CO_2$ and 21% $O_2$ at 37 °C, cells were placed in different incubators with 5% $CO_2$ at 37 °C containing the desired $O_2$ conditions, namely: 21% atmospheric $O_2$, 3% $O_2$ (incubator with $N_2$-regulation) and 65% $O_2$ (air-tight sealed chamber filled with gas mixture) and incubated for 48 h. Subsequently, cells were removed from the different $O_2$ conditions and stimulated with 100 ng/mL LPS for 4 h (52 h time point) or 24 h (72 h time point) in atmospheric $O_2$ with 5% $CO_2$ at 37 °C. This sequential double-hit stimulation model is depicted in Figure 3-1. After the LPS stimulation, supernatant was harvested on ice and stored at -80 °C until further use. Cells were used for RNA isolation (3.2.7.1) or flow cytometry (3.2.6).


**Figure 3-1: Sequential double-hit model for lung immunity.** Cells were placed in different $O_2$ concentrations (21% atmospheric $O_2$, 3% $O_2$ and 65% $O_2$) and incubated for 48 h. Subsequently, cells were removed from the different $O_2$ conditions and stimulated with 100 ng/mL LPS for 4 h (52 h time point) or 24 h (72 h time point) in atmospheric $O_2$.

#### 3.2.4.4 Co-culture of T cells with supernatants from stimulated macrophages

After cell count (see 3.2.4.1) and a 1 h resting phase at 37 °C in differentiation medium containing 1500 U/mL IL-2, $2x10^4$ isolated CD4+ CD25- cells were seeded in 10 µL per well in a round-bottom 96-well plate. Treg inspector beads had a concentration of $2x10^7$ Treg inspector beads/mL loaded with biotinylated CD3/CD28/CD2 antibodies and were used according to the manufacturer's instructions. They were washed and added in a 1:1 bead to cell ratio to all wells except the negative control. Next, 140 µL of differentiation medium was pipetted to the negative controls and medium controls, which were performed in triplicate for normalization. To all other wells, 140 µL of supernatant was added. Supernatants were collected from previously performed experiments using the double-hit stimulation with preterm, term and adult MΦ. All wells were carefully mixed up and down ten times, resulting in an end concentration of 100 U/mL IL-2 within each well. After 6 days of incubation in atmospheric $O_2$ with 5 % $CO_2$ at 37 °C, supernatant was carefully collected on ice and stored at -80 °C, and cells were used for RNA isolation (3.2.7.1).

### 3.2.5 Microscopy

#### 3.2.5.1 Morphology

To compare the morphology of MDMs from preterm and term infants as well as adults after differentiation, three phase contrast pictures per experiment and donor were obtained using a fluorescence microscope at 20x magnification.

#### 3.2.5.2 Indirect immunofluorescence

To assess protein expression of transcription factors and their translocation to the nucleus, immunostaining was used.

Chamber slides were coated with 20-30 µg/mL Cell-Tak in 100 µL sodium bicarbonate buffer for 20 min at room temperature. Wells were then washed twice with 500 µL sterile distilled water and air-dried for 1 h under sterile conditions. After differentiation, $5x10^4$ MΦ per mL were seeded in 400 µL stimulation medium per coated well. After a 1 to 2 h resting and adherence phase in an incubator containing an atmosphere of 5% $CO_2$ and 21% $O_2$ at a temperature of 37 °C, chamber slides were transferred to different incubators with 5% $CO_2$ at 37 °C containing the desired $O_2$ conditions, including 21% atmospheric $O_2$, 3% $O_2$ (incubator with N2-regulation) and 65% $O_2$ (air-tight sealed chamber filled with gas mixture), and incubated for 5 h. In the following description, volumes were specified per chamber. Immediately after the 5 h incubation period, the supernatant was discarded, and cells were fixed by adding 200 µL fixing buffer for 30 min at room temperature. Afterwards, cells were washed three times with 200 µL washing solution and stored in PBS buffer at 4 °C overnight. On the next day, 200 µL permeabilization buffer were added and cells were incubated 5 min at room temperature. Following permeabilization and three washes with 200 µL PBS buffer per wash, non-specific binding sites on cells were blocked for 30 min at room temperature using 200 µL immunostaining buffer. Afterwards, immunostaining buffer was completely removed, and cells were incubated with 100 µL primary antibody diluted as indicated in Table 3-12 in immunostaining buffer for 1 h at room temperature. Next, cells were washed three times with 200 µL PBS buffer and then incubated with 200 µL diluted secondary antibody (as indicated in Table 3-12) for 30 min at 37 °C in the dark. After repeating the washing step three times using 200 µL PBS buffer per wash, cells were incubated with 200 µL DAPI solution (1 ng/mL) for 15 min at room temperature in the dark and washed two times with 200 µL PBS buffer per wash. Following the staining procedure, PBS buffer and chambers were removed to let the slides dry. Using one drop of mounting solution, slides were covered with a coverslip and sealed using nail polish. Slides were stored at 4 °C for up to 2 days to allow them to dry.

#### 3.2.5.3 Analysis of immunofluorescent stained macrophages

Three to four microscopy pictures were obtained per condition at 100x magnification using oil on the objective of the fluorescence microscope. To obtain comparable pictures, the same exposure time was used for each image. Afterwards, pixel intensity of the red channel was analyzed in the nucleus of Nrf2- or HIF-1α-stained cells using ImageJ. Results represent 3 to 4 microscopy pictures per $O_2$ condition for each experiment, including 8 to 12 cells analyzed per picture.

### 3.2.6 Flow cytometry

#### 3.2.6.1 Staining

To determine the expression of proteins on the cell surface and intracellularly, MΦ were stained with fluorescently labeled antibodies and analyzed using flow cytometry as described in the following paragraph.

Directly after differentiation, $5x10^4$ to $1x10^5$ MΦ were transferred into a FACS tube. When staining intracellular proteins, $2x10^5$ to $4x10^5$ cells were transferred per FACS tube. Cells were washed once with 1 mL PBS buffer and centrifuged at 1500 rpm for 5 min at room temperature. The supernatant was discarded by inverting the tube in one continuous motion, leaving the cells in approximately 100 µL PBS buffer. Next, 20 µL FcR blocking reagent was added to all tubes, samples were pulse vortexed, and then incubated for 15 min at room temperature in the dark. The Fixable Viability Dye was pre-diluted 1:100 in PBS buffer. Antibodies against surface proteins were added at dilutions indicated in Table 3-11 using two different FACS panels: 1.) CD14, CD45, and pre-diluted Fixable Viability Dye and 2.) CD11b, CD163, and pre-diluted Fixable Viability Dye. All samples were pulse vortexed and incubated for 25 min at room temperature in the dark. Subsequently, samples were washed with 2 mL of flow cytometry staining buffer or FACS buffer to each tube and centrifuged at 1500 rpm for 5 min at room temperature. Then, supernatant was discarded in one continuous motion by inverting the tubes. For the first panel, cells were resuspended in 150 µL FACS buffer for flow cytometric analysis.

For the second panel, intracellular staining was subsequently performed using the Foxp3/Transcription Factor Staining Buffer Set. Working solution was prepared by mixing 125 µL Fixation/Permeabilization-Concentrate with 875 µL Fixation/Permeabilization-Diluent per sample (1:8). Cells were fixed and permeabilized by adding 1 mL of the working solution, pulse vortexing, and incubating 30 min in the dark. Afterwards, 1 mL of 1x permeabilization buffer from the set was added to all samples, they were centrifuged again at 1500 rpm for 5 min at room temperature, and supernatant was discarded by inverting the tube in one continuous motion. To block unspecific binding sites

intracellularly, 20 µL FcR blocking reagent was added to all tubes, samples were pulse vortexed and incubated for 15 min at room temperature in the dark. Next, an antibody against the intracellular protein CD68 was added in a dilution indicated in Table 3-11, samples were pulse vortexed and incubated for another 30 min at room temperature in the dark. Washing samples was repeated by adding 2 mL 1x permeabilization buffer, centrifugation at 1500 rpm for 5 min at room temperature, and discarding supernatant by inverting the tube in one continuous motion. As a last step, 150 µL flow cytometry staining buffer were added to each sample.

For analysis of surface protein expression on MΦ after stimulation with the double-hit, surface protein staining was performed as described above using the following FACS panel: CD80, CD206, CD200R, CD284 (TLR4), HLA-DR and pre-diluted Fixable Viability Dye.

#### 3.2.6.2 Measurements and gating strategy

All samples and controls were measured with the BD FACSCanto™ II using BD FACS Diva™ software. A total of 20,000 events per sample were measured.

Colors were compensated using unstained and single-stained controls. To generate a positive heat-killed control, 50µL cell suspension obtained after the first washing step described in section 3.2.6.1 were incubated at 65 °C for 2 min, then 2 min on ice and transferred back to half of the remaining living cells. A compensation calculation was performed using BD FACSDiva™ software. Fluorescence minus one (FMO) was used to accurately set the gates for the evaluation of flow cytometry data. A total of 10,000 cells were stained with a mix containing all dyes except for one. Results were used to determine the gating. The gathered data was analyzed using FlowJo® software. The gating strategy is depicted in Figure 3-2 for MΦ. Cells were analyzed for similar size using Forward Scatter (FSC) and similar granularity by Side Scatter (SSC). Single cells were then determined by gating for FSC-Height (FSC-H) by FSC-Area (FSC-A) via exclusion of duplets. Fixable Viability Dye low events were identified as living cells. To further characterize protein expression in MΦ, living singlet cells were analyzed for the different marker expression, setting the gates using FMO controls. To determine marker expression after stimulation with the double-hit, mean fluorescence intensity [MFI] was analyzed to assess the shift in fluorescence intensity for the marker expression in a population of cells.

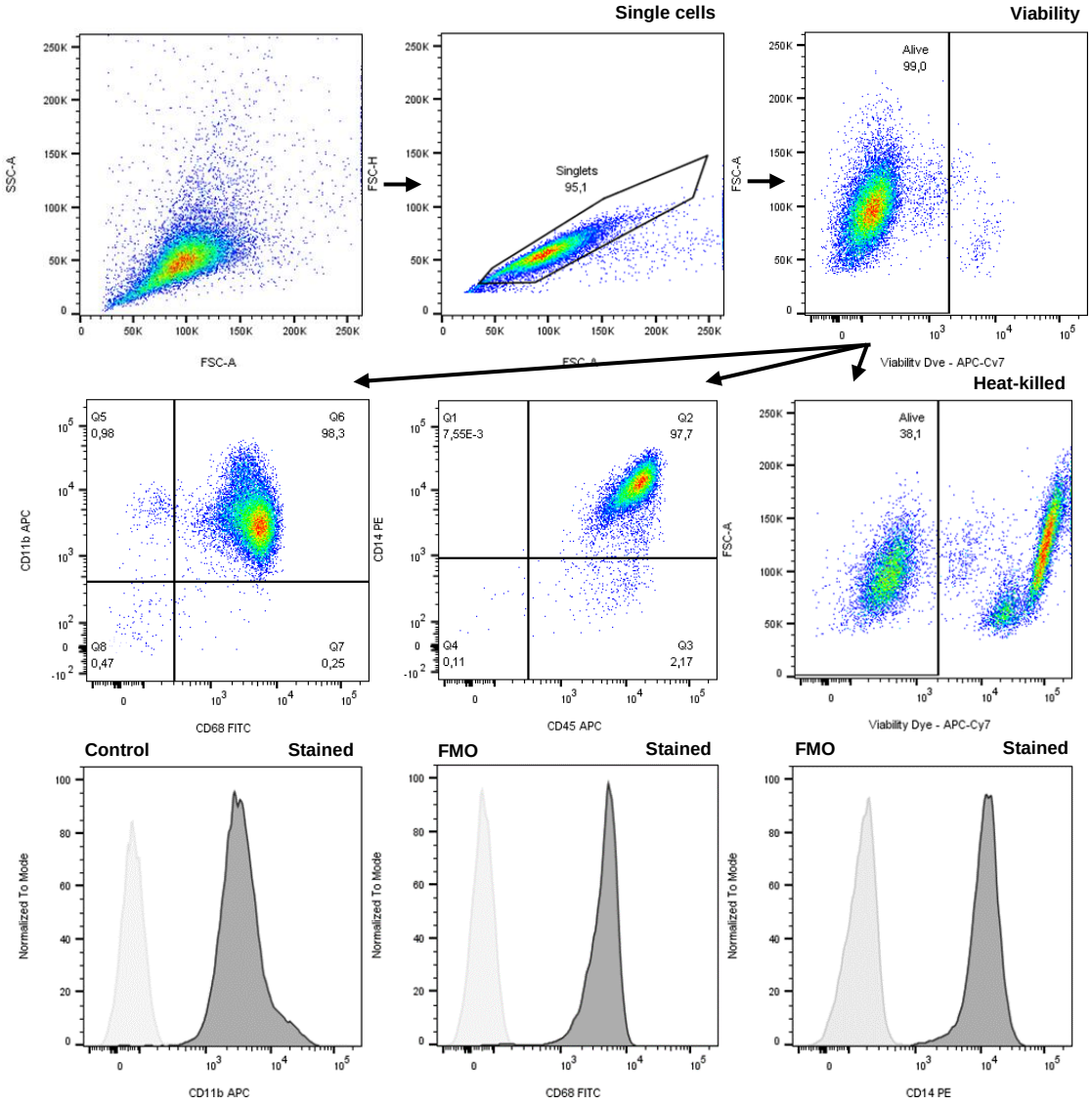


**Figure 3-2: Flow cytometry gating strategy for the analysis of macrophages.** For every sample measured on the BD FACSCanto™ II, evaluation was performed using FlowJo® software. Cells were determined as being singlets and life cells as a starting point and then further gated for marker expression. In this example marker expression of CD11b, CD68 and CD14 is shown as well as a heat-killed control and FMOs of the three markers (histograms).

### 3.2.6.3 Quantitative analysis of cytokines in culture supernatants

To quantify cytokine release, MΦ supernatants were analyzed after the double-hit using the LEGENDplex™ Human M1/M2 Macrophage Panel (10-plex) Kit according to the manufacturer's instructions. After preparing a mixture with 10 different antibody-immobilized beads and reconstituting the Human Macrophage/Microglia Panel Standard Cocktail, a serial dilution of the Standard Cocktail was performed using assay buffer as a diluent. Following preparation of standard dilutions, the 96-well V-bottom plate was loaded with 25 µL assay buffer, 25 µL standard or supernatant and 25 µL bead mixture containing

10 different beads that capture via one specific antibody per bead immobilized on the surface: IL-12p70, TNF-α, IL-6, IL-10, IL-1β, thymus and activation regulated chemokine (TARC, also known as chemokine (C-C motif) ligand (CCL)17), IL-1RA, IL-12p40, IL-23 and interferon γ-induced protein (IP)-10 (also known as C-X-C motif chemokine 10 (CXCL10)). Standards were performed in duplicate. Next, the loaded plate was incubated shaking overnight at 4°C. On the following morning, 25 µL biotinylated secondary detection antibodies were added to the centrifuged and washed plate, and the plate was incubated shaking for 1 h at room temperature. Subsequently, 25 µL streptavidin-phycoerythrin (SA-PE) were transferred to the wells, which bound to the biotinylated detection antibodies, providing fluorescent signal intensities in proportion to the amount of bound analyte. Following an incubation step shaking for 30 min at room temperature, the samples were washed, beads were resuspended using 150 µL 1x wash buffer from the kit, and each sample and the standard were transferred to FACS tubes.

All samples and standards were measured with the BD FACSCanto™ II using BD FACS Diva™ software. Two different bead populations were distinguished by size in the SSC-FSC-plot, and each specific antibody-immobilized bead within a population had a different intensity in its fluorescence signal detected in the APC channel. To quantify the amount of bound analyte, the SA-PE fluorescence signal was detected in the PE channel. Using APC and PE in the flow cytometry setup for detection and quantification of cytokines, no compensation was necessary. A total of 4,000 events of the two bead populations were measured, including approximately 300 events per bead. Gating and analysis were performed using the LEGENDplex v8.0 software according to supplied instructions. The concentration of a particular analyte was determined using a standard curve generated in the same assay.

### 3.2.7 Molecular biology

#### 3.2.7.1 RNA isolation

RNA was isolated by using the NucleoSpin RNA Isolation Kit. β-mercaptoethanol was added to the RNA lysis buffer in a 1:100 dilution. Cells of one well in a 96-well plate were lysed with 200-300 µl RNA lysis buffer and stored at -80 °C until further use. Isolation was performed according to the supplier´s protocol. Samples were thawed, vigorously vortexed, transferred to the violet NucleoSpin Filter and centrifuged to clear the lysate. Afterwards, the flow-through was mixed with an equal amount of 70% ethanol and the mixture was added to the blue NucleoSpin RNA Column and centrifuged for binding of the RNA to the column. By adding MDB buffer onto the membrane of the blue column and centrifugation, it was desalted. Next, DNA was digested by adding 95 µL DNase reaction

mixture and incubating at room temperature for 15 min. After a washing step to inactivate the DNase with RAW2 buffer and two additional washing steps using RA3 buffer, the RNA was eluted using 40 µL RNase-free water, and stored at -80 °C.

#### 3.2.7.2 Reverse transcription PCR

Complementary DNA (cDNA) was generated from an RNA template. The applied scheme of the reverse transcription PCR is shown in Table 3-13.

**Table 3-13: Reverse transcription PCR pipetting scheme**

| Reagent | Volume [µL] |
|---|---|
| 5x reaction buffer | 4.0 |
| Reverse Transcriptase | 1.0 |
| dNTP mix | 2.0 |
| Random hexamer primer | 2.0 |
| RiboLock RNase Inhibitor | 0.5 |
| Nuclease-free water | 5.5 |
| RNA template | 5.0 |

PCR reactions were performed in a thermocycler using the parameters depicted in Table 3-14. After cDNA synthesis, the samples were stored at -20 °C.

**Table 3-14: Reverse transcription PCR temperature profile**

| Temperature program | Temperature [°C] | Time [min] |
|---|---|---|
| Hybridization | 25 | 10 |
| Reverse transcription | 50 | 30 |
| Enzyme inactivation | 85 | 5 |
| Cooling | 4 | forever |

#### 3.2.7.3 Quantitative PCR

Quantitative PCR was performed with the cDNA in a white 96- well plate using the dye SYBR Green. The amount of cDNA and other required ingredients were used according to LightCycler® 480 SYBR Green I Master Kit instructions as indicated in Table 3-15. The cDNA was analyzed with primers listed in Table 3-9 (MOLBIOL) and Table 3-10 (Bio-Rad).

**Table 3-15: Quantitative PCR pipetting scheme per sample**

| Reagent | Volume [µL] MOLBIOL | Volume [µL] Bio-Rad |
|---|---|---|
| Mastermix | 10.0 | 10.0 |
| Forward primer | 0.2 | 1.0 |
| Reverse primer | 0.2 | |
| Nuclease-free water | 7.6 | 7.0 |
| cDNA template | 2.0 | 2.0 |

The PCR was run in a LightCycler using the program depicted in Table 3-16. Evaluation of the data was performed with the LightCycler Data Analysis program. Data were normalized to the corresponding mRNA expression of the housekeeping gene β-Actin. Changes in gene expression were analyzed using the $2^{-\Delta\Delta CT}$ method.

**Table 3-16: Quantitative PCR temperature profile**

| Temperature program | Temperature [°C] | Time [min] | Cycle no. |
|---|---|---|---|
| Initial denaturation | 95 | 10 min | 1 |
| Denaturation | 95 | 10 sec | 45 |
| Annealing | 60 | 10 sec | |
| Elongation | 72 | 20 sec | |
| Melting curve | 95<br>50 | 1 sec<br>30 sec | 1 acquisition every 5 °C |
| Cooling | 40 | forever | 1 |

### 3.2.7.4 RNA sequencing

For sequencing of total RNA samples, the service from the company Novogene was used. Concentration of isolated RNA was determined using the fluorometer Qubit 2.0 and samples with a total amount of more than 50 ng were used. At Novogene, total RNA sample quality control was performed using Nanodrop as preliminary quantification, agarose gel electrophoresis to test degradation and contamination, and the Bioanalyzer Agilent 2100 to check integrity and quantification. After quality control of RNA samples, library preparation was performed using a 250-300 bp insert cDNA library (low-input). Then mRNA was enriched using oligo (dT) beads and randomly fragmented in fragmentation buffer followed by cDNA synthesis using random hexamers and reverse transcriptase. After first-strand synthesis, a custom second-strand synthesis buffer (Illumina) was added with dNTPs, RNase H and Escherichia coli polymerase I to generate the second strand by nick-translation. The final cDNA library was ready after a round of

purification, terminal repair, A-tailing, ligation of sequencing adapters, size selection and PCR enrichment. Library concentration was first quantified using a Qubit 2.0 fluorometer (Life Technologies), and then diluted to 1 ng/µL before checking insert size on an Agilent 2100 and quantifying to greater accuracy by quantitative PCR (library activity > 2nM). Following library preparation, sequencing of the library was performed using an Illumina PE150 platform according to activity and expected data volume.

### 3.2.8 Bioinformatics and statistics

#### 3.2.8.1 Software

Table 3-17 shows all software required for this thesis.

**Table 3-17: Software**

| Software | Distributor | License or freeware |
|---|---|---|
| Acrobat Reader | Adobe INC., Delaware, USA | License |
| BD FACSDiva | BD Bioscience, San Jose, USA | License |
| BZII Analyzer | Keyence, Osaka, Japan | License |
| BZII Viewer | Keyence, Osaka, Japan | License |
| DESeq2 1.22.2 | Bionconductor package | Freeware |
| Excel 2016 | Microsoft Corporation, Redmond, WA, USA | License |
| FASTQC 0.11.5 | Babraham Bioinformatics | Freeware |
| FlowJo® V10 | FlowJo, LLC, Ashland, OR, USA | License |
| GAGE 2.32.0 | Bionconductor package | Freeware |
| GraphPad Prism 7 | GraphPad Software, La Jolla, CA, USA | License |
| ImageJ | ImageJ Project | Freeware |
| KALLISTO 0.43.1 | Github Pachter lab | Freeware |
| LEGENDplex v8.0 | Biolegend, San Diego, CA, USA | License |
| Mendeley | Elsevier, Amsterdam, Netherlands | Freeware |
| MSIGDB library 1.0.6.1 | Github | Freeware |
| R 3.5.2 | R-Project | Freeware |
| Rstudio 1.1.463 | R-Project | Freeware |
| SLEUTH 0.30.0 | Github Pachter lab | Freeware |
| Word 2016 | Microsoft Corporation, Redmond, WA, USA | License |

#### 3.2.8.2 Processing and analysis of raw RNA sequencing data

Quality control of RNA-seq reads was visually inspected using FASTQC. Afterwards, reads were pseudoaligned to human cDNA and ncRNA (Ensembl v94, GRCh38) using KALLISTO with 30 bootstrap cycles. On average, 90% of reads were mapped per sample (total 33 million reads). Quantification files were imported to SLEUTH and pairwise comparisons to 21% $O_2$ (unstimulated baseline) within preterm and term groups were performed (e.g. within term group: 21% $O_2$ versus 21% $O_2$ + LPS; 21% $O_2$ versus 65% $O_2$ + LPS; etc). Significantly different expressed genes were selected based on likelihood ratio tests. Multi-factorial RNA-seq analysis was performed using DESeq2. Gene set enrichment analysis was performed on log2 fold changes from differentially expressed genes using GAGE and Reactome gene sets (provided by MSIGDB library) for pathway analysis. A principal component analysis was performed to inspect the distribution of samples using the mapped RNA-seq data and selecting for the 5,000 most variable genes (R function prcomp with scaling). Results were plotted using the R package REDER.

#### 3.2.8.3 Statistical analysis

Data obtained in the experiments were analyzed using GraphPad Prism except for the principal component analysis (PCA) plot and sequencing data, which were calculated using R. After testing for normal distribution, nonparametric statistical analysis was performed on immunofluorescence, flow cytometry, and cytokine data from MΦ as well as PCR data from T cells. Friedman test for matched data or Kruskal-Wallis for not matched data was used followed by Dunn´s multiple comparison. Sequencing data was analyzed using a two-tailed t-test for comparing two conditions within the groups (see 3.2.8.2), and p-values were corrected for the number of conducted comparisions. For pathway analysis, the “mean of gene set” test statistic was used to evaluate statistically significant differences in pathways within the pairwise comparisons, and p-values were corrected for multiple testing. The threshold for significance was a p-value $< 0.05$ depicted as *, $< 0.01$ as **, $< 0.001$ as *** and $<0.0001$ as ****.

# 4. Results

## 4.1 Clinical characterization of the study cohort

Within the IRoN study cohort preterm infants born between 30+0 and 34+4 weeks of gestation were recruited, and cord blood samples were collected to isolate monocytes for differentiation to MΦ (preterm group). To investigate gestational age-dependent differences, cord blood was also collected from late preterm and term infants who were born above 36+0 weeks of gestation (term group). Peripheral blood samples from healthy adults served as controls (n=17 healthy blood donors, adult group). The overview of clinical characteristics for the whole cohort is depicted in Table 4-1 (see supplementary data for clinical characteristics of each experiment in Table 7-1). No inflammatory or other diseases were reported for included patients during the duration of their hospital stay, except one intra-amniotic infection and one late-onset sepsis in the preterm infant group. However, those infections did not seem to have an impact on the results of this study. All babies were born via Caesarean section, except for three term infants born vaginally. The mode of delivery was comparable between groups.

**Table 4-1: Summary of patient demographics**

| | **Preterm** | **Term** |
|---|---|---|
| **n** | 14 | 19 |
| **Gestational age [weeks]** | 33 ± 1 | 39 ± 1 |
| **Weight [grams]** | 2016 ± 581 | 3536 ± 517 |
| **Male gender [n (%)]** | 9 (64) | 9 (47) |

## 4.2 Characterization of neonatal macrophages after differentiation

MDMs from adult peripheral blood are the most commonly studied type of human MΦ. Since immune cells from infants` blood can differ from immune cells of adults with respect to immune cell function (Kollmann et al. 2012; de Jong et al. 2017) and there are no reports about MDMs from preterm infants, the following results in section 4.2 compare characteristics of MDMs from preterm and term infants as well as adults directly after 6 days of differentiation.

### 4.2.1 Morphology and Viability

To assess the morphology and viability of MDMs from the different groups, microscopy images were obtained after 6 days of differentiation with M-CSF, and flow cytometry analysis was performed using a viability dye.

MDMs from preterm and term infants as well as adults had a similar morphology, with a mixture of spindle-shaped and round-shaped cells forming pseudopodia (Figure 4-1). The median viability of macrophages after differentiation was above 95% for all three groups (Figure 4-2).

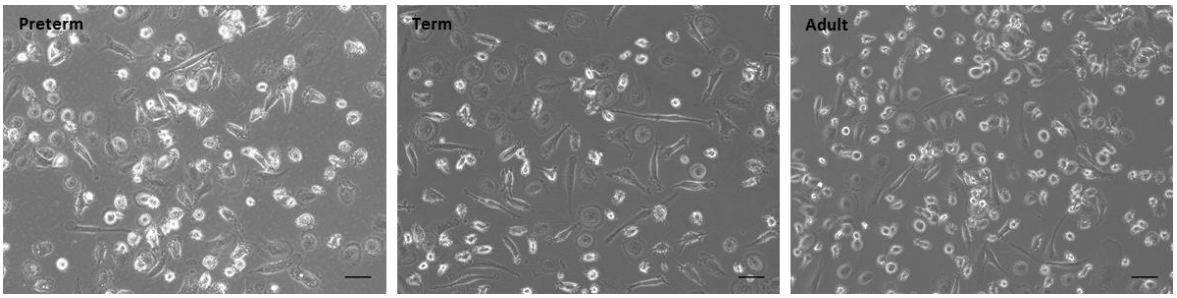


**Figure 4-1: Morphologies of monocyte-derived macrophages (MDMs) from preterm and term infants as well as adults.** Monocytes were differentiated using macrophage colony-stimulating factor (M-CSF) and microscopy images were obtained after 6 days (scale bar 50 µm, n=3 per group).

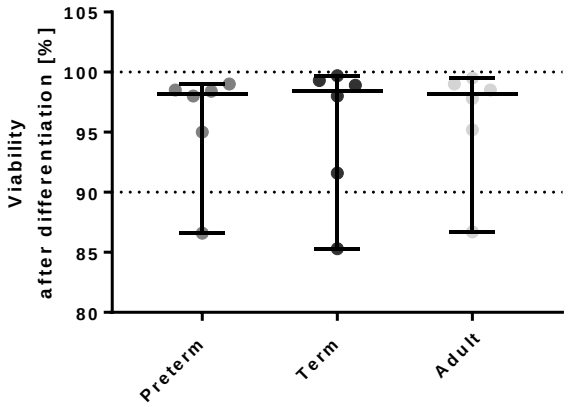


**Figure 4-2: Viability of monocyte-derived macrophages (MDMs) from preterm and term infants as well as adults were similar with a median viability above 95%.** Monocytes were differentiated using macrophage colony-stimulating factor (M-CSF) and viability was assessed using flow cytometry after 6 days (n=6, median with range).

### 4.2.2 Expression of macrophage markers

To investigate expression of macrophage markers on MDMs from preterm and term infants as well as adults, flow cytometry analysis was performed after 6 days of differentiation with M-CSF. Frequencies of cells expressing CD14, CD68 and CD11b were determined.

The frequencies of macrophages expressing CD14, CD68 and CD11b were not statistically significantly different in preterm MDMs compared to term and adult MDMs. For each marker, over 90% of cells were positive in each group (Figure 4-3).

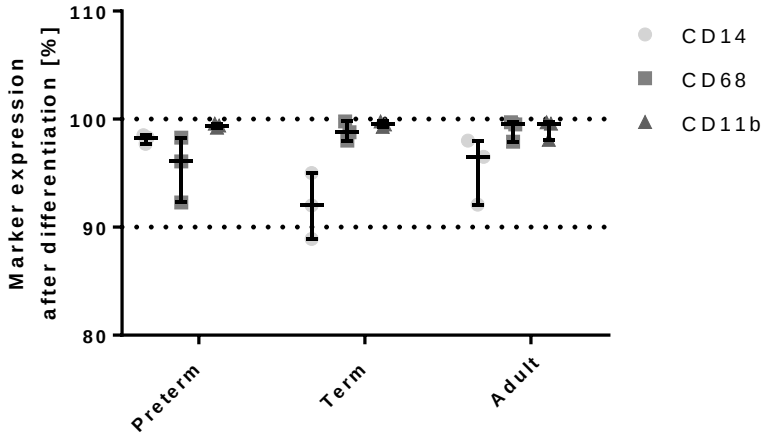


**Figure 4-3: Expression of macrophage markers CD14, CD68 and CD11b was comparable in monocyte-derived macrophages (MDMs) from preterm and term infants as well as adults.** Monocytes were differentiated for 6 days using macrophage colony-stimulating factor (M-CSF) and flow cytometry was performed to determine the frequency of macrophages expressing the markers after differentiation in percentage (n=3, median with range).

In summary, these results indicate that MDMs from preterm and term infants as well as adults had comparable characteristics directly after differentiation with respect to morphology, viability, and expression of macrophages markers.

## 4.3 Immune response of neonatal macrophages in an *ex-vivo* double-hit model for lung immunity

The *ex-vivo* double-hit model for lung immunity was based on two main risk factors for lung developmental deficiencies in preterm infants, abnormal $O_2$ concentrations and infections. After differentiating primary blood monocytes to MDMs, they were cultured for 48 h with different $O_2$ concentrations. Higher $O_2$ (65%) was used to mimic the need for supplemental $O_2$ due to lung immaturity, and lower $O_2$ (3%) to mimic episodes of hypoxia that preterm infants often experience in the first weeks of life (Trembath and Laughon 2012; Martin, Di Fiore, and Walsh 2015). As a control, MDMs were incubated for 48 h under atmospheric $O_2$ (21%). After the incubation period, MDMs were stimulated with 100 ng/mL LPS and incubated under 21% $O_2$ for another 24 h. This sequential second hit with LPS was used to mimic an infection, which preterm infants also often face in the first

weeks of life (Trembath and Laughon 2012). This double-hit model provided the ability to investigate gestational age-dependent differences in response to those key lung exposure factors that contribute to the risk for development of BPD in preterm infants.

### 4.3.1 Oxygen sensing of macrophages

Part of the *ex-vivo* double-hit model was the incubation of cells in various $O_2$ concentrations, including 65% and 3% $O_2$ compared to 21% $O_2$. To verify that MDMs sensed the $O_2$ in the culture conditions used (incubator and air-tight chamber), cells were incubated for 5 h in either 21%, 65% or 3% $O_2$. Afterwards, cells were fixed and antibody-labelled proteins HIF-1α and Nrf2 were detected via immunofluorescence. Generally, under atmospheric $O_2$ conditions both HIF-1α and Nrf2 are degraded in the cytosol. However, HIF-1α is stabilized under low $O_2$ conditions (Nizet and Johnson 2009), whereas Nrf2 increases under high $O_2$ (Cho et al. 2012).

In the used setting, Nrf2 protein was significantly increased in the nucleus of term MDMs incubated under 65% $O_2$ but not under 3% compared to 21% atmospheric $O_2$ (Figure 4-4 A and C). However, HIF1-α protein was exclusively upregulated in the nucleus of MDMs incubated under 3% $O_2$ but not under 65% compared to 21% $O_2$ (Figure 4-4 B and D). The differential upregulation of HIF1-α and Nrf2 protein based on the $O_2$ concentration supports the idea that MDMs sensed the $O_2$ concentrations used in the culture conditions.

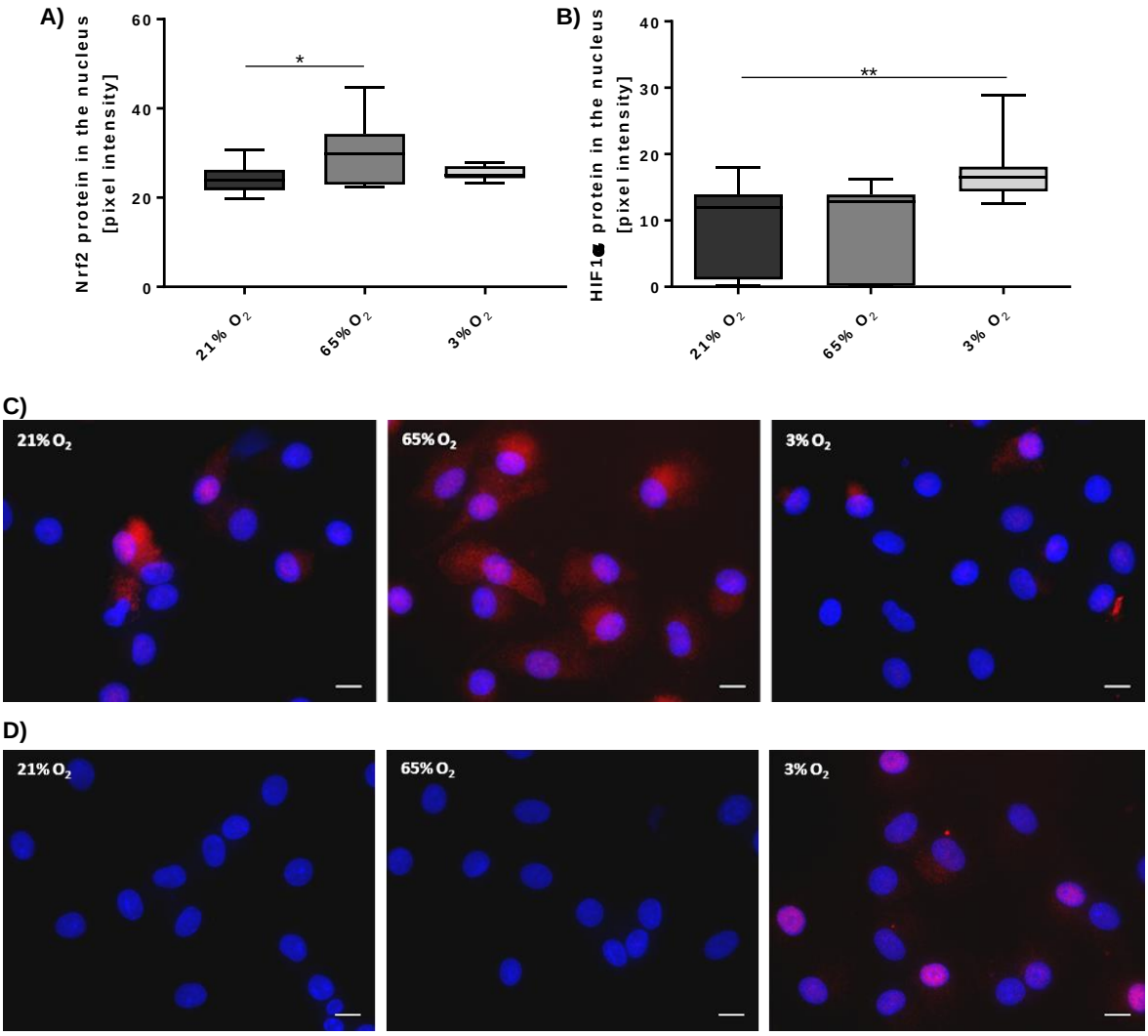


**Figure 4-4: Nuclear factor-like (Nrf)2 protein was significantly upregulated in the nucleus of term monocyte-derived macrophages (MDMs) incubated in 65% $O_2$ whereas Hypoxia-inducible factor (HIF)-1α protein was increased in 3% $O_2$.** A and C) Pixel intensity in the nucleus (blue) of Nrf2 (red) stained cells. B and D) Pixel intensity in the nucleus (blue) of HIF-1α (red) stained cells. Box plots represent 3 to 4 microscopy pictures per $O_2$ condition for each experiment, including 8 to 12 cells analyzed per picture (scale bar 10 µm, n=3, Kruskal-Wallis followed by Dunn´s multiple comparison to 21% $O_2$).

### 4.3.2 Polarization of macrophages

MΦ are highly dynamic immune cells that can exhibit pro- or anti-inflammatory properties depending on their environment (Biswas and Mantovani 2010). To examine polarization of MDMs using the double-hit model, surface protein expression of CD80, CD200R and CD206 was analyzed at 72 h via flow cytometry. Those markers have been used by Jaguin *et al*. to characterize the pro- and anti-inflammatory state of human MDMs (Jaguin et al. 2013). In general, CD80 is a surface protein that provides a costimulatory signal for T cell activation on pro-inflammatory activated MΦ (Mondino and Jenkins 1994). CD200R

is a surface protein mediating an anti-inflammatory signal via cell-cell-contact with epithelial cells, thereby controlling immune responses of MΦ in the lung (Holt et al. 2008). CD206 is a mannose receptor that recognizes glycans from the surface of some microorganisms (Azad, Rajaram, and Schlesinger 2014). Its expression has been shown to remain unaffected after LPS or IL-4 stimulation of MΦ (Jaguin et al. 2013).

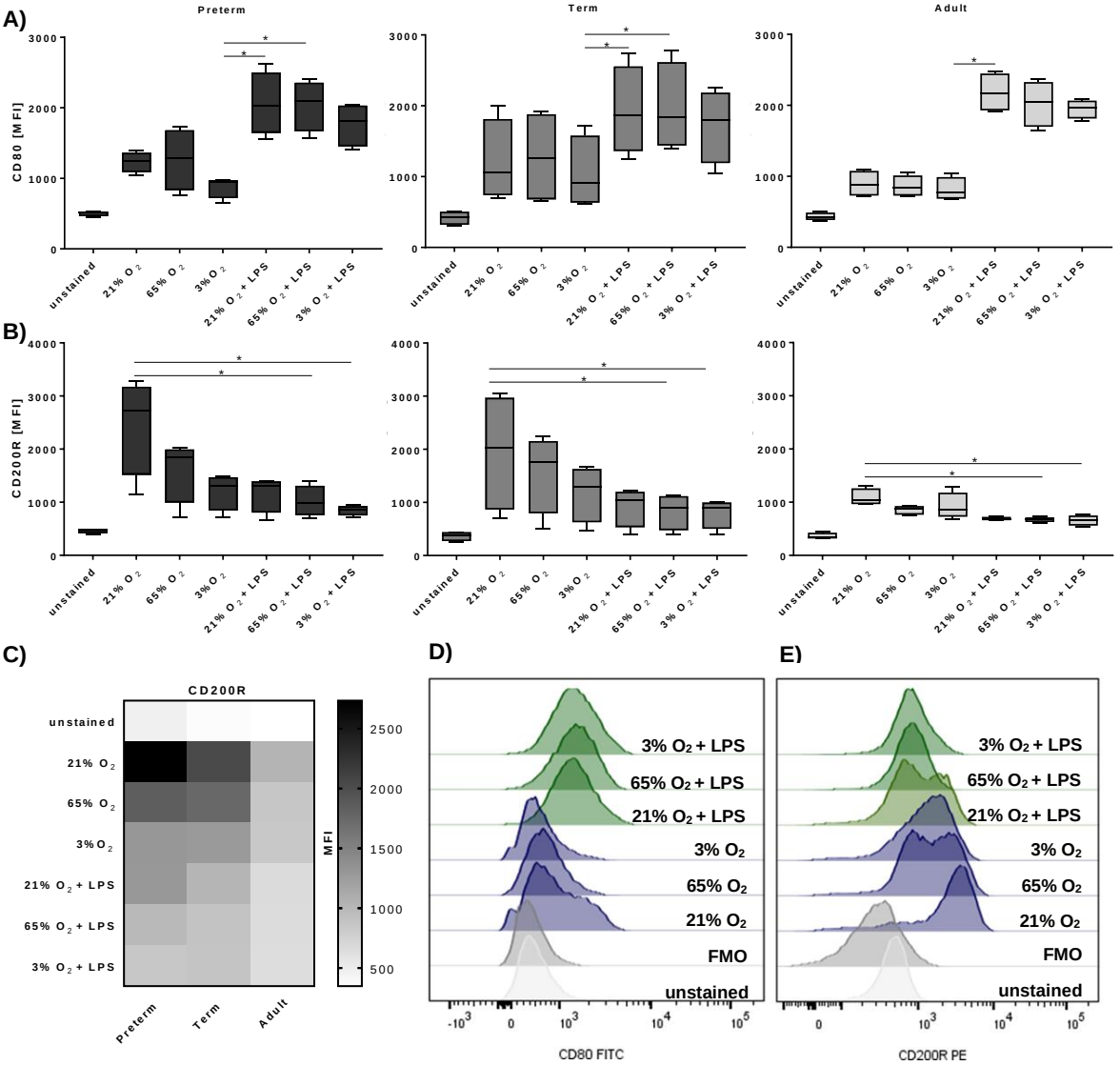


**Figure 4-5: Expression of CD80 was upregulated on macrophages of preterm and term infants as well as adults upon LPS stimulation, while CD200R expression was downregulated.** A) CD80 expression at 72 h depicted as box plots. B, C) CD200R expression at 72 h depicted as box plots and heatmap. Mean fluorescence intensity [MFI] of surface proteins was shown on macrophages in all three groups assessed by flow cytometry after the double-hit model. Histograms for CD80 (D) and CD200R (E) show a representative sample of preterm macrophages (n=4, box plot: Friedman followed by Dunn´s multiple comparison; Heatmap: Median, Kruskal-Wallis followed by multiple comparison to preterm within each condition).

In the *ex-vivo* double-hit model of lung immunity, MDMs from all groups upregulated CD80 surface expression in an LPS-dependent manner (Figure 4-5 A and D). However, CD80 expression was not significantly affected by $O_2$ conditions themselves or by the double-hits with 65% and 3% $O_2$ and subsequent LPS stimulation. For CD200R surface expression, the opposite effect was observed (Figure 4-5 B and E). MDMs from all three groups downregulated CD200R expression upon LPS stimulation. Interestingly, the expression of CD200R showed a tendency to be higher in unstimulated (21% $O_2$) preterm MDMs (baseline), especially compared to adult MDMs at baseline (Figure 4-5 C). No significant changes in CD206 expression were detected (data not shown). The viability of MDMs from all three groups was above 90% after 72 h of stimulation (supplementary data in Figure 7-1).

In summary, MDMs from preterm and term infants as well as adults were polarized towards a pro-inflammatory phenotype in an LPS-dependent manner.

### 4.3.3 Cytokine production by macrophages

Cytokine release is an important aspect of MΦ function. These signaling molecules mediate and regulate inflammation by recruitment of other immune cells and activation of resident cells as well as recruited immune cells (Ryan, Ahmed, and Lakshminrusimha 2008). To analyze cytokine release of MDMs using the double-hit model with key lung exposure factors, the human M1/M2 macrophage cytokine bead array was used to measure cytokine concentration in macrophage supernatants.

MDMs from preterm and term infants as well as adults showed similar production of the inflammatory cytokine TNFα after 52 h, with an upregulation after LPS treatment and an amplification of TNFα release only after the double-hit with 65% $O_2$ and sequential LPS (Figure 4-6 A). The $O_2$ conditions by themselves did not induce a significant TNFα upregulation compared to the 21% $O_2$ control in all three groups. The double-hit with 3% $O_2$ did not have an impact in all three groups either as compared to LPS stimulation alone (Figure 4-6 A). After 72 h, TNFα release by preterm MDMs was similar to the level at 52 h, again with a significant upregulation after the double-hit using 65% $O_2$. However, TNFα release by term and adult MDMs exposed to LPS alone or the double-hits was substantially less at 72 h compared to 52 h.

Production of the inflammatory cytokine IL-6 was upregulated at 52 h upon LPS stimulation for all three groups, although slightly lower in adult MDMs (Figure 4-6 B). However, after 72 h stimulation, further increases in IL-6 release were only detected in preterm MDMs. In addition, the median of 9116 pg/mL IL-6 release at 72 h from preterm

MDMs after the double-hit with 65% $O_2$ showed an amplification compared to LPS treatment alone with a median of 3360 pg/mL.

Release of the regulatory cytokine IL-10 was upregulated upon LPS stimulation at 52 h for all three groups (Figure 4-6 C). However, the double-hit with 65% $O_2$ and LPS showed substantially less upregulation of IL-10 release at 52 h. $O_2$ conditions by themselves compared to 21% $O_2$, as well as the double-hit with 3% $O_2$ compared to LPS at 21% $O_2$ did not appear to influence IL-10 release. The pattern of IL-10 production was similar after 72 h in term and adult MDMs compared to 52 h, but preterm MDMs produced over 10 times more IL-10 upon LPS stimulation at 72 h, regardless of $O_2$ condition.

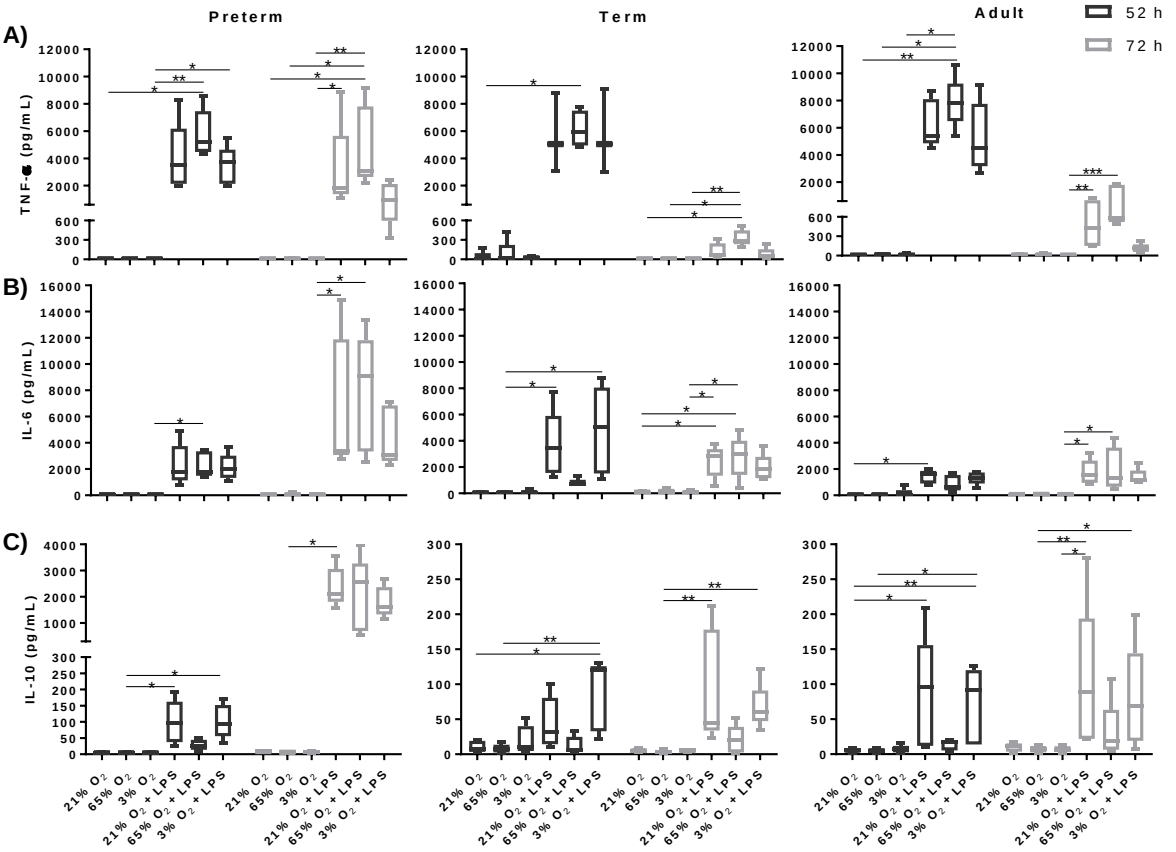


**Figure 4-6: Compared to term infants and adults, macrophages from preterm infants showed a sustained inflammatory response over time, which was exaggerated after the double-hit with 65% $O_2$ and subsequent LPS.** A) TNFα, B) IL-6 and C) IL-10 release after the double-hit measured at 52 h and 72 h from preterm, term and adult macrophages using a cytokine bead array (n=5, box plots, Friedman followed by Dunn´s multiple comparison within time point).

The release of IL-12p70 and IL-23 was investigated because they play a major role in polarization of CD4+ T cells to Th cell type 1 and 17, respectively (Kollmann et al. 2012). During the development of the immune system, Th17 responses seem to be more

dominant in preterm infants early in life, and them shift towards Th1 responses during infancy (Kollmann et al. 2012). In the *ex-vivo* double-hit model of lung immunity, release of IL-12p70 was not detected in any group, whereas IL-12p40, a shared subunit of IL-12p70 and IL-23, was upregulated after 72 h in all three groups upon LPS stimulation (Figure 4-7 A). However, MDMs of term infants and adults downregulated IL-12p40 release after the double-hits with 65% $O_2$ or 3% $O_2$ at 72 h, which was not apparent after the double-hit with 65% $O_2$ in preterm MDMs (Figure 4-7 A). At 52 h, IL-23 release showed the only significant upregulation upon LPS stimulation at 21% $O_2$ by term MDMs (Figure 4-7 B). However, preterm MDMs significantly released IL-23 after 72 h showing an increase after the double-hit with 65% $O_2$ (Figure 4-7 B). Interestingly, adult MDMs showed a similar pattern of IL-23 release after 72 h as preterm MDMs, but with a much lower concentration.

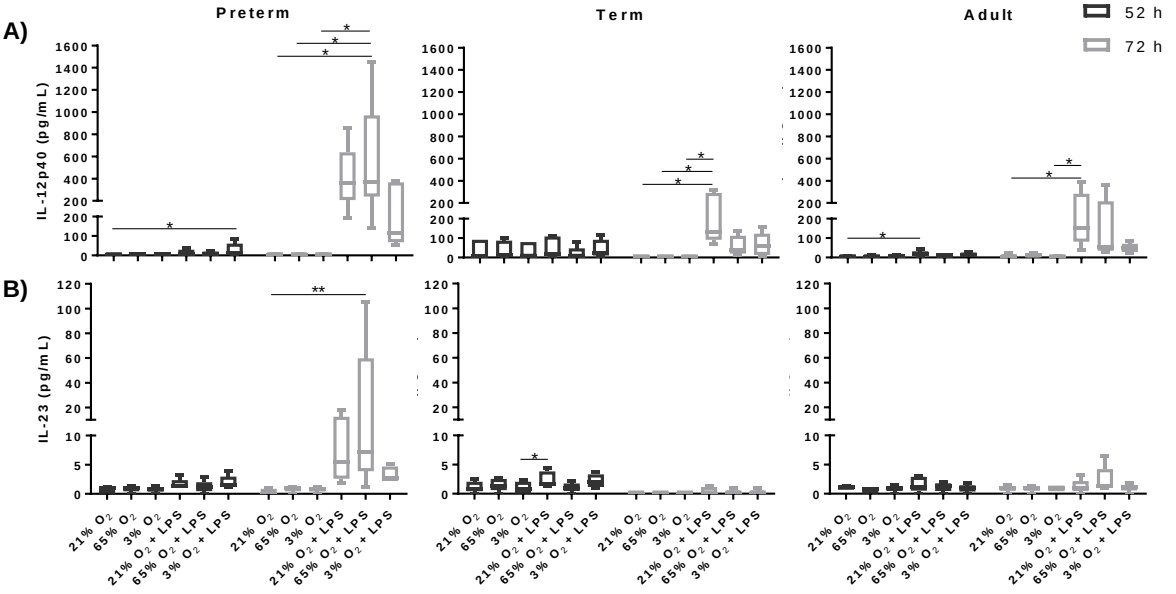


**Figure 4-7: IL-23 release by macrophages was significantly upregulated after the double-hit with 65% $O_2$ and LPS at 72 h in preterm infants, but not in term infants or adults.** A) IL-12p40 and B) IL-23 release after the double-hit at 52 h and 72 h from preterm, term and adult macrophages measured using a cytokine bead array (n=5, box plots, Friedman followed by Dunn´s multiple comparison within time point).

Direct age-dependent comparison of preterm, term and adult MDMs at 72 h was done using heatmaps for TNFα, IL-6, IL-10 and IL-1β as well as IL-12p40 and IL-23 (Figure 4-8). Significant up- and downregulations indicated in these heatmaps were compared to preterm MDMs within the six conditions. TNFα, IL-6, IL-10 and IL-1β demonstrated a significant age-dependent increase of cytokine release by preterm MDMs upon LPS stimulation or the double-hit with 65% $O_2$ compared to term and adult MDMs within the

conditions. The heatmaps also highlight the exaggerated cytokine release after the double-hit with 65% $O_2$ compared to LPS stimulation in 21% $O_2$ by preterm MDMs, as shown in Figure 4-6 and Figure 4-7. In addition, the direct comparison of all three groups at 72 h for IL-12p40 and IL-23 demonstrated a significant age-dependent increase of those cytokines upon stimulation with LPS alone or the double-hit using 65% $O_2$ comparing term and preterm MDMs within the conditions (Figure 4-8).

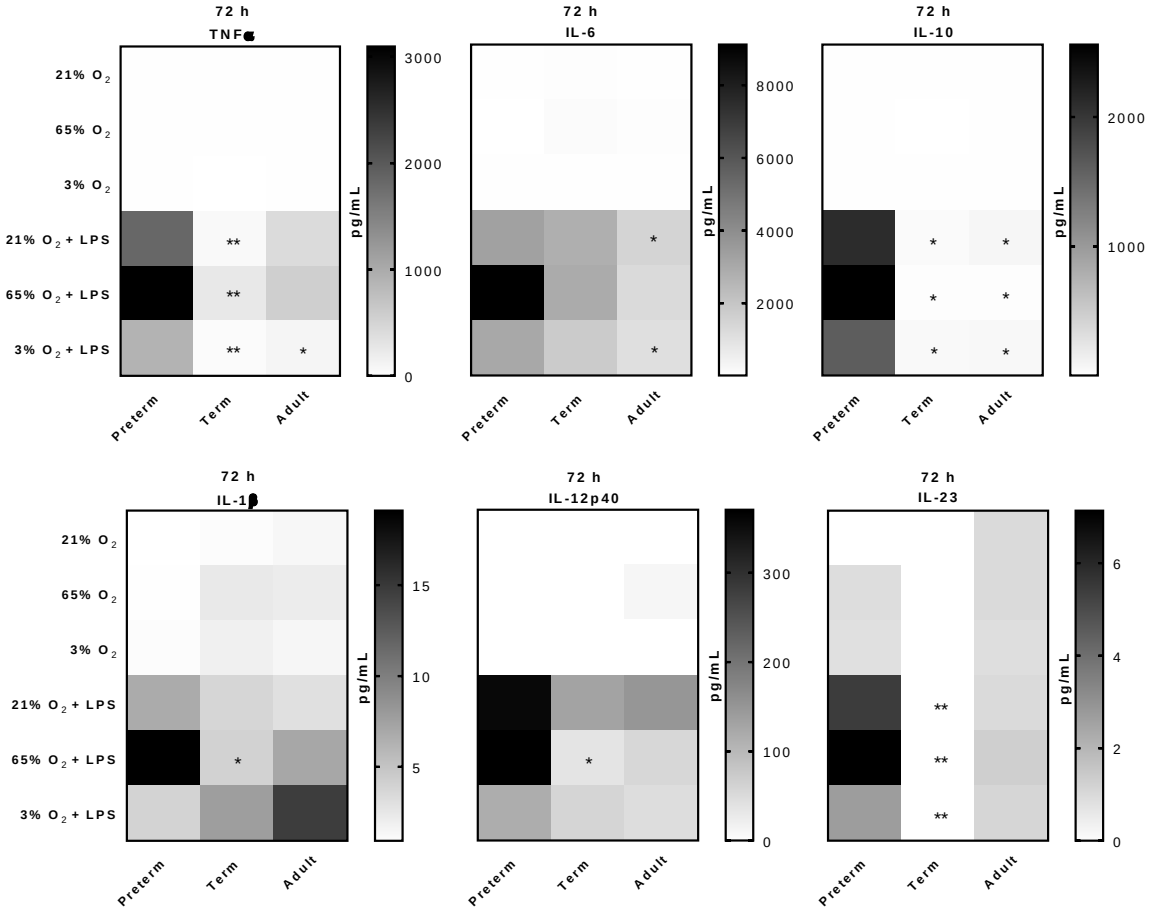


**Figure 4-8: Cytokine release by macrophages upon stimulation showed an age-dependent difference.** Heatmaps of TNFα, IL-6, IL-10, IL-1β, IL-12p40 and IL-23 release after the double-hit at 72 h from preterm, term and adult macrophages measured using a cytokine bead array (n=5, Heatmap: Median, Kruskal-Wallis followed by Dunn´s multiple comparison to preterm within condition).

Another indicator for the recruitment of cells is the release of chemokines from MΦ (Vissers et al. 2015). Therefore, chemokine CXCL10 release was analyzed using the cytokine bead array. CXCL10 showed an upregulation at 52 h in LPS-stimulated MDMs for all three groups, which was not observed in the double-hit with 65% $O_2$ (Figure 4-9).

However, at 72 h CXCL10 was further upregulated in preterm MDMs in an LPS-dependent manner.

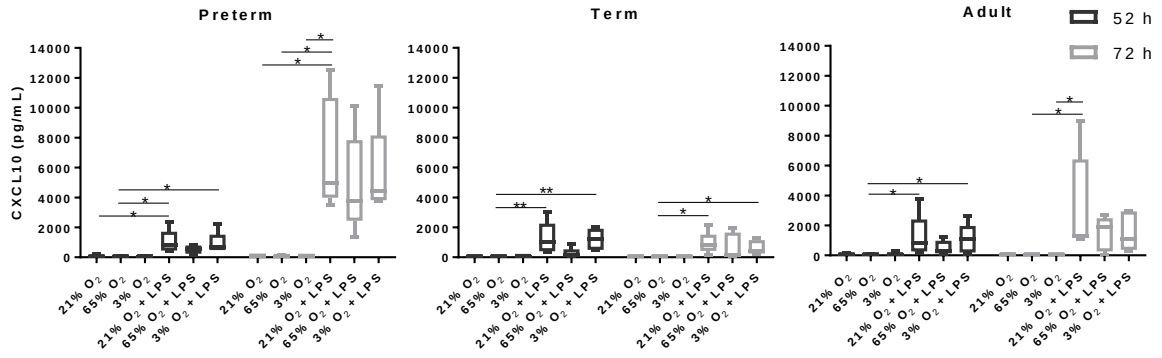


**Figure 4-9: Chemokine CXCL10 release by macrophages was significantly upregulated in preterm and term infants as well as adults upon LPS stimulation at 52 h; at 72 h CXCL10 increased even further for macrophages of preterm infants.** CXCL10 release after the double-hit at 52 h and 72 h from preterm, term and adult macrophages measured using a cytokine bead array (n=5, box plots, Friedman followed by Dunn´s multiple comparison within time point).

In summary, preterm MDMs showed a sustained, upregulated inflammatory cytokine release at the late time point for all analyzed mediators, in contrast to an equal or downregulated cytokine release by term and adult MDMs. In addition, an exaggerated cytokine release of TNFα, IL-6, and IL-1β after the double-hit with 65% $O_2$ was noted in preterm MDMs at the late time point compared to LPS stimulation at 21% $O_2$.

### 4.3.4 Expression of macrophage surface markers

Using the double-hit model for lung immunity, expression of selected surface proteins on preterm, term and adult MDMs was assessed to characterize differences in inflammatory markers due to gestational age or double-hit stimulation. TLR4 was analyzed because it mediates LPS signaling within the cell (Biswas and Mantovani 2010). Human leukocyte antigen – DR isotype (HLA-DR) was investigated because it presents antigens to T cells and thereby activates them (Ettensohn, Duncan, and Jankowski 1989). Surface protein expression of TLR4 and HLA-DR was assessed at 72 h using flow cytometry.

A significantly decreased expression of TLR4 was noted in the double-hit with 3% $O_2$ using adult MDMs but not term MDMs (Figure 4-10 A). Preterm MDMs demonstrated a similar expression pattern of TLR4 as adult MDMs (Figure 4-10 A and D). Interestingly, a direct comparison between the three groups revealed significantly lower surface expression of TLR4 at baseline (21% $O_2$) and upon LPS stimulation on adult MDMs compared to preterm MDMs (Figure 4-10 C). However, basal TLR4 expression was

downregulated to a similar level upon double-hit stimulation with 65% and 3% $O_2$ comparing all three groups within those conditions (Figure 4-10 C).

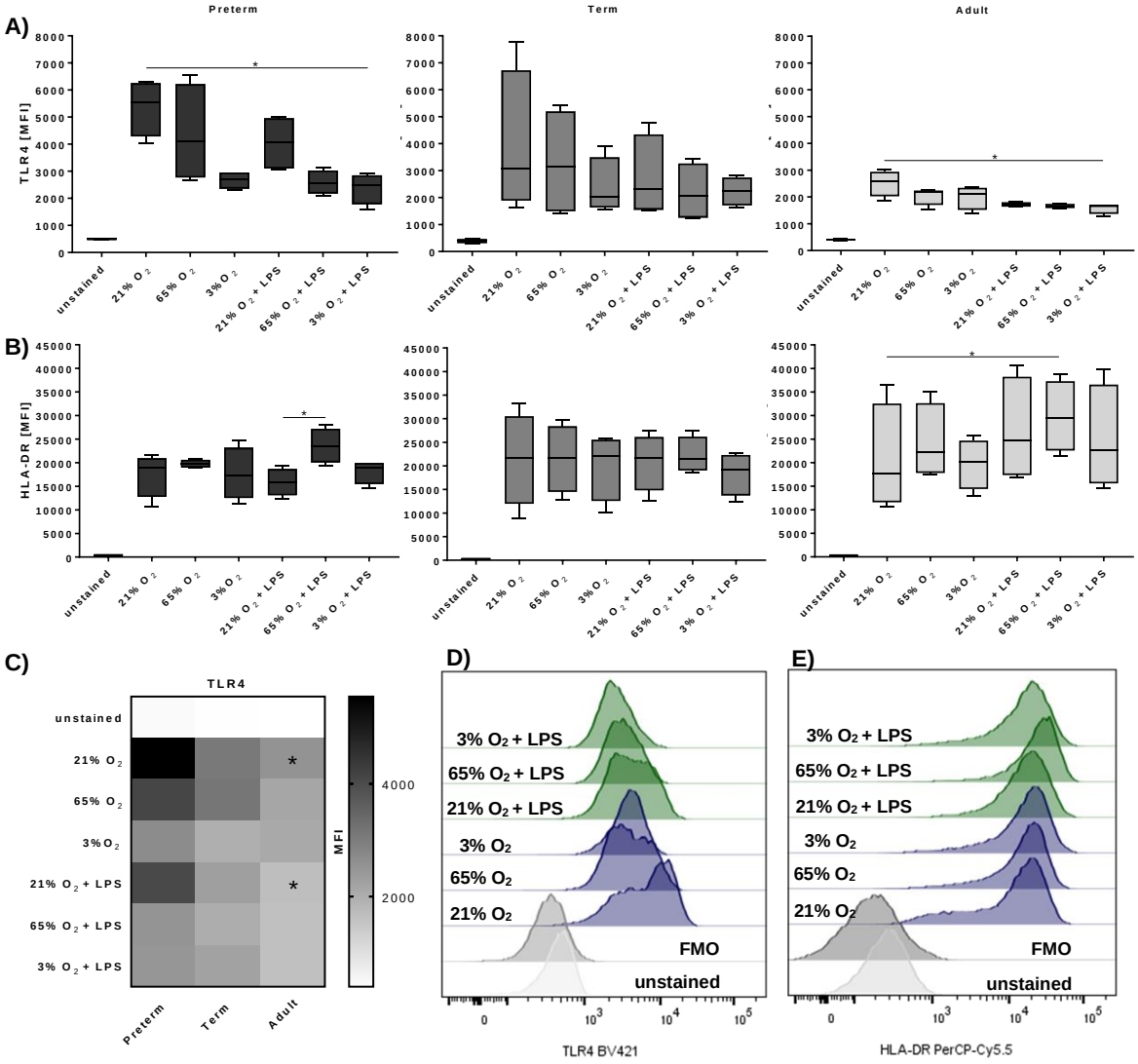


**Figure 4-10: Expression of TLR4 was downregulated upon LPS stimulation of macrophages from preterm and term infants as well as adults, but baseline (21% $O_2$) TLR4 surface expression was significantly lower on adult macrophages compared to preterm macrophages. HLA-DR showed a double-hit dependent significant upregulation after 65% $O_2$ and subsequent LPS.** A and C) TLR4 expression at 72 h depicted as box plots and heatmap. B) HLA-DR expression at 72 h depicted as box plots. Mean fluorescence intensity [MFI] of surface proteins was shown on macrophages in all three groups assessed by flow cytometry using the double-hit model. Histograms of TLR4 (D) and HLA-DR (E) show a representative sample of preterm macrophages (n=4, box plot: Friedman followed by Dunn´s multiple comparison; Heatmap: Median, Kruskal-Wallis followed by multiple comparison to preterm within each condition).

In preterm MDMs, significant upregulation of HLA-DR surface expression was only observed upon double-hit stimulation with 65% $O_2$ and LPS compared to LPS stimulation in 21% $O_2$ (Figure 4-10 B and E). For adult MDMs, HLA-DR surface expression was also significantly upregulated upon double-hit stimulation with 65% $O_2$ and LPS, but compared to 21% $O_2$ exposure (Figure 4-10 B).

In summary, TLR4 surface expression was higher in preterm MDMs at baseline but downregulated to a similar level upon double-hit stimulation compared to term and adult MDMs. This indicates an age-dependent difference in TLR4 expression. For HLA-DR expression, a double-hit effect with 65% $O_2$ was observed.

### 4.3.5 Global transcriptional profile of macrophages

A global transcriptional pathway profile of MDMs after exposure to various $O_2$ concentrations and LPS from preterm and term infants was analyzed at 72 h using an RNA sequencing approach. This approach was used in order to address gestational age-dependent differences in the transcriptome of term and preterm MDMs, as well as potential mechanisms that may contribute to exaggerated immune responses of preterm MDMs after the double-hit with 65% $O_2$ and LPS.

Principal component analysis (PCA) was used to visualize the distribution of samples based on the 5000 most variable genes (Figure 4-11). PCA analysis revealed a clustering of samples depending on LPS stimulation (Figure 4-11, blue ovals) as well as a clustering depending on gestational age (Figure 4-11, red ovals are preterm).

To get an insight into differentially regulated pathways, first differentially expressed genes of MDMs within each condition were assessed compared to unstimulated MDMs (21% $O_2$) from both preterm and term infants. Since the $O_2$ conditions by themselves did not have a significant impact on differentially regulated pathways, only the numbers of differentially expressed genes in LPS-stimulated or double-hit-stimulated MDMs were depicted in Table 4-2. A higher number of genes were differentially regulated by LPS stimulation in MDMs from preterm infants compared to term infants with each $O_2$ condition. The highest number of differentially expressed genes was detected in the double-hit with 65% $O_2$ plus LPS in both groups.

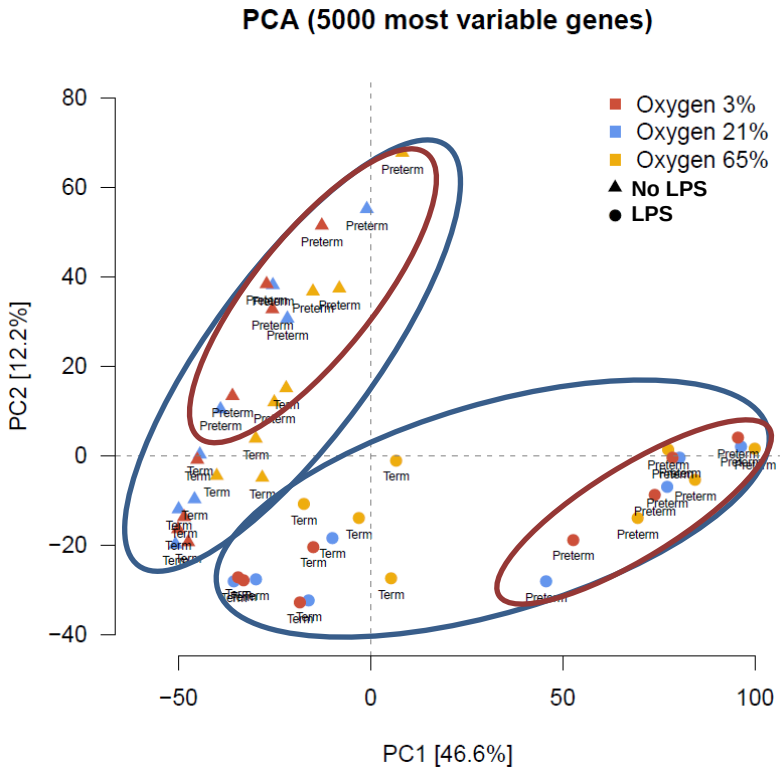


**Figure 4-11: Clustering of RNA samples from macrophages after the double-hit model at 72 h in preterm and term infants depended on LPS stimulation (blue ovals) and gestational age (red ovals: preterm).** Principal component analysis to show distribution of samples based on the 5000 most variable genes in the RNA samples of macrophages.

**Table 4-2: Number of differentially expressed genes in preterm and term macrophages at 72 h** (n=4; t-test corrected for multiple testing).

| | Preterm | | | Term | | |
|---|---|---|---|---|---|---|
| **Comparison** | **up** | **down** | **total** | **up** | **down** | **total** |
| **21% $O_2$ vs. 21% $O_2$ + LPS** | 4535 | 4553 | 9088 | 464 | 59 | 523 |
| **21% $O_2$ vs. 65% $O_2$ + LPS** | 4825 | 5054 | 9879 | 1735 | 1551 | 3286 |
| **21% $O_2$ vs. 3% $O_2$ + LPS** | 4551 | 4667 | 9218 | 531 | 140 | 671 |

Next, differential gene expression of each comparison was used to profile differentially regulated pathways based on the Reactome gene sets (provided by MSIGDB library). To visualize the pathway profiling, a heatmap was generated using the “mean of gene set”-values from the statistical analysis of LPS- and double-hit-stimulated samples. It was used for pathways that were significantly regulated compared to 21% $O_2$ in at least one condition (Figure 4-12), implicating that all significances depicted in the heatmap are comparing the presented condition to baseline MDM gene expression at 21% $O_2$. The pathway profiling revealed differentially regulated pathways in the following categories:

cell cycle/replication, transcription, translation, transport, innate immune system, apoptosis, phagosome, amyloids, and metabolism.

The first two categories, cell cycle/ replication and transcription, seemed to be upregulated in preterm MDMs for some distinct pathways in all three conditions (e.g. “Meiosis” or “RNA polymerase I”). Those pathways were not significantly regulated in term MDMs for any condition. In addition, there was an enhanced downregulation of several cell cycle/replication and transcription pathways in term MDMs after the double-hit with 65% $O_2$ compared to preterm MDMs after exposure to the same condition (Figure 4-12, cell cycle/replication and transcription category depicted in grey).

The next categories, including translation, transport, and cytokine and interferon pathways within the category of the innate immune system, showed significant regulation upon LPS stimulation for both preterm and term MDMs. That regulation was independent of gestational age or double-hit (Figure 4-12, translation, transport, cytokines and interferon signaling pathways depicted in grey). Specifically, pathways belonging to the categories translation and transport were downregulated and pathways belonging to cytokine and interferon signaling were upregulated after LPS stimulation independent of $O_2$ concentration compared to atmospheric 21% $O_2$ alone for both preterm and term MDMs (Figure 4-12, translation, transport, cytokines and interferon signaling pathways depicted in grey).

For the last categories, including interleukins and chemokines of the category innate immune system as well as apoptosis, phagosome, amyloids, and metabolism, differences in pathway regulation based on gestational age as well as double-hit were observed (Figure 4-12). Interleukin signaling (named “Signaling by ILS” depicted in black) was significantly upregulated only in preterm MDMs after LPS stimulation independent of $O_2$ concentration compared to baseline (21% $O_2$), but not in term MDMs in any condition. In addition, this pathway showed a tendency to be even more upregulated upon double-hit with 65% $O_2$ compared to LPS at 21% $O_2$ for preterm MDMs (Figure 4-12, “Signaling by ILS” in black). For the category chemokines depicted in grey, LPS-stimulated term MDMs incubated in 21% $O_2$ showed four significantly upregulated signaling pathways depicted in black, including “Class A1 rhodopsin like receptors”, “GPCR ligand binding”, “Peptide ligand binding receptors”, and “Chemokine receptors bind chemokines” compared to baseline (21% $O_2$). However, after the double-hit with 65% or 3% $O_2$ term MDMs did not significantly upregulate those pathways anymore, except for the “Peptide ligand binding receptor” pathway, which was significantly upregulated upon double-hit stimulation with 3% $O_2$ in term MDMs compared to baseline (Figure 4-12, grey category chemokines). These chemokine pathways showed a different regulation pattern in preterm MDMs. The pathway “Chemokine receptors bind chemokines” demonstrated a greater upregulation in

preterm MDMs after LPS stimulation in 21% $O_2$ compared to term MDMs in the same condition. In addition, preterm MDMs also showed a greater upregulation in the black-depicted pathways “Peptide ligand binding receptors”, and “Chemokine receptors bind chemokines”, comparing both double-hit stimulations with term MDMs (Figure 4-12, grey category chemokines). Furthermore, in preterm MDMs the pathway “Chemokine receptors bind chemokines” showed a tendency to be even more amplified in the double-hit with 65% $O_2$ compared to LPS stimulation in 21% $O_2$ (Figure 4-12, grey category chemokines). The pathways apoptosis, phagosome, amyloids, and “tricarboxylic acid (TCA) cycle and electron transport” depicted in black at the bottom of Figure 4-12 generally only showed a regulation of pathways in preterm MDMs compared to term MDMs of any condition (Figure 4-12). In preterm MDMs, upregulation of apoptosis and phagosome pathways seemed to be substantially higher in the double-hit with 3% $O_2$ compared to LPS alone or the double-hit with 65% $O_2$. The amyloid pathway showed an LPS-dependent, significant upregulation in preterm MDMs, but not term MDMs. The “TCA cycle and electron transport” pathway was significantly downregulated only upon double-hit stimulations of preterm MDMs, but not after LPS stimulation in 21% $O_2$.

In summary, the differentially expressed pathway profiling of preterm and term MDMs stimulated with the double-hit model revealed gestational age-dependent differences with regard to cell cycle, transcription, interleukin, chemokine, apoptosis, and phagosome signaling as well as amyloids and TCA/respiratory electron transport. All those pathways were upregulated in preterm MDMs except for the TCA/respiratory electron transport, which was downregulated. Evaluating the effects of double-hit exposure compared to LPS stimulation in 21% $O_2$, term MDMs showed a downregulation of cell cycle and transcription after double-hit with 65% $O_2$, which was not observed in preterm MDMs. Preterm MDMs demonstrated a downregulation in TCA/respiratory electron transport upon both double-hit stimulations compared to LPS stimulation in 21% $O_2$, which was not observed in term MDMs. In addition, chemokine (“Chemokine receptors bind chemokines”) signaling was more upregulated in preterm MDMs than in term MDMs, especially comparing the double-hit conditions between preterm and term MDMs. A tendency of enhanced interleukin (Signaling by ILS) was evident upon double-hit stimulation with 65% $O_2$ compared to LPS stimulation in 21% $O_2$ in preterm MDMs and enhanced apoptosis and phagosome signaling upon double-hit with 3% $O_2$.

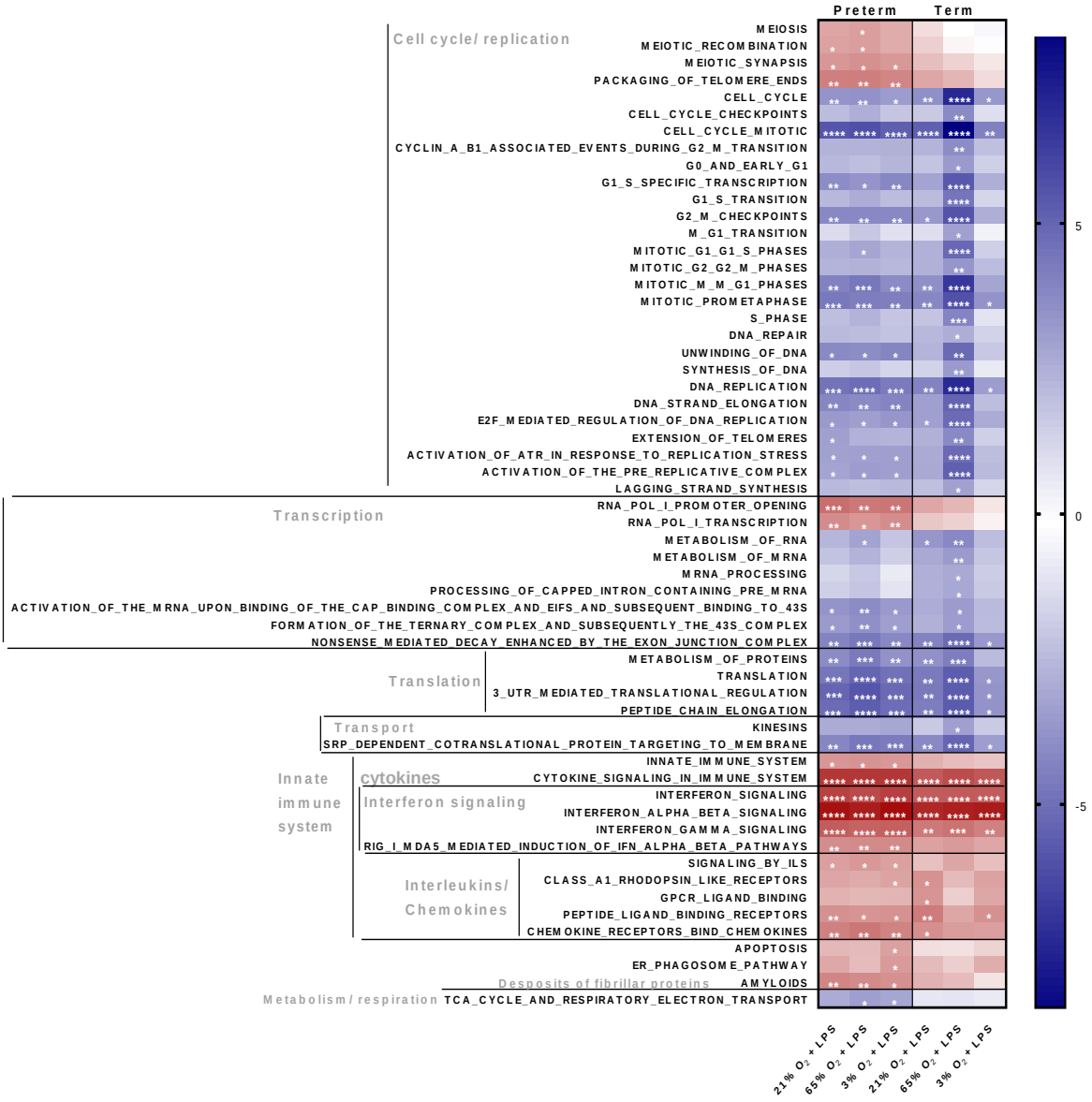


**Figure 4-12: Pathways profile of macrophages from preterm and term infants at 72 h upon double-hit based on the Reactome gene sets (provided by MSIGDB library) after input of differentially regulated genes.** The heatmap shows the "mean of gene set"-values from the statistical analysis of LPS- and double-hit stimulated samples for pathways which were significantly regulated compared to 21% $O_2$ in at least one condition. The following categories were detected: cell cycle/ replication, transcription, translation, intracellular transport, innate immune system, apoptosis, phagosome, amyloids, and metabolism. Within those categories, pathway regulation showed differences regarding gestational age as well as double-hit stimulation (n=4; "mean of gene set" test statistic within the pairwise comparisons to baseline (21% $O_2$) and p-values were corrected for multiple testing).

## 4.4 Determination of CD4 T cell polarization induced by macrophage supernatants

To investigate the effects of cytokine release from preterm, term and adult MDMs, macrophage supernatants were used to induce neonatal CD4 T cell polarization *in vitro*. CD4 T cells were isolated from term cord blood and incubated for 6 days with macrophage supernatants harvested at 72 h following the double-hit exposure, along with CD3/CD28/CD2 beads and IL-2 to support proliferation. Incubation of CD4 T cells with medium, CD3/CD28/CD2 beads and IL-2 served as a control. Expression of T cell lineage-specific transcription factor mRNA was used to evaluate T cell polarization. RORC was used as an indicator of Th17 polarization, TBX21 as an indicator of Th1 polarization, FOXP3 as an indicator of Treg polarization, and GATA3 as an indicator of Th2 polarization (Roy, Rizvi, and Awasthi 2019).

RORC mRNA expression increased upon incubation of CD4 T cells with preterm macrophage supernatants harvested at 72 h after LPS stimulation and both double-hit stimulations in an LPS-dependent manner compared to control (Figure 4-13 A), which was only significant for 21% $O_2$ or 3% $O_2$ plus LPS stimulation. A similar effect was demonstrated with CD4 T cells incubated with adult macrophage supernatant, but only upon LPS stimulation in 21% $O_2$ at 72 h. For TBX21 mRNA expression, no significant changes were detected in any group (Figure 4-13 B). However, there was a general trend of upregulated TBX21 mRNA upon incubation with supernatants from macrophages for all groups stimulated with LPS, which seemed to be even more pronounced in CD4 T cells incubated with term macrophage supernatant upon both double-hits harvested at 72 h. FOXP3 mRNA expression showed a tendency to be downregulated in CD4 T cells upon incubation with supernatants from MDMs after LPS stimulation harvested at 72 h for all groups (Figure 4-13 C). GATA3 mRNA expression showed no change in T cells compared to control for any condition in any group (data not shown).

For direct comparison of mRNA expression in CD4 T cells incubated with preterm, term and adult macrophage supernatants harvested after 72 h of LPS or double-hit stimulation, heatmaps were generated (Figure 4-14). Those heatmaps revealed a significantly lower FOXP3 mRNA expression after incubation with supernatants of preterm MDMs upon 65% $O_2$ or double-hit with 65% $O_2$ abd LPS compared to adult macrophage supernatants in the same conditions (Figure 4-14). In addition, the heatmaps demonstrated the above-described increased RORC mRNA expression upon use of LPS-stimulated preterm macrophage supernatants and increased TBX21 mRNA expression upon use of double-hit-stimulated term macrophage supernatants.

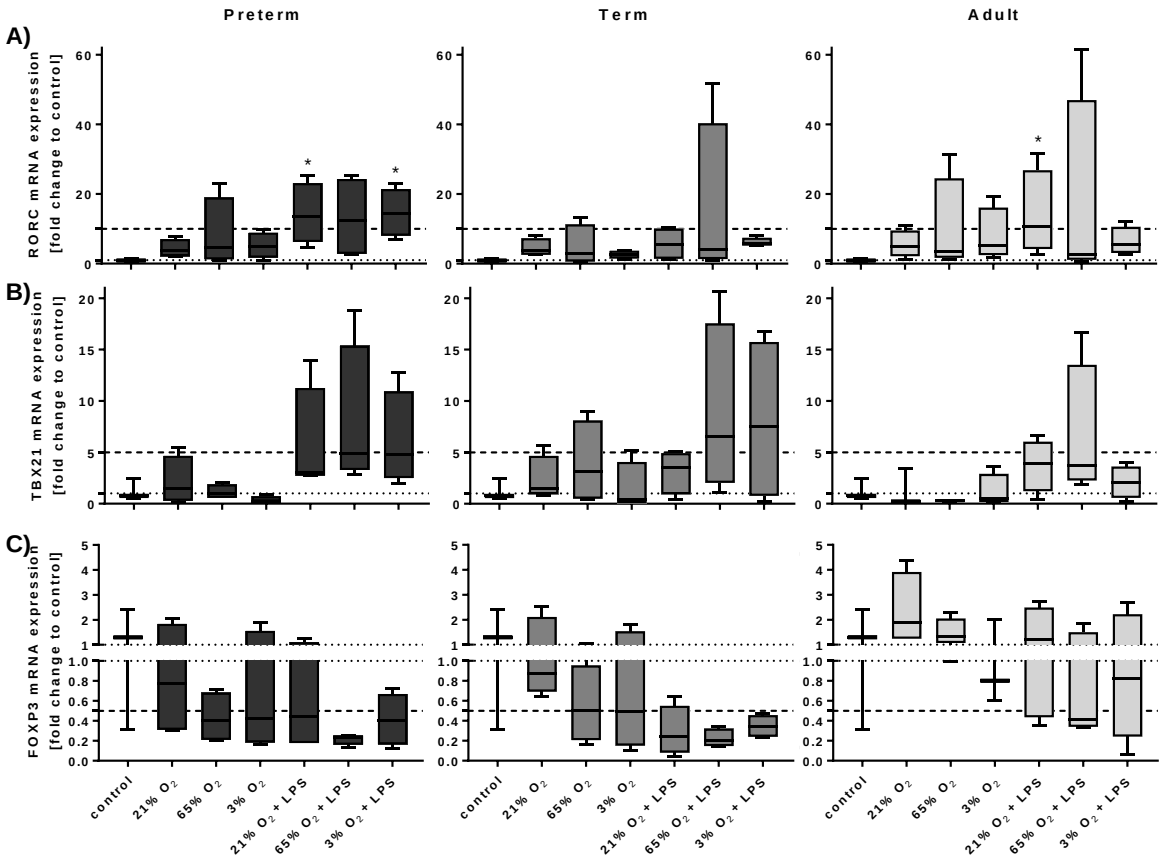


**Figure 4-13: Significantly increased RORC mRNA expression in CD4 T cells incubated with preterm macrophage supernatant upon LPS stimulation.** Box plots of RORC (A), TBX21 (B) and FOXP3 (C) mRNA expression normalized to β-Actin depicted as a fold change to the medium control. mRNA was isolated from CD4 T cells after 6 days of incubation with supernatants of preterm, term and adult macrophages upon stimulation with the double-hit model at 72 h. The dotted line at 1 indicates the normalization level and the second dotted line is an auxiliary line for comparison between plots (n=4; box plot: Friedman followed by Dunn´s multiple comparison to control).

Taken together, these findings suggest that cytokine release by MDMs from preterm infants led to a Th17-dominant polarization when those macrophages were stimulated with LPS and both double-hits, which was not detected when term and adult MDMs were stimulated with the double-hits. Furthermore, a decreased Treg polarization was demonstrated when preterm MDMs were stimulated with 65% $O_2$ and LPS compared to the same stimulation in adult MDMs.

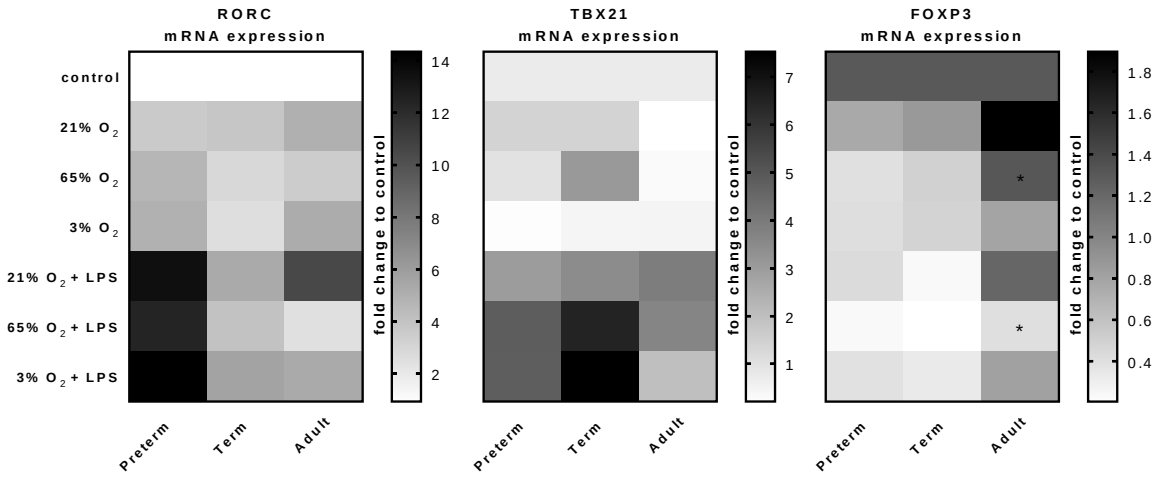


**Figure 4-14: Significantly reduced FOXP3 mRNA expression in CD4 T cells incubated with preterm macrophage supernatant upon 65% $O_2$ and double-hit with 65% $O_2$ and LPS compared to adult macrophage supernatants.** Heatmaps of RORC, TBX21 and FOXP3 mRNA expression normalized to β-Actin depicted as a fold change to the medium control. mRNA was isolated from CD4 T cells after 6 days of incubation with supernatants of preterm, term and adult macrophages upon stimulation with the double-hit model at 72 h (n=4; Heatmap: Median, Kruskal-Wallis followed by Dunn´s multiple comparison to preterm within condition).

# 5. Discussion

## 5.1 *Ex-vivo* double-hit model for lung immunity using human monocyte-derived macrophages of preterm infants – Rationale for the model

Most of the studies investigating lung diseases of preterm infants have been performed in animal models due to a limitation of available lung tissue from preterm infants (Lambert and Culley 2017). The results of this thesis are based on an *ex-vivo* double-hit model for lung immunity using primary human MDMs of preterm infants. The following paragraphs discuss the relevance of this model and its implications for BPD in preterm infants.

### 5.1.1 *Ex-vivo* model using primary human monocyte-derived macrophages of preterm infants

The use of primary human MDMs, in contrast to animal models, has the advantage of providing insight into the immune response of human cells. This is important because species-related differences in immune responses have been described, such as different MΦ responses to glucocorticoids in mice and humans (Jubb et al. 2016). Another example of those differences is the distinct arginine metabolism of MΦ that varies across species (Young et al. 2018). The arginine metabolism is an important characteristic metabolic pathway of an anti-inflammatory MΦ phenotype (Arora et al. 2018). In addition, the *ex-vivo* double-hit model used in this thesis focuses on MDMs from preterm infants, which is the primary risk group to develop BPD during the postnatal period (Data from GNN, Trembath and Laughon 2012; Tröger et al. 2014). It is already well established that the immune system of infants differs from that of adults, with a tendency towards more regulatory mechanisms that are thought to be important for microbiota development during infancy (Pettengill, van Haren, and Levy 2014; Debock and Flamand 2014; Kollmann et al. 2017). The microbiome establishment of preterm infants can be disturbed by several factors. In our recent cohort study, we demonstrated that a Bacilli-dominated gut dysbiosis is associated with a dysregulation of the immune-microbiota interplay and an increased sepsis risk (Graspeuntner et al. 2018). For several immune cell types, such as T cells and monocytes, a difference in abundance or function has also been demonstrated in preterm infants relative to term infants (Kollmann et al. 2012; de Jong et al. 2017). Monocytes of preterm infants have been reported to be deficient for cytokine production, which may contribute to the susceptibility to infections (Wisgrill et al. 2016; de Jong et al. 2017). However, there is a paucity of data investigating immune cell functions of MΦ from preterm infants. MΦ are especially important for local immune responses within tissues, such as mucosal-associated lung and gut tissues (Torow et al. 2017; Wisgrill et al. 2018).

In the context of this study, the immune responses of MΦ from preterm infants are of special interest because of their central role in BPD development, which has been demonstrated in several animal models (Vozzelli et al. 2004; Johnson et al. 2009; Velten et al. 2010; Blackwell et al. 2011; Syed and Bhandari 2013; Drummond et al. 2015; Arora et al. 2018). Therefore, primary monocytes from preterm infants have been isolated and differentiated to macrophages using M-CSF, which induces a macrophage phenotype after *in vitro* differentiation of adult and term monocytes (Pixley and Stanley 2004; Gleissner 2012; Wisgrill et al. 2016). A comparable MΦ phenotype of preterm infants after monocyte differentiation with M-CSF has been demonstrated to term and adult MDMs with regard to morphology (Figure 4-1), viability (Figure 4-2) and the phenotypic markers CD14, CD68, and CD11b (Figure 4-3, Aggarwal, King, and D'Alessio 2014). Those results suggest that MDMs from preterm infants have been responsive to M-CSF, generating a similar MΦ phenotype as monocytes from term infants and adults. MDMs of preterm infants provide a useful model to study immune responses related to lung immunity due to their tissue-specific abundance (Dos Santos et al. 2013). However, it needs to be considered that this model cannot account for environmental factors in the context of lung tissue *in vivo*, which might influence important MΦ responses. To interpret results presented in this thesis, it should also be noted that monocytes of infants have been obtained from umbilical cord blood, which provides sufficient sample material from highly vulnerable infants. There is, however, a mild risk for contamination with maternal blood during clinical sampling. Future studies need to consider peripheral blood of infants and laboratory methods adjusted to use minimal-volume samples.
Despite these limitations, primary MDMs of preterm infants provide a useful *ex-vivo* model for studying immune responses in a context that is relevant to highly vulnerable infants.

### 5.1.2 Double-hit model with key lung exposure factors - oxygen and infection

BPD is a multifactorial disease. The main risk factors, which also shape the pulmonary immune response, are supplemental $O_2$, respiratory support such as mechanical ventilation due to RDS, infection, and nutritional deficits (Trembath and Laughon 2012; Niedermaier and Hilgendorff 2015). Animal models suggest that type, frequency and intensity of an insult can influence the immune response in BPD development, which seems to be stronger with increasing intensity and frequency of different insults (Jobe 2011, 2012; Buczynski, Maduekwe, and O'Reilly 2013; Nold et al. 2013). The double-hit model used in this thesis has mimicked two of the before mentioned key lung exposure factors, which are often encountered by preterm infants in the first weeks of life.

(Trembath and Laughon 2012; Niedermaier and Hilgendorff 2015). Oxygen toxicity due to supplemental $O_2$ has been modeled by exposure of preterm MΦ to 65% $O_2$. Alternatively, preterm MΦ have been exposed to 3% $O_2$ to mimic hypoxic episodes of infants caused by RDS. Nrf2 upregulation upon 65% $O_2$ exposure and HIF-1α upregulation upon 3% $O_2$ exposure has verified $O_2$ sensing of MΦ in those experiments (Figure 4-4). However, it needs to be taken into account that those $O_2$ concentrations can differ in a clinical setting. For instance, infants are often exposed to intermittent $O_2$ depending on their condition. Subsequently, preterm MΦ have been stimulated with LPS to model a gram-negative infection. LPS stimulation has been useful for verification and comparision of obtained data because of its frequent use to stimulate MΦ *in vitro*. However, pathogens causing sepsis in infants are often Gram-positive, e.g. Coagulase-negative staphylococci (Tröger et al. 2014). Hence, future studies should also focus on different infectious stimuli in this model, e.g. toll-like receptor agonists or heat-inactivated bacteria. The double-hit challenge of MΦ has led to a phenotype characterized by upregulation of CD80 and downregulation of CD200R in preterm and term infants and adults, which has occurred mainly after LPS stimulation independently of $O_2$ condition (Figure 4-5). A comparable pro-inflammatory phenotype of adult MΦ has been described after M-CSF differentiation and LPS stimulation (Jaguin et al. 2013), suggesting that in the used settings the double-hit stimulation revealed a pro-inflammatory phenotype in MDMs of all different age groups. In summary, the *ex-vivo* double-hit model for lung immunity using MDMs reflects human-specific immune responses in highly vulnerable infants, which are particularly related to the multifactorial BPD development. In addition, the pro-inflammatory MΦ phenotype after using the double-hit model is consistent with the MΦ phenotype that has been shown to contribute to lung injury in animal models (Jankov et al. 2001; Kalymbetova et al. 2018)

## 5.2 Sustained pro-inflammatory responses in preterm macrophages

Infants have a distinct immune system that differs from that of adults. It is characterized by a general hypo-responsiveness, more immunoregulatory factors, and a bias towards Th2 and Th17 responses (for more detail see 1.2.2; Levy et al. 2006; Debock and Flamand 2014; Pettengill, van Haren, and Levy 2014; Kollmann et al. 2012; Pagel et al. 2016). In addition, a gestational age-dependent difference in immune cell function has been reported, including differences in monocyte cytokine production relative to term infants (de Jong et al. 2017). In the context of BPD development in preterm infants, MΦ are likely to play a key role in the immature lung immunity of preterm infants because they maintain the balance between an appropriate inflammatory response to harmful insults and continued tissue remodeling and maintenance of homeostasis during lung development.

(Blackwell et al. 2011; Loering et al. 2019). In addition, lung injury leads to recruitment of MDMs (Jankov et al. 2001; Velten et al. 2010). In the absence of solid data on MDM characteristics in preterm infants, the aim has been to investigate gestational age-dependent differences between immune responses of human MΦ from preterm and term infants compared to adults using the *ex-vivo* double-hit model for lung immunity.

### 5.2.1 Sustained cytokine release in preterm macrophages, partially due to increased basal TLR4 surface expression

Cytokine release for activation and recruitment of other cells is one of the major immunological functions of MΦ (Turner et al. 2014). In this thesis, cytokine release by preterm MDMs has been determined after different stimulations. Although the release of TNFα, IL-6, IL-1β, IL-23, IL-10 and CXCL10 has been comparable to term and adult MDMs at an early 52 h time point, all cytokine levels have been sustained and further upregulated only in preterm MDMs at a later 72 h time point after stimulation (Figure 4-6, Figure 4-7, Figure 4-8, Figure 4-9). This result suggests a dysregulated sustained pro-inflammatory cytokine release by preterm MDMs. In another study, term MDMs have been shown to secrete similar levels of TNFα, IL-1, IL-6 and IL-10 after LPS stimulation as adult MDMs (Wisgrill et al. 2018), which is comparable to the results of this thesis. Mononuclear cells from term infants have shown a distinct pattern of cytokine production with moderately less TNF-α, but as much or even more IL-1β, IL-6, IL-23, and IL-10 compared to adult cells after LPS stimulation (Kollmann et al. 2009; Corbett et al. 2010; Nguyen et al. 2010). However, in preterm peripheral blood mononuclear cells, monocytes and lymphocytes, less production of cytokines such as TNFα, IL-6 and IL-10 has been shown after LPS stimulation compared to term infants (Härtel et al. 2005; Schultz et al. 2007; Härtel et al. 2008; Wisgrill et al. 2016; de Jong et al. 2017). In addition, production of TNFα, IL-6 and IL-10 has been shown to positively correlate with gestational age (Härtel et al. 2005; Härtel et al. 2008; Strunk et al. 2012). Those results have been determined in whole blood or using mononuclear cells isolated from cord blood, which are known to include inhibitory factors such as adenosine or Tregs (Pettengill, van Haren, and Levy 2014; Pagel et al. 2016). Nevertheless, purified preterm monocytes have also shown a decreased TNFα, IL-6 and IL-1β secretion and similar IL-10 secretion after LPS stimulation compared to monocytes from term infants (Shen et al. 2013; de Jong et al. 2017). The mechanism for reduced cytokine production by monocytes from preterm infants remains unknown (de Jong et al. 2017). However, cytokine release of preterm MDMs determined in this thesis have shown an opposed effect with increased production. In addition, patterns of cytokine release by preterm MDMs, including increased TNFα,

IL-6, IL-1β, and IL-23, have been consistent with a Th17 polarization, because the combination of those cytokines together with TGFβ (not analyzed in this thesis) have been shown to induce a Th17 phenotype in neonatal but not adult naïve T cells (Korn et al. 2009; Black et al. 2012). This is supported by a general Th17 bias in preterm infants (Kollmann et al. 2012). In particular, IL-23 is important for Th17 maintenance and expansion when there is a lack of IL-12 (McKenzie, Kastelein, and Cua 2006), which has also been obvious for preterm MDM characteristics in the used setting.

Initial upregulation of IL-10 release upon LPS stimulation has been comparable in preterm, term and adult MDMs. After LPS stimulation other studies have seen IL-10 upregulation in mononuclear blood cells and MDMs of term infants, likely serving as an immunoregulatory mechanism (Kollmann et al. 2009; Wisgrill et al. 2018). However, preterm MDMs have shown a 10-fold higher upregulation of IL-10 release at the late 72 h time point upon LPS stimulation compared to term and adult MDMs (Figure 4-6, Figure 4-8). Higher IL-10 levels have been shown by others to be produced after LPS stimulation of whole blood from preterm infants, with a decline over the first year of life (Kollmann et al. 2012). One possible reason for upregulated IL-10 is the sustained upregulation of pro-inflammatory cytokines in preterm MDMs described above, which as a consequence may stimulate further upregulation of regulatory IL-10 to prevent injury due to pro-inflammatory mediators (Rojas et al. 2017). IL-10 is also involved in different inflammatory immune processes. It regulates B cell survival and differentiation, and favors B cell effector function by stimulating plasma cell differentiation in viral infections (Rojas et al. 2017). In the presence of M-CSF, IL-10 may also contribute to inflammatory processes by facilitating monocyte differentiation into TNFα-responsive macrophages via the upregulation of TNF receptor on the cell surface, resulting in enhanced production of IL-6 and IL-1β (Takasugi et al. 2006).

MΦ phenotypes are generally classified into pro- and anti-inflammatory phenotypes with a high plasticity to switch between phenotypes depending on their environment (Mosser and Edwards 2008). In this classical MΦ phenotyping, IL-10 production is exclusive to the context of anti-inflammatory MΦ (Biswas and Mantovani 2010). However, there exists a concept of a switched MΦ phenotype, which may respond to pro-inflammatory stimuli with reprogramming towards the anti-inflammatory MΦ phenotype or respond to anti-inflammatory stimuli with reprogramming towards the pro-inflammatory MΦ phenotype. This switched MΦ phenotype has been associated with lung diseases in adults (Malyshev and Malyshev 2015). Assuming a dysregulated pro-inflammatory preterm MΦ phenotype upon stimulation as discribed above, it may be that preterm MΦ respond in a pro-inflammatory manner to IL-10 comparable to the switched phenotype. Future studies to further define preterm MDM response to IL-10 will assist in addressing that possibility.

In order to define an underlying mechanism for the upregulated sustained cytokine release in preterm MDMs, TLR4 surface expression has been analyzed. Increased basal TLR4 surface expression has been detected on preterm MDMs compared to adult MDMs (Figure 4-10). This result might at least in part explain the sustained and further upregulated cytokine release of preterm MDMs compared to term and adult MDMs upon LPS stimulation. Other studies have analyzed cytokine production and TLR4 expression in preterm monocytes. Levels of cytokine production by monocytes have positively correlated with gestational age, as has TLR4 expression (Shen et al. 2013; Wisgrill et al. 2016). Those correlations suggest that TLR4 might contribute to detected cytokine levels in monocytes of preterm infants. Although preterm MDMs have shown increased basal TLR4 and sustained cytokine production as opposed to preterm monocytes, it seems that TLR4 is part of the mechanism for produced cytokine amounts.

### 5.2.2 Global transcriptome pathway profile points to a more activated macrophage phenotype in preterm infants

Transcriptome analysis can identify global changes within a cell population on an mRNA level. Transcriptome studies using whole blood, leukocytes, and neutrophils from term infants have confirmed the general concept of an attenuated immune response compared to older children or adults (Wynn et al. 2011; Mathias et al. 2017). Comparing the leukocyte transcriptome of term infants to older children or those of neonatal to adult mice has revealed an attenuation of their inflammatory response upon sepsis onset, exhibiting less cell recruitment and less production of ROS and cytokines (Wynn et al. 2011; Gentile et al. 2014). Compared to adult neutrophils, term neutrophils have failed to effectively upregulate genes associated with activation, phagocytosis, and chemotaxis in response to LPS stimulation (Mathias et al. 2017). Furthermore, preterm leukocytes and neutrophils have been characterized by significantly downregulated cytokine- and chemokine-related pathways, reduced pathogen recognition, and antimicrobial activity compared to leukocytes and neutrophils from term born infants (Kwinta et al. 2017; Raymond et al. 2017). The investigation of mononuclear cells from cord blood of term infants has demonstrated a more diverse and robust expression of genes encoding pro-inflammatory cytokines, chemokines and growth factors compared to neutrophils (Davidson et al. 2013). However, there are conflicting results on a transcriptome level comparing preterm and term monocytes. Jong *et al.* have demonstrated comparable transcriptome profiles after stimulation, whereas Kan *et al.* have reported a remarkable downregulation of metabolic genes belonging to OXPHOS and glycolytic pathways. The latter has pointed towards a downregulated immune response, which has been consistent with reduced cytokine

release of preterm monocytes compared to term monocytes (de Jong et al. 2018; Kan et al. 2018).

MΦ are less well studied on a transcriptome level. Neonatal murine MΦ have exhibited increased activity of pro-inflammatory pathways at baseline compared to adult MΦ (Winterberg et al. 2015). In the experiments decribed in this thesis, preterm MDMs have also demonstrated upregulated innate immune pathways, such as interleukin and chemokine pathways, after 72 h of stimulation compared to term MDMs (Figure 4-12, interleukins and chemokines depicted in grey). This result has been consistent with increased cytokine and chemokine release in preterm MDMs compared to term and adult MDMs (see 5.2.1, Figure 4-6, Figure 4-9). In addition, cell cycle activation and upregulated transcription has been detected on a gene expression level in preterm MDMs. Those results suggest a more activated MΦ phenotype upon stimulation compared to term MDMs (Figure 4-12). Furthermore, the TCA/respiratory electron transport pathway has been downregulated in preterm MDMs compared to term MDMs. This supports the notion of an activated phenotype even more, because downregulation of these pathways indicates a switch in energy metabolism from OXPHOS to glycolysis, which has been described for pro-inflammatory MΦ (Mills and O'Neill 2016; O'Neill, Kishton, and Rathmell 2016). In summary, transcriptome pathway profiling of preterm MDMs has confirmed a pro-inflammatory and generally more activated MΦ phenotype upon stimulation compared to term MDMs. This MΦ phenotype has also been found in the lung upon activation (Hussell and Bell 2014; Aggarwal, King, and D'Alessio 2014).

### 5.2.3 Polarization towards pro-inflammatory Th17 response by released cytokines from preterm macrophages

The cytokine composition released by preterm MDMs in the experiments described above has been consistent with a Th17 rather than a Th1 polarization due to increased IL-23 release and no detection of IL-12 (McKenzie, Kastelein, and Cua 2006). This is supported by the concept that infants are distinct in their immune response, which has been characterized by a bias towards Th17 function (Kollmann et al. 2012). In general, MΦ are one of the main sources for IL-23, which is released due to a strong inflammatory insult. IL-23 rapidly activates resident immune cells, who recruit neutrophils (McKenzie, Kastelein, and Cua 2006; Mosser and Edwards 2008). IL-23 is also important for maintenance and expansion of Th17 cells, which provide an essential immune defense at mucosal surfaces, especially against intracellular pathogens (Bystrom et al. 2018; Y. Li et al. 2018). In addition, IL-23, in combination with other cytokines released by MΦ, can activate naïve T cells and influence Th17 polarization (McKenzie, Kastelein, and Cua

2006; Mosser and Edwards 2008). Th17 cells have been associated with chronic inflammatory diseases such as severe asthma (McKenzie, Kastelein, and Cua 2006; Mosser and Edwards 2008; Manni, Robinson, and Alcorn 2014). In adult mouse models of acute lung injury, pro-inflammatory MΦ in the lung have induced a Th17 phenotype that has resulted in tissue damage and neutrophil infiltration (Nagato et al. 2015; Tu et al. 2017). Increased Th17 abundance has also been associated with respiratory viral infection of newborn infants (Stoppelenburg et al. 2014) and intra-amniotic infection (Rito et al. 2017). However, the role of Th17 cells in those infections is not clear. Monocytes of preterm infants, who developed necrotizing enterocolitis, have been shown to preferentially support Th17 polarization as opposed to Treg polarization (Pang et al. 2018). In a mouse model of necrotizing enterocolitis, Th17 cells have been shown to be required for gut pathology (Egan et al. 2015). In another neonatal mouse model, systemic inflammation leading to lung injury has also been mediated by Th17 cells in the lung (Jia et al. 2018). Those studies further suggest the importance of Th17 cells in infants` immune responses with an emphasis on infections at mucosal surfaces. In the experiments described in this thesis, supernatants of preterm MDMs have increased the polarization of naïve neonatal T cells towards Th17 in an LPS-dependent manner, which has not been detected using supernatants of term MDMs (Figure 4-13).

The results from the experiments suggest that dysregulated and more activated pro-inflammatory MΦ of preterm infants mediate a pro-inflammatory environment by Th17 polarization, potentially enhancing pro-inflammatory tissue injury, which has not been the case with term or adult MDMs.

## 5.3 Exaggerated pro-inflammatory immune responses of preterm macrophages after double-hit with key lung exposure factors

Preterm infants are highly susceptible to sustained lung inflammation, which can be triggered by exposure to supplemental $O_2$ and infections (Ryan, Ahmed, and Lakshminrusimha 2008; Trembath and Laughon 2012). Sustained lung inflammation can lead to lung developmental arrest characterized by reduced alveolarization and vascularization (Niedermaier and Hilgendorff 2015). To understand the underlying mechanisms, an *ex-vivo* double-hit model for lung immunity using human MDMs of preterm infants has been developed to characterize effects of key lung exposure factors on MΦ function.

### 5.3.1 Cytokine release is exaggerated and HLA-DR surface expression is upregulated in preterm macrophages after challenge with key lung exposure factors

For preterm infants, supplemental $O_2$ has been the first described exposure factor leading to severe lung injury and subsequent BPD (Northway Jr, Rosan, and Porter 1967). More recently, epidemiological studies have described BPD as a multifactorial disease (Trembath and Laughon 2012; Klinger et al. 2013; Tröger et al. 2014, data from GNN). Due to their prematurity, preterm infants are often exposed to more than one risk factor for BPD in the first weeks of life. Most animal models of BPD have investigated lung injury after increased $O_2$ concentrations or after administration of antenatal LPS as the only challenge (Bonikos et al. 1975; Randell, Mercer, and Young 1990; Warner et al. 1998; Kramer, Kallapur, Moss, et al. 2009; Weichelt et al. 2013; Drummond et al. 2015; Jobe 2015). However, other studies have suggested that the type and frequency of exposure factors shape lung immunity differently as compared to only one challenge, which has a central role for multifactorial diseases such as BPD development. In those studies, neonatal animals have been exposed to a combination of sequential challenges such as intra-amniotic LPS and increased $O_2$ or increased $O_2$ followed by infection (Velten et al. 2010; Nold et al. 2013; Syed and Bhandari 2013; Cui et al. 2016). The results of those studies have demonstrated an exaggerated immune response in the lungs, in terms of cytokine and chemokine release and increased MΦ influx and activation, with a more severe BPD phenotype after the double-hit (Velten et al. 2010; Nold et al. 2013; Syed and Bhandari 2013; Cui et al. 2016). In the experiments described in this thesis, MDMs of preterm infants have released increased amounts of pro-inflammatory cytokines (TNFα, IL-6, and IL-1β) after the double-hit with 65% O2 and subsequent LPS challenge compared to LPS stimulation alone (Figure 4-6, Figure 4-8). TNFα, IL-6, and IL-1β have also been described to be upregulated in blood, bronchoalveolar lavage fluids, and tracheal aspirates of infants who subsequently developed BPD, and in lungs of neonatal animals exposed to increased $O_2$ (Kotecha et al. 1996; Jonsson et al. 1997; Patterson et al. 1998; Ambalavanan et al. 2009; Deng, Mason, and Auten 2000; Choo-Wing et al. 2007; Johnson et al. 2009; Nold et al. 2013). Exaggerated cytokine release by preterm MDMs suggests a central role of MΦ to mediate lung injury in preterm infants developing BPD.

IL-10, generally described as a regulatory cytokine, has previously been reported to be downregulated in tracheal aspirates and upregulated in blood of preterm infants, who develop BPD (Ambalavanan et al. 2009; V. Bhandari 2010). In this thesis, preterm MDMs have shown a downregulation of IL-10 after a double-hit with 65% $O_2$ and LPS at an early

52 h time point compared to LPS stimulation at 21% $O_2$. This result supports the theory of an imbalanced exaggerated pro-inflammatory immune response after stimulation with key lung exposure factors (Figure 4-6). The IL-10 release by preterm MDMs has been similar in adult and term MDMs at the early time point. However, preterm MDMs have increased the IL-10 release 10-fold compared to adult and term MDMs at the late 72 h time point in an LPS-dependent manner. As discussed above (5.2.1), the function of increased IL-10 release by preterm MDMs in this context remains to be investigated in the future.

In addition to cytokine release, the antigen presentation for priming and activating T cells is an important MΦ-mediated function (Ettensohn, Duncan, and Jankowski 1989; Arnold et al. 2015). Lymphocyte responses in the context of BPD are not well characterized. Two studies have found decreased T cell frequencies in cord blood of preterm infants who subsequently developed BPD. An explanation for this result might be the recruitment of lymphocytes from the blood stream to the lung in BPD patients (Turunen et al. 2009; Misra et al. 2015). In the experiments of this thesis, preterm MDMs have shown increased surface expression of HLA-DR, an MHC class II cell surface receptor to prime T cells, after double-hit challenge with 65% $O_2$ and LPS compared to LPS stimulation alone (Figure 4-10). This result indicates an enhanced capacity for T cell priming upon challenge with key lung exposure factors. Other studies have shown that MDMs have the capacity to drive T cell polarization, in particular Th17 polarization (Ettensohn, Duncan, and Jankowski 1989; Arnold et al. 2015).

In summary, sequential challenge of preterm MDMs with the key lung exposure factors of 65% $O_2$ and then LPS has led to an exaggerated immune response with enhanced T cell priming capacity compared to LPS challenge at 21% $O_2$. Those results indicate an excessive inflammatory environment in the lung of preterm infants after key lung exposure factors and a potential role for increased lymphocyte responses adding to the inflammatory conditions.

### 5.3.2 Global transcriptome pathway profile suggests an enhanced immune cell recruitment and more activated phenotype of preterm macrophages after challenge with key lung exposure factors

There is a very limited number of studies investigating the transcriptome of immune cells or lung tissue in the context of neonatal lung diseases. Mei *et al*. have analyzed the transcriptome of term infants with and without RDS in peripheral blood. In that analysis, three groups of differentially regulated genes have been identified in the blood of term infants with RDS: cellular processes, innate immune response, and pathogen recognition response (Mei et al. 2018). The majority of differentially regulated pathways in those

groups have been associated with immunological mechanisms and pathogen recognition via antigen presentation (Exemplary differentially regulated pathways: tumor necrosis factor (TNF) signaling pathway, influenza A pathway, and *Staphylococcus aureus* infection) (Mei et al. 2018). Those results have confirmed the importance of the immunological response in neonatal lung diseases, although the sample size of that study was very small (n=4 RDS infants and n=2 control infants) (Mei et al. 2018). Another global transcriptome study has been performed in a preterm rabbit model after 7 days of 95% $O_2$ exposure (Salaets et al. 2015). Dysregulation of inflammation, lung development, vascular development and ROS metabolism pathways have been identified in lung tissue upon increased $O_2$ exposure (Salaets et al. 2015). In addition, networks of interconnecting pathways have demonstrated the interaction of immunity and development of the lung (Salaets et al. 2015). In this thesis, the analysis of global transcriptome pathway profiles of preterm MDMs using the double-hit model has also identified upregulation of innate immune pathways, especially chemokine signaling, which has been upregulated upon 65% $O_2$ exposure and LPS (Figure 4-12). This upregulation correlates with data from other studies, which have shown inceased chemokine production in tracheal aspirates of infants developing BPD (Baier et al. 2004) and in the lungs of neonatal animals exposed to increased $O_2$ (Vozzelli et al. 2004; Weichelt et al. 2013; Nold et al. 2013). In lungs of neonatal animals exposed to increased $O_2$, chemokines have led to immune cell recruitment from the blood, contributing to lung injury and developmental arrest of the lung in animal models (Auten et al. 2001; Jankov et al. 2001; Weichelt et al. 2013). That effect has been exaggerated after multiple challenges with LPS and increased $O_2$ (Nold et al. 2013).

In addition, pathway profiling done in this thesis has revealed an upregulation of cell cycle activation in preterm MDMs upon 65% $O_2$ exposure and LPS compared to term MDMs after the double-hit with 65% $O_2$ (Figure 4-12). This supports the notion of a more activated preterm MΦ phenotype after multiple challenges. Furthermore, the TCA/respiratory electron transport pathway has been downregulated in preterm MDMs after the double-hits compared to LPS alone. This indicates a switch in the energy metabolism from OXPHOS toward glycolysis, which is associated with a pro-inflammatory MΦ phenotype (Mills and O'Neill 2016; O'Neill, Kishton, and Rathmell 2016). Ratner *et al.* has also demonstarted that reduced OXPHOS in neonatal mice exposed to increased $O_2$ induces an arrest of alveolar development (Ratner et al. 2009).

In summary, the global transcriptome pathways profile of human preterm MDMs further supports the idea of a dysregulated, pro-inflammatory activated phenotype after exposure to the double-hit with 65% $O_2$ and LPS compared to LPS challenge alone. In addition, known features of BPD, such as enhanced cell recruitment due to exaggerated

chemokine release and reduced OXPHOS, could be seen in preterm MDMs, indicating a well-suited model for further investigations.

### 5.3.3 Decreased Treg polarization by cytokines released from preterm macrophages after challenge with key lung exposure factors

The nature of lymphocyte responses in neonatal lung diseases is largely unknown. Adaptive immune responses are considered more relevant in the chronic phase of lung diseases, which are not well studied in animal models. In neonatal rabbits, there has been a lymphocytic infiltrate after chronic exposure to increased $O_2$ (Ryan, Ahmed, and Lakshminrusimha 2008). In another animal model, lung injury and subsequent lymphocyte response in the lung has been induced through systemic inflammation in neonatal mice (Jia et al. 2018). The lymphocyte response has been mediated via TLR4-dependent activation of lung epithelial cells, which has led to increased pro-inflammatory Th17 cells and a reduction of Tregs (Jia et al. 2018). The Th17/Treg imbalance has been required for the development of lung injury and has also been apparent in human lung tissue (Jia et al. 2018). Those observations may be relevant for BPD development in preterm infants, because systemic inflammation secondary to sepsis is one of the main risk factors for BPD (Trembath and Laughon 2012). In the experiments described in this thesis, preterm MDMs have preferentially increased Th17 polarization compared to term and adult MDMs (5.2.3; Figure 4-13). Furthermore, pronounced decrease of Treg polarization has been observed with preterm MDMs upon double-hit stimulation with 65% $O_2$ compared to adult MDMs exposed to the same condition (Figure 4-14). Those results indicate that cytokines released from dysregulated pro-inflammatory preterm MDMs have mediated a Th17/Treg imbalance after key lung exposure factors. The Th17/Treg imbalance has been due to an age-dependent upregulation of Th17 polarization upon any stimulation, and a combined effect of age and key lung exposure factors leading to less pronounced Treg polarization. Interestingly, Treg polarization has been decreased in preterm MDMs after exposure to the double-hit with 65% $O_2$ despite very large amounts of released IL-10. IL-10 is known to be important for the maintenance of Treg function (Rojas et al. 2017). As described above, IL-10 release of preterm MDMs might have a different function than the known anti-inflammatory effects in this context (5.2.1). Another reason for decreased Treg polarization might be the responsiveness of neonatal lymphocytes to IL-10, since reduced expression of IL-10 receptor on lymphocytes from term cord blood has been reported (Schultz et al. 2007). In addition, reduced responsiveness to IL-10 in lymphocytes could be due to increased $O_2$ exposure, such as it has been seen for IL-4 responsiveness of MΦ. *In vitro*, MΦ exposed to increased $O_2$ have enhanced their polarization towards a pro-

inflammatory phenotype upon LPS stimulation and have inhibited their polarization towards an anti-inflammatory phenotype upon IL-4 stimulation (Syed and Bhandari 2013). The mechanism to inhibit the anti-inflammatory MΦ phenotype upon IL-4 and increased $O_2$ exposure is unclear. However, this mechanism may be relevant for decrease of Treg polarization despite high amounts of IL-10 after double-hit exposure with 65% $O_2$ and LPS.

T cells are the least abundant immune cell type in the developing lung (Dos Santos et al. 2013; Torow et al. 2017), which could argue against there being relevant effects of a Th17/Treg imbalance in the preterm lung upon exposure to BPD risk factors. However, in the event of lung injury, lymphocytes are likely recruited from the blood stream to the lung. This idea is supported by two studies demonstrating a decreased T cell frequency in blood in the context of lung injury (Turunen et al. 2009; Misra et al. 2015). Another T cell source in the developing lung are Tregs, which can be detected in substantial numbers (Thome et al. 2016). The MΦ-mediated Th17/Treg imbalance after key lung exposure factors described above could also result from high Treg numbers, which are characteristic for the developing lung and have a high plasticity towards a Th17 phenotype depending on the cytokine environment (Omenetti and Pizarro 2015). Rito *et al.* have also shown an association between exposure of preterm infants to intra-amniotic infection and elevated cord blood frequencies of IL-17+ Treg cells (Rito et al. 2017), although IL-17 is the main effector cytokine of Th17 cells (Omenetti and Pizarro 2015). In an LPS-induced intra-amniotic infection model using fetal rhesus macaques, Th17 cytokines have predominantly been expressed by FoxP3+CD4+ T cells and not by their FoxP3− counterparts. Bi-functional IL17+FoxP3+ T cells have exhibited a phenotype of inflammatory RORc+ Treg compared to typical FoxP3+ T cells (Rueda et al. 2016). Therefore, the two most likely sources of lymphocyte responses in preterm infants developing BPD are recruitment of naïve T cells from the blood and repolarization of Tregs at the mucosal lung surface in the developing lung. Those possibilities need to be analyzed in suitable animal models in the future.

This thesis is the first study to associate exaggerated pro-inflammatory MΦ responses with a Th17/Treg imbalance in preterm infants after key lung exposure factors. This discovery has the potential to identify new treatment options for preterm infants who develop BPD, since targeting the Th17/Treg axis is already recognized as a treatment option for inflammatory-mediated diseases in adults (Fasching et al. 2017). Various novel candidate molecules to beneficially re-shape the Th17/Treg imbalance have recently shown promising results in animal models (Fasching et al. 2017).

## 5.4 Conclusion

BPD development in preterm infants leads to substantial long-term problems and a reduced quality of life. The central goal of this thesis is to contribute to new insights into mechanisms of effector cells that mediate sustained pulmonary inflammation leading to BPD development. An *ex-vivo* double-hit model for lung immunity has been developed in which responses of primary MDMs from preterm infants have been compared to term infants and adults following exposure to relevant stimuli in a sequential manner.

MDMs of preterm infants have shown gestational age-dependent differences in immune responses compared to term infants and adults after different stimulations. Those changes have been characterized by a dysregulated and sustained pro-inflammatory cytokine release, upregulated chemokine signaling and cell cycle activation, and downregulated TCA/respiratory electron transport signaling on a transcriptome level. In addition, supernatants of preterm MDMs have shown a predominant Th17 polarization upon LPS stimulation independently of $O_2$ concentration compared to term and adult MDMs. Especially after the double-hits, term MDMs have shown a predominant Th1 polarization. These data suggest that dysregulated and increasingly activated pro-inflammatory MDMs in preterm infants mediate a sustained pro-inflammatory environment with distinct cytokine and chemokine release. The pro-inflammatory environment leads to a Th17 polarization of CD4 T cells, potentially enhancing tissue injury in a manner that is distinct from term and adult MDMs. Enhanced basal TLR4 surface expression on preterm MDMs may at least in part explain the sustained cytokine release compared to term and adult MDMs (Summary of results “Preterm *vs.* term”: Table 5-1).

Furthermore, exposure of preterm MDMs to a double-hit using 65% $O_2$ and subsequent LPS stimulation have revealed an exaggerated immune response compared to LPS stimulation alone. After the double-hit, preterm MDMs have enhanced cytokine release, chemokine signaling and cell cycle activation even further, and reduced TCA/respiratory electron transport signaling more compared to LPS stimulation alone. Moreover, HLA-DR surface expression on preterm MDMs has been upregulated after a double-hit with 65% $O_2$ and LPS compared to LPS challenge alone, and supernatants of preterm MDMs have mediated a decreased Treg polarization upon double-hit stimulation with 65% $O_2$ compared to adult MDMs (Summary of results “65% double-hit *vs*. LPS”: Table 5-1). Hence, sequential challenge of preterm MDMs with 65% $O_2$ and LPS has enhanced the dysregulated, and increasingly activated pro-inflammatory MDM phenotype due to gestational age-dependent differences. That phenotype has been characterized by an exaggerated immune response with enhanced T cell priming capacity. In addition, decreased Treg polarization by released cytokines from preterm MDMs after double-hit

with 65% $O_2$, in conjunction with enhanced Th17 polarization described as a gestational age-dependent effect, suggests a Th17/ Treg imbalance. This imbalance has been mediated by preterm MDMs after key lung exposure factors, and has not been detected in term and adult MDMs.

**Table 5-1: Summary of differences in the immune response of macrophages after stimulation with LPS alone and the double hit with 65% $O_2$.** The column "Preterm versus term" macrophages shows changes in the investigated parameters upon any stimulation used in this thesis. The column "65% double-hit versus LPS" illustrates the differences of preterm macrophages between those stimulations (+: upregulated; ++: further upregulated; =: unchanged in compared groups/conditions; - downregulated; --: further downregulated; *:Comparison at basline (21%O2), not at stimulated conditions; **: Comparison within 65% double-hit condition between the groups adult and preterm macrophages, not between the conditions 65% double-hit and LPS).

| | **Stimulated MΦ** | **Preterm MΦ** |
|---|---|---|
| Compared groups | Preterm *vs*. term | 65% double-hit *vs*. LPS |
| **Cell cycle signaling** | **+** | **++** |
| **Interleukin signaling & release** | **+** | **++** |
| **Chemokine signaling & release** | **+** | **++** |
| **TLR4 surface expression** | **+*** | **=** |
| **HLA-DR surface expression** | **=** | **+** |
| **Th17 polarization** | **+** | **=** |
| **Treg polarization** | **=** | **-**** |
| **TCA+ETC signaling** | **-** | **--** |

This is the first study describing immune responses of MDMs from preterm infants. The combined effect of both gestational age-dependent differences and double-hit stimulation with increased $O_2$ seems to drive the exaggerated chronic inflammation mediated by preterm MΦ leading to a Th17/Treg dysbalance (Figure 5-1). The pro-inflammatory, and more activated MΦ phenotype in preterm infants, leading to enhanced cytokine and chemokine release described in this study, is consistent with the immune response described *in vivo* in the lungs of different animal models after exposure to increased $O_2$. The new aspect of a Th17/Treg imbalance that is described in this thesis might substantially contribute to ongoing inflammation in the lung, potentially indicating a novel therapeutic target for patients with BPD.

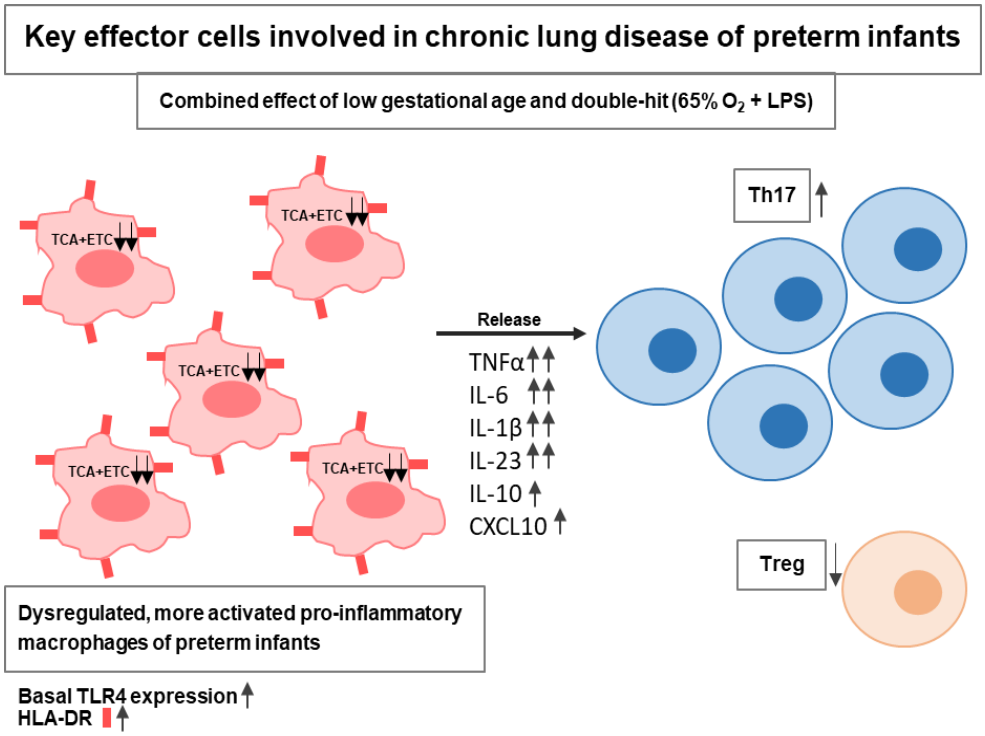


**Figure 5-1: Key effector cells and their immune response potentially involved in chronic lung disease of preterm infants.** This illustration summarizes the combined effects of low gestational age and multiple challenges with key lung exposure factors (65% $O_2$ and LPS) mediated by macrophages from preterm infants that were discovered in this study. Abbreviations: lipopolysaccharide (LPS); tricarboxylic acid cycle and electron transport (TCA+ETC); Toll-like receptor 4 (TLR4); human leukocyte antigen - DR isotype (HLA-DR); tumor necrosis factor α (TNFα); interleukin (IL); chemokine (C-X-C motif) ligand 10 (CXCL10), T helper cell (Th); regulatory T cell (Treg).

## 5.5 Outlook

Dysregulated human preterm MΦ responses lead to exaggerated inflammation, inducing a Th17/Treg imbalance due to age-dependent differences and key lung exposure factors. In this study, dysregulated MΦ responses have been confirmed in human preterm MDMs, and a Th17/Treg dysbalance has been associated for the first time with BPD development.

One major goal in the future is to discover the mechanism driving the dysregulated, more activated MΦ phenotype of preterm infants, which has great potential to identify a candidate predictive biomarker or targeted treatment for BPD. For that purpose, transcriptome data from MDMs of term and preterm infants after the double-hit with key lung exposure factors could reveal mechanistic differences by identifying key regulators

and activity of genes in order to build an interactive model for BPD development. Changes in the metabolism have already indicated to play a crucial role after challenge with key lung exposure factors by the pathway profiling of preterm MDMs, which have not been seen in term MDMs. In addition, a comparison of transcriptome data from term and preterm MDMs over time could reveal a regulatory mechanism or lack of such a mechanism, resulting in sustained cytokine release in preterm MDMs, but not in term MDMs, at a late time point.

The Th17/Treg imbalance should also be a focus of future research, because those effector cells have been shown to drive many inflammatory diseases, especially at mucosal surfaces, and have the potential for new therapeutic strategies. Animal models should be the first approach to confirm and further characterize the Th17/Treg imbalance in a double-hit model for BPD development. Moreover, efforts should be made to restore the balance of pro- and anti-inflammation by comparing different treatment strategies. Possible treatment candidates are IL-17 antibodies to neutralize the main effector cytokine of Th17 cells, and blockade of IL-23 receptor, which would potentially attenuate the Th17 functions.

## 6. References


Abman, Steven H., Eduardo Bancalari, and Alan Jobe. 2017. “The Evolution of Bronchopulmonary Dysplasia after 50 Years.” *American Journal of Respiratory and Critical Care Medicine* 195 (4): 421–24. https://doi.org/10.1164/rccm.201611-2386ed.

Aggarwal, Neil R., Landon S. King, and Franco R. D’Alessio. 2014. “Diverse Macrophage Populations Mediate Acute Lung Inflammation and Resolution.” *American Journal of Physiology-Lung Cellular and Molecular Physiology* 306 (8): L709–25. https://doi.org/10.1152/ajplung.00341.2013.

Aghai, Zubair H., Aruna Kode, Judy G. Saslow, Tarek Nakhla, Sabeena Farhath, Gary E. Stahl, Riva Eydelman, Louise Strande, Paola Leone, and Irfan Rahman. 2007. “Azithromycin Suppresses Activation of Nuclear Factor-Kappa B and Synthesis of pro-Inflammatory Cytokines in Tracheal Aspirate Cells from Premature Infants.” *Pediatric Research* 62 (4): 483–88. https://doi.org/10.1203/PDR.0b013e318142582d.

Alvira, Cristina M. 2014. “Nuclear Factor-Kappa-B Signaling in Lung Development and Disease: One Pathway, Numerous Functions.” *Birth Defects Research Part A - Clinical and Molecular Teratology* 100: 202–16. https://doi.org/10.1002/bdra.23233.

Alvira, Cristina M., Aida Abate, Guang Yang, Phyllis A. Dennery, and Marlene Rabinovitch. 2007. “Nuclear Factor-KB Activation in Neonatal Mouse Lung Protects against Lipopolysaccharide-Induced Inflammation.” *American Journal of Respiratory and Critical Care Medicine* 175 (8): 805–15. https://doi.org/10.1164/rccm.200608-1162OC.

Ambalavanan, Namasivayam, Waldemar A Carlo, Carl T D ’Angio, Scott A Mcdonald, Abhik Das, Diana Schendel, Poul Thorsen, and Rosemary D Higgins. 2009. “Cytokines Associated with Bronchopulmonary Dysplasia or Death in Extremely Low Birth Weight Infants.” *Pediatrics* 123 (4): 1132–1141. https://doi.org/10.1542/peds.2008-0526.

Arnold, Christina E., Peter Gordon, Robert N. Barker, and Heather M. Wilson. 2015. “The Activation Status of Human Macrophages Presenting Antigen Determines the Efficiency of Th17 Responses.” *Immunobiology* 220: 10–19. https://doi.org/10.1016/j.imbio.2014.09.022.

Arora, Shweta, Kapil Dev, Beamon Agarwal, Pragnya Das, and Mansoor Ali Syed. 2018. “Macrophages: Their Role, Activation and Polarization in Pulmonary Diseases.” *Immunobiology* 223: 383–96. https://doi.org/10.1016/j.imbio.2017.11.001.

Auten, Richard L., S. Nicholas Mason, David T. Tanaka, Karen Welty-Wolf, and Mary H. Whorton. 2001. “Anti-Neutrophil Chemokine Preserves Alveolar Development in Hyperoxia-Exposed Newborn Rats.” *American Journal of Physiology-Lung Cellular and Molecular Physiology* 281: L336–44. https://doi.org/10.1152/ajplung.2001.281.2.l336.

Azad, Abul K, Murugesan V S Rajaram, and Larry S Schlesinger. 2014. “Exploitation of the Macrophage Mannose Receptor (CD206) in Infectious Disease Diagnostics and Therapeutics.” *Journal of Cytology & Molecular Biology* 10 (1). https://doi.org/10.13188/2325-4653.1000003.

Baier, R. John, Abdul Majid, Haroon Parupia, John Loggins, and Thomas E. Kruger. 2004. “CC Chemokine Concentrations Increase in Respiratory Distress Syndrome and Correlate with Development of Bronchopulmonary Dysplasia.” *Pediatric Pulmonology* 37 (2): 137–48. https://doi.org/10.1002/ppul.10417.

Balany, Jherna, and Vineet Bhandari. 2015. “Understanding the Impact of Infection, Inflammation, and Their Persistence in the Pathogenesis of Bronchopulmonary Dysplasia.” *Front. Med.* 2: 90. https://doi.org/10.3389/fmed.2015.00090.

Beck, Stacy, Daniel Wojdyla, Lale Say, Ana Pilar Betran, Mario Merialdi, Jennifer Harris Requejo, Craig Rubens, Ramkumar Menon, and Paul F A Van Look. 2010. “The Worldwide Incidence of Preterm Birth: A Systematic Review of Maternal Mortality and Morbidity.” *Bulletin of the World Health Organization* 88: 31–38. https://doi.org/10.2471/BLT.08.062554.

Belderbos, M.E., G.M. van Bleek, O. Levy, M.O. Blanken, M.L. Houben, L. Schuijff, J.L.L. Kimpen, and L. Bont. 2009. “Skewed Pattern of Toll-like Receptor 4-Mediated Cytokine Production in Human Neonatal Blood: Low LPS-Induced IL-12p70 and High IL-10 Persist throughout the First Month of Life.” *Clin Immunol.* 133 (2): 228–37. https://doi.org/10.1016/j.clim.2009.07.003.

Benjamin, John T., Rebekah J. Smith, Brian A. Halloran, Timothy J. Day, David R. Kelly, and Lawrence S. Prince. 2007. “FGF-10 Is Decreased in Bronchopulmonary Dysplasia and Suppressed by Toll-like Receptor Activation.” *American Journal of Physiology-Lung Cellular and Molecular Physiology* 292 (2): L550–58. https://doi.org/10.1152/ajplung.00329.2006.

Bhandari, Anita, and Vineet Bhandari. 2013. “Biomarkers in Bronchopulmonary Dysplasia.” *Paediatric Respiratory Reviews* 14: 173–179. https://doi.org/10.1016/j.prrv.2013.02.008.

Bhandari, V. 2010. “Hyperoxia-Derived Lung Damage in Preterm Infants Vineet.” *Semin Fetal Neonatal Med.* 15 (4): 223–29. https://doi.org/10.1016/j.siny.2010.03.009.

Bhattacharya, Soumyaroop, Diana Go, Daria L. Krenitsky, Heidi L. Huyck, Siva Kumar Solleti, Valerie A. Lunger, Leon Metlay, et al. 2012. “Genome-Wide Transcriptional Profiling Reveals Connective Tissue Mast Cell Accumulation in Bronchopulmonary Dysplasia.” *American Journal of Respiratory and Critical Care Medicine* 186 (4): 349–58. https://doi.org/10.1164/rccm.201203-0406OC.

Biswas, Subhra K, and Alberto Mantovani. 2010. “Macrophage Plasticity and Interaction with Lymphocyte Subsets: Cancer as a Paradigm.” *Nature Reviews Immunology* 11 (10): 889–96. https://doi.org/10.1038/ni.1937.

Black, Allison, Suniti Bhaumik, Richard L. Kirkman, Casey T. Weaver, and David A. Randolph. 2012. “Developmental Regulation of Th17-Cell Capacity in Human Neonates.” *European Journal of Immunology* 42 (2): 311–19. https://doi.org/10.1002/eji.201141847.

Blackwell, Timothy S., Ashley N. Hipps, Yasutoshi Yamamoto, Wei Han, Whitney J. Barham, Michael C. Ostrowski, Fiona E. Yull, and Lawrence S. Prince. 2011. “NF-KB Signaling in Fetal Lung Macrophages Disrupts Airway Morphogenesis.” *Journal of Immunology* 187 (5): 2740–47. https://doi.org/10.4049/jimmunol.1101495.

Bonikos, D S, K G Bensch, S K Ludwin, and W H Northway. 1975. “Oxygen Toxicity in the Newborn. The Effect of Prolonged 100 per Cent O2 Exposure on the Lungs of Newborn Mice.” *Laboratory Investigation* 32 (5): 619–35.

Britt, Rodney D., Markus Velten, Trent E. Tipple, Leif D. Nelin, and Lynette K. Rogers. 2013. “Cyclooxygenase-2 in Newborn Hyperoxic Lung Injury.” *Free Radic Biol Med*, 502–11. https://doi.org/10.1016/j.freeradbiomed.2013.04.012.

Buczynski, Bradley W., Echezona T. Maduekwe, and Michael A. O’Reilly. 2013. “The Role of Hyperoxia in the Pathogenesis of Experimental BPD.” *Semin Perinatol.* 37 (2): 69–78. https://doi.org/10.1053/j.semperi.2013.01.002.

Bystrom, Jonas, Felix I.L. Clanchy, Taher E. Taher, Mohammed Al-Bogami, Voon H. Ong, David J. Abraham, Richard O. Williams, and Rizgar A. Mageed. 2018. “Functional and Phenotypic Heterogeneity of Th17 Cells in Health and Disease.” *European Journal of Clinical Investigation*. https://doi.org/10.1111/eci.13032.

Cho, Hye-Youn, Bennett van Houten, Xuting Wang, Laura Miller-DeGraff, Jennifer Fostel, Wesley Gladwell, Ligon Perrow, et al. 2012. “ Targeted Deletion of Nrf2 Impairs Lung Development and Oxidant Injury in Neonatal Mice .” *Antioxidants & Redox Signaling* 17 (8): 1066–82. https://doi.org/10.1089/ars.2011.4288.

Cho, Hye-Youn, Xuting Wang, Jianying Li, Douglas A. Bell, and Steven R. Kleeberger. 2016. “Potential Therapeutic Targets in Nrf2-Dependent Protection against Neonatal Respiratory Distress Disease Predicted by CDNA Microarray Analysis and Bioinformatics Tools.” *Current Opinion in Toxicology* 1: 125–33. https://doi.org/10.1016/j.cotox.2016.10.006.

Choo-Wing, Rayman, Jonathan H. Nedrelow, Robert J. Homer, Jack A. Elias, and Vineet Bhandari. 2007. “Developmental Differences in the Responses of IL-6 and IL-13 Transgenic Mice Exposed to Hyperoxia.” *American Journal of Physiology-Lung Cellular and Molecular Physiology* 293: L142–50. https://doi.org/10.1152/ajplung.00434.2006.

Coalson, Jacqueline J., Vicki T. Winter, Theresa Siler-Khodr, and Bradley A. Yoder. 1999. “Neonatal Chronic Lung Disease in Extremely Immature Baboons.” *American Journal of Respiratory and Critical Care Medicine* 160: 1333–46. https://doi.org/10.1164/ajrccm.160.4.9810071.

Contreras, Mariana, Nitya Hariharan, June Lewandoski, Wayne Ciesielski, Rebecca Koscik, and Jerry Zimmerman. 1996. “Bronchoalve Olar Oxyradical Inflammatory Elements Herald Bronchopulmonary Dysplasia.” *Critical Care Medicine* 24 (1): 29–37.

Corbett, Nathan P., Darren Blimkie, Kevin C. Ho, Bing Cai, Darren P. Sutherland, Arlene Kallos, Juliet Crabtree, et al. 2010. “Ontogeny of Toll-like Receptor Mediated Cytokine Responses of Human Blood Mononuclear Cells.” *PLoS ONE* 5 (11). https://doi.org/10.1371/journal.pone.0015041.

Cui, Tracy X, Bhargavi Maheshwer, Jun Y Hong, Adam M Goldsmith, J Kelley Bentley, and Antonia P Popova. 2016. “Hyperoxic Exposure of Immature Mice Increases the Inflammatory Response to Subsequent Rhinovirus Infection: Association with Danger Signals.” *Journal of Immunology* 196 (11): 4692–4705. https://doi.org/10.4049/jimmunol.1501116.

Davidson, Dennis, Alla Zaytseva, Veronika Miskolci, Susana Castro-Alcaraz, Ivana Vancurova, and Hardik Patel. 2013. “Gene Expression Profile of Endotoxin-Stimulated Leukocytes of the Term New Born: Control of Cytokine Gene Expression by Interleukin-10.” *PLoS ONE* 8 (1): e53641. https://doi.org/10.1371/journal.pone.0053641.

Day, Colby L., and Rita M. Ryan. 2017. “Bronchopulmonary Dysplasia: New Becomes Old Again!” *Pediatric Research* 81 (1–2): 210–13. https://doi.org/10.1038/pr.2016.201.

Debock, Isabelle, and Véronique Flamand. 2014. “Unbalanced Neonatal CD4 + T-Cell Immunity.” https://doi.org/10.3389/fimmu.2014.00393.

Deng, Hui, S. Nicholas Mason, and Richard L. Auten. 2000. “Lung Inflammation in Hyperoxia Can Be Prevented by Antichemokine Treatment in Newborn Rats.” *American Journal of Respiratory and Critical Care Medicine* 162 (6): 2316–23. https://doi.org/10.1164/ajrccm.162.6.9911020.

Dowling, David J., and Ofer Levy. 2014. “Ontogeny of Early Life Immunity.” *Trends in Immunology* 35 (7): 299–310. https://doi.org/10.1016/j.it.2014.04.007.

Doyle, Lex W., and Peter J. Anderson. 2009. “Long-Term Outcomes of Bronchopulmonary Dysplasia.” *Seminars in Fetal and Neonatal Medicine* 14: 391–95. https://doi.org/10.1016/j.siny.2009.08.004.

Drummond, Shelley, Shalini Ramachandran, Eneida Torres, Jian Huang, Dorothy Hehre, Cleide Suguihara, and Karen C. Young. 2015. “CXCR4 Blockade Attenuates Hyperoxia Induced Lung Injury in Neonatal Rats.” *Neonatology* 107 (4): 304–11. https://doi.org/10.1159/000371835.

Egan, Charlotte E, Chhinder P Sodhi, Misty Good, Joyce Lin, Hongpeng Jia, Yukihiro Yamaguchi, Peng Lu, et al. 2015. “Toll-like Receptor 4–Mediated Lymphocyte Influx Induces Neonatal Necrotizing Enterocolitis.” *The Journal of Clinical Investigation* 126 (2): 495–508. https://doi.org/10.1172/JCI83356.

Elberson, V. D., L. C. Nielsen, H. Wang, and H. S.V. Kumar. 2015. “Effects of Intermittent Hypoxia and Hyperoxia on Angiogenesis and Lung Development in Newborn Mice.” *Journal of Neonatal-Perinatal Medicine* 8 (4): 313–22. https://doi.org/10.3233/NPM-15814134.

Ettensohn, D B, P G Duncan, and M J Jankowski. 1989. “The Role of Human Alveolar Macrophages in the Allogeneic and Autologous Mixed Leucocyte Reactions.” *Clin Exp Immunol* 75: 432–37.

Fasching, Patrizia, Martin Stradner, Winfried Graninger, Christian Dejaco, and Johannes Fessler. 2017. “Therapeutic Potential of Targeting the Th17/Treg Axis in Autoimmune Disorders.” *Molecules* 22: 134. https://doi.org/10.3390/molecules22010134.

Galli, Stephen J, Niels Borregaard, and Thomas A Wynn. 2011. “Phenotypic and Functional Plasticity of Cells of Innate Immunity: Macrophages, Mast Cells and Neutrophils.” *Nature Reviews Immunology* 12 (11). https://doi.org/10.1038/ni.2109.

Gentile, Lori F, Dina C Nacionales, M Cecilia Lopez, Erin Vanzant, Angela Cuenca, Alex G Cuenca, Ricardo Ungaro, et al. 2014. “Protective Immunity and Defects in the Neonatal and Elderly Immune Response to Sepsis.” *J Immunol* 192 (7): 3156–65. https://doi.org/10.4049/jimmunol.1301726.

Gleditsch, Dorothy D., Laurie P. Shornick, Juliette Van Steenwinckel, Pierre Gressens, Ryan P. Weisert, and Joyce M. Koenig. 2014. “Maternal Inflammation Modulates Infant Immune Response Patterns to Viral Lung Challenge in a Murine Model.” *Pediatric Research* 76 (1): 33–40. https://doi.org/10.1038/pr.2014.57.

Gleissner, Christian A. 2012. “Macrophage Phenotype Modulation by CXCL4 in Atherosclerosis.” *Frontiers in Physiology* 3: 1. https://doi.org/10.3389/fphys.2012.00001.

Goedicke-Fritz, Sybelle, Christoph Härtel, Gabriela Krasteva-Christ, Matthias V. Kopp, Sascha Meyer, and Michael Zemlin. 2017. “Preterm Birth Affects the Risk of Developing Immune-Mediated Diseases.” *Frontiers in Immunology* 8: 1266. https://doi.org/10.3389/fimmu.2017.01266.

Gortner, Ludwig, Björn Misselwitz, David Milligan, Jennifer Zeitlin, Louis Kollée, Klaus Boerch, Rocco Agostino, et al. 2011. “Rates of Bronchopulmonary Dysplasia in Very Preterm Neonates in Europe: Results from the MOSAIC Cohort.” *Neonatology* 99 (2): 112–17. https://doi.org/10.1159/000313024.

Graspeuntner, S, S Waschina, S Künzel, N Twisselmann, T K Rausch, K Cloppenborg-Schmidt, J Zimmermann, et al. 2018. “Gut Dysbiosis with Bacilli Dominance and Accumulation of Fermentation Products Precedes Late-Onset Sepsis in Preterm Infants.” *Clinical Infectious Diseases* XX: 1–10. https://doi.org/10.1093/cid/ciy882.

Guilliams, Martin, Ismé De Kleer, Sandrine Henri, Sijranke Post, Leen Vanhoutte, Sofie De Prijck, Kim Deswarte, Bernard Malissen, Hamida Hammad, and Bart N Lambrecht. 2013. “Alveolar Macrophages Develop from Fetal Monocytes That Differentiate into Long-Lived Cells in the First Week of Life via GM-CSF.” *The Journal of Experimental Medicine* 210 (10): 1977–92. https://doi.org/10.1084/jem.20131199.

Härtel, C, I Osthues, J Rupp, B Haase, K Röder, W Göpel, E Herting, and C Schultz. 2008. “Characterisation of the Host Inflammatory Response to Staphylococcus Epidermidis in Neonatal Whole Blood.” *Arch Dis Child Fetal Neonatal Ed* 93: F140–45. https://doi.org/10.1136/adc.2007.124685.

Härtel, Christoph, N. Adam, T. Strunk, P. Temming, M. Müller-Steinhardt, and C. Schultz. 2005. “Cytokine Responses Correlate Differentially with Age in Infancy and Early Childhood.” *Clinical and Experimental Immunology* 142 (3): 446–53. https://doi.org/10.1111/j.1365-2249.2005.02928.x.

Hilgendorff, Anne, Irwin Reiss, Harald Ehrhardt, Oliver Eickelberg, and Cristina M. Alvira. 2014. “Chronic Lung Disease in the Preterm Infant: Lessons Learned from Animal Models.” *American Journal of Respiratory Cell and Molecular Biology* 50 (2): 233–45. https://doi.org/10.1165/rcmb.2013-0014TR.

Holt, Patrick G., Deborah H. Strickland, Matthew E. Wikström, and Frode L. Jahnsen. 2008. “Regulation of Immunological Homeostasis in the Respiratory Tract.” *Nature Reviews Immunology* 8 (2): 142–52. https://doi.org/10.1038/nri2236.

Hou, Yanli, Min Liu, Cristiana Husted, Chihhsin Chen, Kavitha Thiagarajan, Jennifer L. Johns, Shailaja P. Rao, and Cristina M. Alvira. 2015. “Activation of the Nuclear Factor-KB Pathway during Postnatal Lung Inflammation Preserves Alveolarization by Suppressing Macrophage Inflammatory Protein-2.” *American Journal of Physiology-Lung Cellular and Molecular Physiology* 309 (6): L593–604. https://doi.org/10.1152/ajplung.00029.2015.

Howson, Eds CP, MV Kinney, and JE Lawn. 2012. “Born Too Soon - The Global Action Report on Preterm Birth.” Genova.

Hussell, Tracy, and Thomas J. Bell. 2014. “Alveolar Macrophages: Plasticity in a Tissue-Specific Context.” *Nature Reviews Immunology* 14: 81–93. https://doi.org/10.1038/nri3600.

Islam, Jessica Y., Roberta L. Keller, Judy L. Aschner, Tina V. Hartert, and Paul E. Moore. 2015. “Understanding the Short- and Long-Term Respiratory Outcomes of Prematurity and Bronchopulmonary Dysplasia.” *American Journal of Respiratory and Critical Care Medicine* 192 (2): 134–56. https://doi.org/10.1164/rccm.201412-2142PP.

Jackson, Courtney M., Casey B. Wells, Meredith E. Tabangin, Jareen Meinzen-Derr, Alan H. Jobe, and Claire A. Chougnet. 2017. “Pro-Inflammatory Immune Responses in Leukocytes of Premature Infants Exposed to Maternal Chorioamnionitis or Funisitis.” *Pediatr Res.* 81 (2): 384–90. https://doi.org/10.1038/pr.2016.232.

Jaguin, Marie, Noémie Houlbert, Olivier Fardel, and Valérie Lecureur. 2013. “Polarization Profiles of Human M-CSF-Generated Macrophages and Comparison of M1-Markers in Classically Activated Macrophages from GM-CSF and M-CSF Origin.” *Cellular Immunology* 281: 51–61. https://doi.org/10.1016/j.cellimm.2013.01.010.

Jankov, Robert P., Xiaoping Luo, Rosetta Belcastro, Ian Copland, Helena Frndova, Stephen J. Lye, John R. Hoidal, Martin Post, and A. Keith Tanswell. 2001. “Gadolinium Chloride Inhibits Pulmonary Macrophage Influx and Prevents O2-Induced Pulmonary Hypertension in the Neonatal Rat.” *Pediatric Research* 50 (2): 172–83. https://doi.org/10.1203/00006450-200108000-00003.

Jia, Hongpeng, Chhinder P. Sodhi, Yukihiro Yamaguchi, Peng Lu, Mitchell R. Ladd, Adam Werts, William B. Fulton, Sanxia Wang, Thomas Prindle, and David J. Hackam. 2018. “Toll Like Receptor 4 Mediated Lymphocyte Imbalance Induces Nec-Induced Lung Injury.” *Shock*. https://doi.org/10.1097/shk.0000000000001255.

Jobe, Alan H. 2012. “Effects of Chorioamnionitis on the Fetal Lung.” *Clinics in Perinatology* 39 (3): 441–57. https://doi.org/10.1016/j.clp.2012.06.010.

Jobe, Alan H. 2011. “The New Bronchopulmonary Dysplasia.” *Curr Opin Pediatr .* 23 (2): 167–72. https://doi.org/10.1097/MOP.0b013e3283423e6b.

Jobe, Alan H. 2015. “Animal Models, Learning Lessons to Prevent and Treat Neonatal Chronic Lung Disease.” *Front. Med.* 2: 49. https://doi.org/10.3389/fmed.2015.00049.

Jobe, Alan H, and Eduardo Bancalari. 2001. “NICHD / NHLBI / ORD Workshop Summary: Bronchopulmonary Dysplasia.” *American Journal of Respiratory and Critical Care MedicineCritical Care Medicine* 163: 1723–29.

Johnson, Ben Hur, Man Yi, Azhar Masood, Rosetta Belcastro, Jun Li, Samuel Shek, Crystal Kantores, Robert P. Jankov, and A. Keith Tanswell. 2009. “A Critical Role for the IL-1 Receptor in Lung Injury Induced in Neonatal Rats by 60% O2.” *Pediatric Research* 66 (3): 260–65. https://doi.org/10.1203/PDR.0b013e3181b1bcd2.

Johnston, Carl J., Terry W. Wright, Christina K. Reed, and Jacob N. Finkelstein. 1997. “Comparison of Adult and Newborn Pulmonary Cytokine MRNA Expression after Hyperoxia.” *Experimental Lung Research* 23 (6): 537–52. https://doi.org/10.3109/01902149709039242.

Jones, Christina V., Maliha A. Alikhan, Megan O’Reilly, Foula Sozo, Timothy M. Williams, Richard Harding, Graham Jenkin, and Sharon D. Ricardo. 2014. “The Effect of CSF-1 Administration on Lung Maturation in a Mouse Model of Neonatal Hyperoxia Exposure.” *Respiratory Research* 15: 110. https://doi.org/10.1186/s12931-014-0110-5.

Jones, Craig A., Rowena G. Cayabyab, Kenny Y.C. Kwong, Cynthia Stotts, Betty Wong, Hasnah Hamdan, Parviz Minoo, and Robert A. Delemos. 1996. “Undetectable Interleukin (IL)-10 and Persistent IL-8 Expression Early in Hyaline Membrane Disease: A Possible Developmental Basis for the Predisposition to Chronic Lung Inflammation in Preterm Newborns.” *Pediatric Research* 39: 966–75. https://doi.org/10.1203/00006450-199606000-00007.

Jong, Emma de, David G. Hancock, Christine Wells, Peter Richmond, Karen Simmer, David Burgner, Tobias Strunk, and Andrew J. Currie. 2018. “Exposure to Chorioamnionitis Alters the Monocyte Transcriptional Response to the Neonatal Pathogen Staphylococcus Epidermidis.” *Immunology and Cell Biology*, 1–13. https://doi.org/10.1111/imcb.12037.

Jong, Emma de, Tobias Strunk, David Burgner, Pascal M. Lavoie, and Andrew Currie. 2017. “The Phenotype and Function of Preterm Infant Monocytes: Implications for Susceptibility to Infection.” *Journal of Leukocyte Biology* 102 (3): 645–56. https://doi.org/10.1189/jlb.4ru0317-111r.

Jonsson, B, K Tullus, A Brauner, Y Lu, and G Noack. 1997. “Early Increase OfTNFalpha and IL-6 in Tracheobronchial Aspirate Fluid Indicator of Subsequent Chronic Lung Disease in Preterm Infants.” *Archives OfDisease in Childhood* 77: F198–201.

Jubb, Alasdair W., Robert S. Young, David A. Hume, and Wendy A. Bickmore. 2016. “Enhancer Turnover Is Associated with a Divergent Transcriptional Response to Glucocorticoid in Mouse and Human Macrophages.” *The Journal of Immunology* 196 (2): 813–22. https://doi.org/10.4049/jimmunol.1502009.

Kalymbetova, Tatiana V., Balachandar Selvakumar, José Alberto Rodríguez-Castillo, Miša Gunjak, Christina Malainou, Miriam Ruth Heindl, Alena Moiseenko, et al. 2018. “Resident Alveolar Macrophages Are Master Regulators of Arrested Alveolarization in Experimental Bronchopulmonary Dysplasia.” *Journal of Pathology* 245 (2): 153–59. https://doi.org/10.1002/path.5076.

Kan, Bernard, Christina Michalski, Helen Fu, Hilda H.T. Au, Kelsey Lee, Elizabeth A. Marchant, Maye F. Cheng, et al. 2018. “Cellular Metabolism Constrains Innate Immune Responses in Early Human Ontogeny.” *Nature Communications* 9: 4822. https://doi.org/10.1038/s41467-018-07215-9.

Kasahara, Kazuki, Yoko Matsumura, Kouji Ui, Kei Kasahara, Yuko Komatsu, Keiichi Mikasa, and Eiji Kita. 2012. “Intranasal Priming of Newborn Mice with Microbial Extracts Increases Opsonic Factors and Mature CD11c+ Cells in the Airway.” *American Journal of Physiology-Lung Cellular and Molecular Physiology* 303: L834–43. https://doi.org/10.1152/ajplung.00031.2012.

Kasat, Kavita, Hardik Patel, Olena Predtechenska, Ivana Vancurova, and Dennis Davidson. 2014. “Anti-Inflammatory Actions of Endogenous and Exogenous Interleukin-10 versus Glucocorticoids on Macrophage Functions of the Newly Born.” *J Perinatol* 34 (5): 380–85. https://doi.org/10.1038/jp.2014.16.

Kaur, Manminder, Thomas Bell, Samira Salek-Ardakani, and Tracy Hussell. 2015. “Macrophage Adaptation in Airway Inflammatory Resolution.” *European Respiratory Review* 24: 510–15. https://doi.org/10.1183/16000617.0030-2015.

Kleer, Ismé De, Fabienne Willems, Bart Lambrecht, and Stanislas Goriely. 2014. “Ontogeny of Myeloid Cells.” *Frontiers in Immunology* 5 (AUG): 1–11. https://doi.org/10.3389/fimmu.2014.00423.

Klinger, Gil, Nir Sokolover, Valentina Boyko, Lea Sirota, Liat Lerner-Geva, and Brian Reichman. 2013. “Perinatal Risk Factors for Bronchopulmonary Dysplasia in a National Cohort of Very-Low-Birthweight Infants.” *American Journal of Obstetrics and Gynecology* 208: 115.e1-115.e9. https://doi.org/10.1016/j.ajog.2012.11.026.

Kollmann, Tobias R., Juliet Crabtree, Annie Rein-Weston, Darren Blimkie, Francis Thommai, Xiu Yu Wang, Pascal M. Lavoie, et al. 2009. “Neonatal Innate TLR-Mediated Responses Are Distinct from Those of Adults.” *Journal of Immunology* 183 (11): 7150–60. https://doi.org/10.4049/jimmunol.0901481.

Kollmann, Tobias R., Beate Kampmann, Sarkis K. Mazmanian, Arnaud Marchant, and Ofer Levy. 2017. “Protecting the Newborn and Young Infant from Infectious Diseases: Lessons from Immune Ontogeny.” *Immunity* 46: 350–63. https://doi.org/10.1016/j.immuni.2017.03.009.

Kollmann, Tobias R., Ofer Levy, Ruth R. Montgomery, and Stanislas Goriely. 2012. “Innate Immune Function by Toll-like Receptors: Distinct Responses in Newborns and the Elderly.” *Immunity* 37 (5): 771–83. https://doi.org/10.1016/j.immuni.2012.10.014.

Korn, Thomas, Estelle Bettelli, Mohamed Oukka, and Vijay K Kuchroo. 2009. “IL-17 and Th17 Cells.” *Annual Review of Immunology* 27: 485–517. https://doi.org/10.1146/annurev.immunol.021908.132710.

Kotecha, S., B. Chan, N. Azam, M. Silverman, and R. J. Shaw. 1995. “Increase in Interleukin-8 and Soluble Intercellular Adhesion Molecule-1 in Bronchoalveolar Lavage Fluid from Premature Infants Who Develop Chronic Lung Disease.” *Archives of Disease in Childhood* 72: F90–96. https://doi.org/10.1136/fn.72.2.f90.

Kotecha, S., L. Wilson, A. Wangoo, M. Silverman, and R. J. Shaw. 1996. “Increase in Interleukin (IL)-1β and IL-6 in Bronchoalveolar Lavage Fluid Obtained from Infants with Chronic Lung Disease of Prematurity.” *Pediatric Research* 40: 250–56. https://doi.org/10.1203/00006450-199608000-00010.

Kramer, Boris W., Suhas G. Kallapur, Timothy J. Moss, Ilias Nitsos, John P. Newnham, and Alan H. Jobe. 2009. “Intra-Amniotic LPS Modulation of TLR Signaling in Lung and Blood Monocytes of Fetal Sheep.” *Innate Immunity* 15 (2): 101–7. https://doi.org/10.1177/1753425908100455.

Kramer, Boris W., Suhas Kallapur, John Newnham, and Alan H. Jobe. 2009. “Prenatal Inflammation and Lung Development.” *Seminars in Fetal and Neonatal Medicine* 14 (1): 2–7. https://doi.org/10.1016/j.siny.2008.08.011.

Kumar, Vasantha H.S., Huamei Wang, and Lori Nielsen. 2018. “Adaptive Immune Responses Are Altered in Adult Mice Following Neonatal Hyperoxia.” *Physiological Reports* 6 (2): 1–10. https://doi.org/10.14814/phy2.13577.

Kwinta, Przemko, Renata Bokiniec, Miroslaw Bik-Multanowski, Clara Cecilie Gunther, Agnieszka Grabowska, Teofila Ksiazek, Anna Madetko-Talowska, et al. 2017. “Comparison of Whole Genome Expression Profile between Preterm and Full-Term Newborns.” *Ginekologia Polska* 88 (8): 434–41. https://doi.org/10.5603/GP.a2017.0080.

Lal, Charitharth Vivek, and Namasivayam Ambalavanan. 2015a. “Biomarkers, Early Diagnosis, and Clinical Predictors of Bronchopulmonary Dysplasia.” *Clinics in Perinatology* 42: 739–754. https://doi.org/10.1016/j.clp.2015.08.004.

Lal, Charitharth Vivek, and Namasivayam Ambalavanan. 2015b. “Genetic Predisposition to Bronchopulmonary Dysplasia.” *Seminars in Perinatology* 39: 584–591. https://doi.org/10.1053/j.semperi.2015.09.004.

Lambert, Laura, and Fiona J. Culley. 2017. “Innate Immunity to Respiratory Infection in Early Life.” *Frontiers in Immunology* 8: 1570. https://doi.org/10.3389/fimmu.2017.01570.

Landry, Jennifer S., Tiffany Chan, Larry Lands, and Dick Menzies. 2011. “Long-Term Impact of Bronchopulmonary Dysplasia on Pulmonary Function.” *Canadian Respiratory Journal* 18 (5): 265–70. https://doi.org/10.1155/2011/547948.

Lawrence, Donald W., and Joyce M. Koenig. 2012. “Enhanced Phagocytosis in Neonatal Monocyte-Derived Macrophages Is Associated with Impaired SHP-1 Signaling.” *Immunological Investigations* 41: 129–43. https://doi.org/10.3109/08820139.2011.595471.

Levy, Ofer. 2007. “Innate Immunity of the Newborn: Basic Mechanisms and Clinical Correlates.” *Nature Reviews Immunology* 7: 379–90. https://doi.org/10.1038/nri2075.

Levy, Ofer, Melissa Coughlin, Bruce N. Cronstein, Rene M. Roy, Avani Desai, and Michael R. Wessels. 2006. “The Adenosine System Selectively Inhibits TLR-Mediated TNF-α Production in the Human Newborn.” *Journal of Immunology* 177 (3): 1956–66.

Li, Huai Dong, Qing Xiang Zhang, Zhi Mao, Xing Jie Xu, Nai Yi Li, and Hui Zhang. 2015. “Exogenous Interleukin-10 Attenuates Hyperoxia-Induced Acute Lung Injury in Mice.” *Experimental Physiology* 100 (3): 331–40. https://doi.org/10.1113/expphysiol.2014.083337.

Li, Yonghong, Chaojun Wei, Hui Xu, Jing Jia, Zhenhong Wei, Rui Guo, Yanjuan Jia, et al. 2018. “The Immunoregulation of Th17 in Host against Intracellular Bacterial Infection.” *Mediators of Inflammation*. https://doi.org/10.1155/2018/6587296.

Loering, Svenja, Guy J.M. Cameron, Malcolm R. Starkey, and Philip M. Hansbro. 2019. “Lung Development and Emerging Roles for Type 2 Immunity.” *Journal of Pathology* 247 (5): 686–96. https://doi.org/10.1002/path.5211.

Malyshev, Igor, and Yuri Malyshev. 2015. “Current Concept and Update of the Macrophage Plasticity Concept: Intracellular Mechanisms of Reprogramming and M3 Macrophage "Switch" Phenotype.” *BioMed Research International*. https://doi.org/10.1155/2015/341308.

Manni, Michelle L., Keven M. Robinson, and John F. Alcorn. 2014. “A Tale of Two Cytokines: IL-17 and IL-22 in Asthma and Infection.” *Expert Review of Respiratory Medicine* 8 (1): 25–42. https://doi.org/10.1586/17476348.2014.854167.

Maródi, L., K. Goda, A. Palicz, and G. Szabó. 2001. “Cytokine Receptor Signalling in Neonatal Macrophage: Defective STAT-1 Phosphorylation in Response to Stimulation with IFN-γ.” *Clinical and Experimental Immunology* 126: 456–60. https://doi.org/10.1046/j.1365-2249.2001.01693.x.

Martin, Richard J., Juliann M. Di Fiore, and Michele C. Walsh. 2015. “Hypoxic Episodes in Bronchopulmonary Dysplasia.” *Clin Perinatol* 42: 825–838. https://doi.org/10.1016/j.clp.2015.08.009.

Mathias, Brittany, Juan C. Mira, Jonathan P. Rehfuss, Jaimar C. Rincon, Ricardo Ungaro, Dina C. Nacionales, Cecilia Lopez, Henry V. Baker, Lyle L. Moldawer, and Shawn D. Larson. 2017. “LPS Stimulation of Cord Blood Reveals a Newborn-Specific Neutrophil Transcriptomic Response and Cytokine Production.” *Shock* 47 (5): 606–14. https://doi.org/10.1097/SHK.0000000000000800.

McKenzie, Brent S., Robert A. Kastelein, and Daniel J. Cua. 2006. “Understanding the IL-23-IL-17 Immune Pathway.” *Trends in Immunology* 27 (1): 17–23. https://doi.org/10.1016/j.it.2005.10.003.

Mei, Hua, Yuheng Zhang, Chunzhi Liu, Yayu Zhang, Chunli Liu, Dan Song, Chun Xin, et al. 2018. “Messenger RNA Sequencing Reveals Similar Mechanisms between Neonatal and Acute Respiratory Distress Syndrome.” *Molecular Medicine Reports* 17: 59–70. https://doi.org/10.3892/mmr.2017.7891.

Mills, Evanna L., and Luke A. O’Neill. 2016. “Reprogramming Mitochondrial Metabolism in Macrophages as an Anti-Inflammatory Signal.” *European Journal of Immunology* 46: 13–21. https://doi.org/10.1002/eji.201445427.

Misra, Ravi S., Syed Shah, Deborah J. Fowell, Hongyue Wang, Kristin Scheible, Sara K. Misra, Heidie Huyck, et al. 2015. “Preterm Cord Blood CD4+ T Cells Exhibit Increased IL-6 Productionin Chorioamnionitis and Decreased CD4+ T Cells in Bronchopulmonary Dysplasia.” *Human Immunology* 76: 329–38. https://doi.org/10.1016/j.humimm.2015.03.007.

Mondino, A., and M. K. Jenkins. 1994. “Surface Proteins Involved in T Cell Costimulation.” *Journal of Leukocyte Biology* 55 (6): 805–15. https://doi.org/10.1002/jlb.55.6.805.

Mosser, David M, and Justin P Edwards. 2008. “Exploring the Full Spectrum of Macrophage Activation.” *Nature Reviews. Immunology* 8 (12): 958–69. https://doi.org/10.1038/nri2448.

Nagato, Akinori C., Frank S. Bezerra, André Talvani, Beatriz J. Aarestrup, and Fernando M. Aarestrup. 2015. “ Hyperoxia Promotes Polarization of the Immune Response in Ovalbumin-Induced Airway Inflammation, Leading to a TH 17 Cell Phenotype .” *Immunity, Inflammation and Disease* 3 (3): 321–37. https://doi.org/10.1002/iid3.71.

Näsänen-Gilmore, Pieta, Marika Sipola-Leppänen, Marjaana Tikanmä Ki, Hanna Maria Matinolli, Johan G. Eriksson, Marjo Riitta Järvelin, Marja Vääräsmä Ki, Petteri Hovi, and Eero Kajantie. 2018. “Lung Function in Adults Born Preterm.” *PLoS ONE* 13 (10): 1–15. https://doi.org/10.1371/journal.pone.0205979.

Nguyen, Muriel, Elke Leuridan, Tong Zhang, Dominique De Wit, Fabienne Willems, Pierre van Damme, Michel Goldman, and Stanislas Goriely. 2010. “Acquisition of Adult-like TLR4 and TLR9 Responses during the First Year of Life.” *PLoS ONE* 5 (4): e10407. https://doi.org/10.1371/journal.pone.0010407.

Niedermaier, Sophie, and Anne Hilgendorff. 2015. “Bronchopulmonary Dysplasia - an Overview about Pathophysiologic Concepts.” *Molecular and Cellular Pediatrics* 2 (2). https://doi.org/10.1186/s40348-015-0013-7.

Nizet, Victor, and Randall S Johnson. 2009. “Interdependence of Hypoxic and Innate Immune Responses.” *Nature Reviews. Immunology* 9 (9): 609–17.

Nkadi, Paul O., T. Allen Merritt, and De-Ann M. Pillers. 2009. “An Overview of Pulmonary Surfactant in the Neonate: Genetics, Metabolism, and the Role of Surfactant in Health and Disease.” *Mol Genet Metab.* 97 (2): 95–101. https://doi.org/10.1016/j.ymgme.2009.01.015.

Nold, M. F., N. E. Mangan, I. Rudloff, S. X. Cho, N. Shariatian, T. D. Samarasinghe, E. M. Skuza, et al. 2013. “Interleukin-1 Receptor Antagonist Prevents Murine Bronchopulmonary Dysplasia Induced by Perinatal Inflammation and Hyperoxia.” *PNAS* 110 (35): 14384–89. https://doi.org/10.1073/pnas.1306859110.

Northway Jr, W H, R C Rosan, and D Y Porter. 1967. “Pulmonary Disease Following Respirator Therapy of Hyaline-Membrane Disease. Bronchopulmonary Dysplasia.” *The New England Journal of Medicine* 276 (7): 357–68. https://doi.org/10.1056/NEJM196702162760701.

O’Neill, Luke A.J., Rigel J. Kishton, and Jeff Rathmell. 2016. “A Guide to Immunometabolism for Immunologists.” *Nature Reviews Immunology* 16 (9): 553–65. https://doi.org/10.1038/nri.2016.70.

Omenetti, Sara, and Theresa T. Pizarro. 2015. “The Treg/Th17 Axis: A Dynamic Balance Regulated by the Gut Microbiome.” *Frontiers in Immunology* 6: 639. https://doi.org/10.3389/fimmu.2015.00639.

Onland, Wes, Thomas P Debray, Matthew M Laughon, Martijn Miedema, Filip Cools, Lisa M Askie, Jeanette M Asselin, et al. 2013. “Clinical Prediction Models for Bronchopulmonary Dysplasia: A Systematic Review and External Validation Study.” *BMC Pediatrics* 13 (1). https://doi.org/10.1186/1471-2431-13-207.

Pagel, J., A. Hartz, J. Figge, C. Gille, S. Eschweiler, K. Petersen, L. Schreiter, et al. 2016. “Regulatory T Cell Frequencies Are Increased in Preterm Infants with Clinical Early-Onset Sepsis.” *Clinical and Experimental Immunology*. https://doi.org/10.1111/cei.12810.

Pang, Yin, Xiaoya Du, Xueli Xu, Mengjie Wang, and Zhichang Li. 2018. “Monocyte Activation and Inflammation Can Exacerbate Treg/Th17 Imbalance in Infants with Neonatal Necrotizing Enterocolitis.” *International Immunopharmacology* 59: 354–60. https://doi.org/10.1016/j.intimp.2018.04.026.

Patterson, Angela, Vicki Taciak, Judith Lovchik, Renee Fox, Andrew Campbell, and Rose Viscardi. 1998. “Ureaplasma Urealyticum Respiratory Tract Colonization Is Associated with an Increase in Interleukin 1-Beta and Tumor Necrosis Factor Alpha Relative to Interleukin 6 in Tracheal Aspirates of Preterm Infants.” *Pediatric Infectious Disease Journal* 17 (4): 321–28.

Pettengill, Matthew Aaron, Simon Daniël van Haren, and Ofer Levy. 2014. “Soluble Mediators Regulating Immunity in Early Life.” *Frontiers in Immunology* 5: 457. https://doi.org/10.3389/fimmu.2014.00457.

Pixley, Fiona J., and E. Richard Stanley. 2004. “CSF-1 Regulation of the Wandering Macrophage: Complexity in Action.” *Trends in Cell Biology* 14 (11): 628–38. https://doi.org/10.1016/j.tcb.2004.09.016.

Popova, Antonia P. 2013. “Mechanisms of Bronchopulmonary Dysplasia.” *Journal of Cell Communication and Signaling* 7: 119– 127. https://doi.org/10.1007/s12079-013-0190-x.

Prince, Lynne R., Nicola C. Maxwell, Sharonjit K. Gill, David H. Dockrell, Ian Sabroe, Eamon P. McGreal, Sailesh Kotecha, and Moira K. Whyte. 2014. “Macrophage Phenotype Is Associated with Disease Severity in Preterm Infants with Chronic Lung Disease.” *PLoS ONE* 9 (8). https://doi.org/10.1371/journal.pone.0103059.

Principi, Nicola, Giada Maria Di Pietro, and Susanna Esposito. 2018. “Bronchopulmonary Dysplasia: Clinical Aspects and Preventive and Therapeutic Strategies.” *Journal of Translational Medicine* 16 (1): 1–13. https://doi.org/10.1186/s12967-018-1417-7.

Prosser, Amy, Julie Hibbert, Tobias Strunk, Chooi Heen Kok, Karen Simmer, Peter Richmond, David Burgner, and Andrew Currie. 2013. “Phagocytosis of Neonatal Pathogens by Peripheral Blood Neutrophils and Monocytes from Newborn Preterm and Term Infants.” *Pediatric Research* 74 (5): 503–10. https://doi.org/10.1038/pr.2013.145.

Pryhuber, Gloria S. 2015. “Postnatal Infections and Immunology Affecting Chronic Lung Disease of Prematurity.” *Clin Perinatol.* 42 (4): 697–718. https://doi.org/10.1016/j.clp.2015.08.002.

Randell, S H, R R Mercer, and S L Young. 1990. “Neonatal Hyperoxia Alters the Pulmonary Alveolar and Capillary Structure of 40-Day-Old Rats.” *Am J Pathology* 136 (6): 1259–66.

Ratner, Veniamin, Anatoly Starkov, Dzmitry Matsiukevich, Richard A. Polin, and Vadim S. Ten. 2009. “Mitochondrial Dysfunction Contributes to Alveolar Developmental Arrest in Hyperoxia-Exposed Mice.” *American Journal of Respiratory Cell and Molecular Biology* 40 (5): 511–18. https://doi.org/10.1165/rcmb.2008-0341RC.

Raymond, Steven L., Brittany J. Mathias, Tyler J. Murphy, Jaimar C. Rincon, María Cecilia López, Ricardo Ungaro, Felix Ellett, et al. 2017. “Neutrophil Chemotaxis and Transcriptomics in Term and Preterm Neonates.” *Transl Res.* 190: 4–15. https://doi.org/10.1016/j.trsl.2017.08.003.

Reddy, Narsa M., Steven R. Kleeberger, Thomas W. Kensler, Masayuki Yamamoto, Paul M. Hassoun, and Sekhar P. Reddy. 2009. “Disruption of Nrf2 Impairs the Resolution of Hyperoxia-Induced Acute Lung Injury and Inflammation in Mice.” *The Journal of Immunology* 182: 7264–7271. https://doi.org/10.4049/jimmunol.0804248.

Rito, Daniel C., Luke T. Viehl, Paula M. Buchanan, Seema Haridas, and Joyce M. Koenig. 2017. “Augmented Th17-Type Immune Responses in Preterm Neonates Exposed to Histologic Chorioamnionitis.” *Pediatric Research* 81 (4): 639–45. https://doi.org/10.1038/pr.2016.254.

Rivera, Lidys, Roopa Siddaiah, Christiana Oji-Mmuo, Gabriela R. Silveyra, and Patricia Silveyra. 2016. “Biomarkers for Bronchopulmonary Dysplasia in the Preterm Infant.” *Front. Pediatr* 4 (33). https://doi.org/10.3389/fped.2016.00033.

Roberts, Devender, Julie Brown, Nancy Medley, and Stuart R Dalziel. 2017. “Antenatal Corticosteroids for Accelerating Fetal Lung Maturation for Women at Risk of Preterm Birth.” *Cochrane Database of Systematic Reviews* 3: CD004454. https://doi.org/10.1002/14651858.CD004454.pub3.

Rojas, José M., Miguel Avia, Verónica Martín, and Noemí Sevilla. 2017. “IL-10: A Multifunctional Cytokine in Viral Infections.” *Journal of Immunology Research* 6104054. https://doi.org/10.1155/2017/6104054.

Rosen, Dennis, Jong Hwan Lee, Frank Cuttitta, Fatema Rafiqi, Simone Degan, and Mary E. Sunday. 2006. “Accelerated Thymic Maturation and Autoreactive T Cells in Bronchopulmonary Dysplasia.” *American Journal of Respiratory and Critical Care Medicine* 174 (1): 75–83. https://doi.org/10.1164/rccm.200511-1784OC.

Roy, Suyasha, Zaigham Abbas Rizvi, and Amit Awasthi. 2019. “Metabolic Checkpoints in Differentiation of Helper T Cells in Tissue Inflammation.” *Frontiers in Immunology* 9: 3036. https://doi.org/10.3389/fimmu.2018.03036.

Rueda, Cesar M., Pietro Presicce, Courtney M. Jackson, Lisa A. Miller, Suhas G. Kallapur, Alan H. Jobe, and Claire A. Chougnet. 2016. “LPS-Induced Chorioamnionitis Promotes IL-1-Dependent Inflammatory FoxP3+ CD4+ T Cells in the Fetal Rhesus Macaque.” *Journal of Immunology* 196 (9): 3706–3715. https://doi.org/10.4049/jimmunol.1502613.

Ryan, Rita M., Qadeer Ahmed, and Satyan Lakshminrusimha. 2008. “Inflammatory Mediators in the Immunobiology of Bronchopulmonary Dysplasia.” *Clinical Reviews in Allergy and Immunology* 34 (2): 174–90. https://doi.org/10.1007/s12016-007-8031-4.

Salaets, Thomas, Jute Richter, Paul Brady, Julio Jimenez, Taro Nagatomo, Jan Deprest, and Jaan Toelen. 2015. “Transcriptome Analysis of the Preterm Rabbit Lung after Seven Days of Hyperoxic Exposure.” *PLoS ONE* 10 (8): e0136569. https://doi.org/10.1371/journal.pone.0136569.

Santos, Angela Batista Gomes Dos, Daniella Binoki, Luis Fernando F Silva, Bianca Bergamo de Araujo, Irene Den Otter, Raquel Annoni, Michael Tsokos, et al. 2013. “Immune Cell Profile in Infants’ Lung Tissue.” *Annals of Anatomy* 195: 596– 604. https://doi.org/10.1016/j.aanat.2013.05.003.

Schultz, C., T. Strunk, P. Temming, N. Matzke, and C. Härtel. 2007. “Reduced IL-10 Production and -Receptor Expression in Neonatal T Lymphocytes.” *Acta Paediatrica, International Journal of Paediatrics* 96 (8): 1122–25. https://doi.org/10.1111/j.1651-2227.2007.00375.x.

Sharma, Ashish Arunkumar, Roger Jen, Rollin Brant, Mihoko Ladd, Qing Huang, Amanda Skoll, Christof Senger, Stuart E. Turvey, Nico Marr, and Pascal M. Lavoie. 2014. “Hierarchical Maturation of Innate Immune Defences in Very Preterm Neonates.” *Neonatology* 106 (1): 1–9. https://doi.org/10.1159/000358550.

Shen, Chung Min, Shih Chang Lin, Dau Ming Niu, and Yu Ru Kou. 2013. “Development of Monocyte Toll-like Receptor 2 and Toll-like Receptor 4 in Preterm Newborns during the First Few Months of Life.” *Pediatric Research* 73 (5): 685–91. https://doi.org/10.1038/pr.2013.36.

Shennan, A T, M S Dunn, A Ohlsson, K Lennox, and E M Hoskins. 1988. “Abnormal Pulmonary Outcomes in Premature Infants: Prediction from Oxygen Requirement in the Neonatal Period.” *Pediatrics* 82 (4): 527–32.

Sime, Patricia J., Zhou Xing, Frank L. Graham, Karl G. Csaky, and Jack Gauldie. 1997. “Adenovector-Mediated Gene Transfer of Active Transforming Growth Factor- B1 Induces Prolonged Severe Fibrosis in Rat Lung.” *Journal of Clinical Investigation* 100 (4): 768–76. https://doi.org/10.1172/JCI119590.

Speer, C P. 2006. “Pulmonary Inflammation and Bronchopulmonary Dysplasia.” *Journal of Perinatology* 26: 57–62. https://doi.org/10.1038/sj.jp.7211476.

Stoll, Barbara J., Nellie I. Hansen, Edward F. Bell, Michele C. Walsh, Waldemar A. Carlo, Seetha Shankaran, Abbot R. Laptook, et al. 2015. “Trends in Care Practices, Morbidity, and Mortality of Extremely Preterm Neonates, 1993-2012.” *JAMA - Journal of the American Medical Association*. https://doi.org/10.1001/jama.2015.10244.

Stoppelenburg, Arie J., Sytze De Roock, Marije P. Hennus, Louis Bont, and Marianne Boes. 2014. “Elevated Th17 Response in Infants Undergoing Respiratory Viral Infection.” *American Journal of Pathology* 184 (5): 1274–79. https://doi.org/10.1016/j.ajpath.2014.01.033.

Stouch, Ashley N., Rinat Zaynagetdinov, Whitney J. Barham, Amanda M. Stinnett, James C. Slaughter, Fiona E. Yull, Hal M. Hoffman, Timothy S. Blackwell, and Lawrence S. Prince. 2014. “IKKβ Activity Drives Fetal Lung Macrophage Maturation Along a Non-M1/M2 Paradigm.” *J Immunol.* 193 (3): 1184–93. https://doi.org/10.4049/jimmunol.1302516.

Strunk, Tobias, Amy Prosser, Ofer Levy, Victoria Philbin, Karen Simmer, Dorota Doherty, Adrian Charles, Peter Richmond, David Burgner, and Andrew Currie. 2012. “Responsiveness of Human Monocytes to the Commensal Bacterium Staphylococcus Epidermidis Develops Late in Gestation.” *Pediatric Research* 72 (1): 10–18. https://doi.org/10.1038/pr.2012.48.

Syed, Mansoor A., and Vineet Bhandari. 2013. “Hyperoxia Exacerbates Postnatal Inflammation-Induced Lung Injury in Neonatal BRP-39 Null Mutant Mice Promoting the M1 Macrophage Phenotype.” *Mediators of Inflammation* 457189. https://doi.org/10.1155/2013/457189.

Takasugi, Koji, Masahiro Yamamura, Mitsuhiro Iwahashi, Fumio Otsuka, Jiro Yamana, Katsue Sunahori, Masanori Kawashima, Masao Yamada, and Hirofumi Makino. 2006. “Induction of Tumour Necrosis Factor Receptor-Expressing Macrophages by Interleukin-10 and Macrophage Colony-Stimulating Factor in Rheumatoid Arthritis.” *Arthritis Research and Therapy* 8 (4): R126. https://doi.org/10.1186/ar2015.

Thome, Joseph J.C., Kara L. Bickham, Yoshiaki Ohmura, Masaru Kubota, Nobuhide Matsuoka, Claire Gordon, Tomer Granot, et al. 2016. “Early-Life Compartmentalization of Human T Cell Differentiation and Regulatory Function in Mucosal and Lymphoid Tissues.” *Nature Medicine* 22: 72–77. https://doi.org/10.1038/nm.4008.

Thorkelsson, Thordur, and Gunnlaugur Sigfusson. 2014. “Neonatal Lung Diseases.” *Pediatric Critical Care Medicine*, 249–62. https://doi.org/10.1007/978-1-4471-6356-5_14.

Torow, N., B. J. Marsland, M. W. Hornef, and E. S. Gollwitzer. 2017. “Neonatal Mucosal Immunology.” *Mucosal Immunology* 10 (1): 5–17. https://doi.org/10.1038/mi.2016.81.

Trembath, Andrea, and Matthew Laughon. 2012. “Predictors of Bronchopulmonary Dysplasia.” *Clin Perinatol.* 39 (3): 585–601. https://doi.org/10.1016/j.clp.2012.06.014.

Tröger, Birte, Wolfgang Göpel, Kirstin Faust, Thilo Müller, Gerhard Jorch, Ursula Felderhoff-Müser, Ludwig Gortner, et al. 2014. “Risk for Late-Onset Blood-Culture Proven Sepsis in Very-Low-Birth Weight Infants Born Small for Gestational Age: A Large Multicenter Study from the German Neonatal Network.” *The Pediatric Infectious Disease Journal* 33 (3): 238–43. https://doi.org/10.1097/INF.0000000000000031.

Tu, Guo wei, Yi Shi, Yi jun Zheng, Min jie Ju, Hong yu He, Guo guang Ma, Guang wei Hao, and Zhe Luo. 2017. “Glucocorticoid Attenuates Acute Lung Injury through Induction of Type 2 Macrophage.” *Journal of Translational Medicine* 15: 181. https://doi.org/10.1186/s12967-017-1284-7.

Tucker, Janet, and William Mcguire. 2004. “Epidemiology of Preterm Birth.” *BMJ* 329: 675–78. https://doi.org/10.1136/bmj.329.7467.675.

Turner, Mark D., Belinda Nedjai, Tara Hurst, and Daniel J. Pennington. 2014. “Cytokines and Chemokines: At the Crossroads of Cell Signalling and Inflammatory Disease.” *Biochimica et Biophysica Acta - Molecular Cell Research* 1843 (11): 2563–82. https://doi.org/10.1016/j.bbamcr.2014.05.014.

Turunen, Riikka, Outi Vaarala, Irmeli Nupponen, Eero Kajantie, Sanna Siitonen, Aulikki Lano, Heikki Repo, and Sture Andersson. 2009. “Activation of T Cells in Preterm Infants with Respiratory Distress Syndrome.” *Neonatology* 96 (4): 248–58. https://doi.org/10.1159/000220764.

Twisselmann, Nele, Yannic C. Bartsch, Julia Pagel, Christian Wieg, Annika Hartz, Marc Ehlers, and Christoph Härtel. 2019. “IgG Fc Glycosylation Patterns of Preterm Infants Differ with Gestational Age.” *Frontiers in Immunology* 10. https://doi.org/10.3389/fimmu.2018.03166.

Velten, Markus, Kathryn M. Heyob, Lynette K. Rogers, and Stephen E. Welty. 2010. “Deficits in Lung Alveolarization and Function after Systemic Maternal Inflammation and Neonatal Hyperoxia Exposure.” *Journal of Applied Physiology* 108 (5): 1347–56. https://doi.org/10.1152/japplphysiol.01392.2009.

Vissers, Marloes, Inge Schreurs, Jop Jans, Jacco Heldens, Ronald de Groot, Marien I. de Jonge, and Gerben Ferwerda. 2015. “Antibodies Enhance CXCL10 Production during RSV Infection of Infant and Adult Immune Cells.” *Cytokine* 76: 458–64. https://doi.org/10.1016/j.cyto.2015.07.024.

Vozzelli, Michael A, S Nicholas Mason, Mary H Whorton, and Richard L Auten. 2004. “Antimacrophage Chemokine Treatment Prevents Neutrophil and Macrophage Influx in Hyperoxia-Exposed Newborn Rat Lung.” *Am J Physiol Lung Cell Mol Physiol* 286: L488–L493. https://doi.org/10.1152/ajplung. 00414.2002.

Walsh, M. C., Qing Yao, Patricia Gettner, Ellen Hale, Monica Collins, Angelita Hensman, Ruth Everette, et al. 2004. “Impact of a Physiologic Definition on Bronchopulmonary Dysplasia Rates.” *PEDIATRICS* 114 (5). https://doi.org/10.1542/peds.2004-0204.

Warner, B B, L A Stuart, R A Papes, and J R Wispé. 1998. “Functional and Pathological Effects of Prolonged Hyperoxia in Neonatal Mice.” *The American Journal of Physiology* 275 (1 Pt 1): L110-7. http://www.ncbi.nlm.nih.gov/pubmed/9688942.

Weichelt, Ulrike, Ruhuye Cay, Thomas Schmitz, Evelyn Strauss, Marco Sifringer, Christoph Bührer, and Stefanie Endesfelder. 2013. “Prevention of Hyperoxia-Mediated Pulmonary Inflammation in Neonatal Rats by Caffeine.” *European Respiratory Journal* 41 (4): 966–73. https://doi.org/10.1183/09031936.00012412.

Winterberg, Thomas, Gertrud Vieten, Tatiana Meier, Yi Yu, Mandy Busse, Christian Hennig, Gesine Hansen, Roland Jacobs, Benno M. Ure, and Joachim F. Kuebler. 2015. “Distinct Phenotypic Features of Neonatal Murine Macrophages.” *European Journal of Immunology* 45 (1): 214–24. https://doi.org/10.1002/eji.201444468.

Wisgrill, Lukas, Alina Groschopf, Elisabeth Herndl, Kambis Sadeghi, Andreas Spittler, Angelika Berger, and Elisabeth Förster-Waldl. 2016. “Reduced TNF-α Response in Preterm Neonates Is Associated with Impaired Nonclassic Monocyte Function.” *Journal of Leukocyte Biology* 100. https://doi.org/10.1189/jlb.4a0116-001rr.

Wisgrill, Lukas, Isabelle Wessely, Andreas Spittler, Elisabeth Förster-Waldl, Angelika Berger, and Kambis Sadeghi. 2018. “Human Lactoferrin Attenuates the Proinflammatory Response of Neonatal Monocyte-Derived Macrophages.” *Clin Exp Immunol.* 192 (3): 315–324. https://doi.org/10.1111/cei.13108.

Wright, Clyde J., Fadeke Agboke, Fengming Chen, Ping La, Guang Yang, and Phyllis A. Dennery. 2010. “NO Inhibits Hyperoxia-Induced NF-KappaB Activation in Neonatal Pulmonary Microvascular Endothelial Cells.” *Pediatric Research* 68 (6): 484–489. https://doi.org/10.1203/PDR.0b013e3181f917b0.

Wynn, James L., Natalie Z. Cvijanovich, Geoffrey L. Allen, Neal J. Thomas, Robert J. Freishtat, Nick Anas, Keith Meyer, et al. 2011. “The Influence of Developmental Age on the Early Transcriptomic Response of Children with Septic Shock.” *Molecular Medicine* 17 (11–12): 1146–56. https://doi.org/10.2119/molmed.2011.00169.

Young, Rachel, Stephen J. Bush, Lucas Lefevre, Mary E. B. McCulloch, Zofia M. Lisowski, Charity Muriuki, Lindsey A. Waddell, et al. 2018. “Species-Specific Transcriptional Regulation of Genes Involved in Nitric Oxide Production and Arginine Metabolism in Macrophages.” *ImmunoHorizons* 2 (1): 27–37. https://doi.org/10.4049/immunohorizons.1700073.

Zhang, Lei, Yi Wang, Guorao Wu, Weining Xiong, Weikuan Gu, and Cong Yi Wang. 2018. “Macrophages: Friend or Foe in Idiopathic Pulmonary Fibrosis?” *Respiratory Research* 19 (1): 170. https://doi.org/10.1186/s12931-018-0864-2.

**Other references**

Section 3.2.1.2: Pediatric Committee of the European Union (PDCO) (2006). Available online at: https://www.ema.europa.eu/en/human-regulatory/overview/paediatric-medicines/paediatric-regulation.

Section 1.1: German Neonatal Network (GNN) initiated and implemented at the Department of Pediatrics at the University of Lübeck in 2009 (Prof. Dr. Göpel, Prof. Dr. Herting).

**Permissions for reprinted figures:**

Figure 1-5: Reprinted by permission from Elsevir Inc.: Elsevir Inc.; *Immunity*; “Innate Immune Function by Toll-like Receptors: Distinct Responses in Newborns and the Elderly.”; Kollmann, Tobias R., Ofer Levy, Ruth R. Montgomery, and Stanislas Goriely; © 2012 Elsevir, Inc. (2012).

Figure 1-6: Reprinted by permission from Springer Nature Customer Service Centre GmbH: Springer Nature Publishing AG; *Mucosal Immunology*; “Neonatal Mucosal Immunology.”; Torow, N., B. J. Marsland, M. W. Hornef, and E. S. Gollwitzer; © 2017 Springer Nature Publishing AG (2017).

Figure 1-8: Reprinted by permission from John Wiley & Sons, Inc.: John Wiley & Sons, Inc., *Journal of Leukocyte Biology*; “The Phenotype and Function of Preterm Infant Monocytes: Implications for Susceptibility to Infection.”; Jong, Emma de, Tobias Strunk, David Burgner, Pascal M. Lavoie, and Andrew Currie; © 2017 Society for Leukocyte Biology (2017).

# 7. Appendix

## 7.1 Supplementary data

### 7.1.1 Supplementary figure

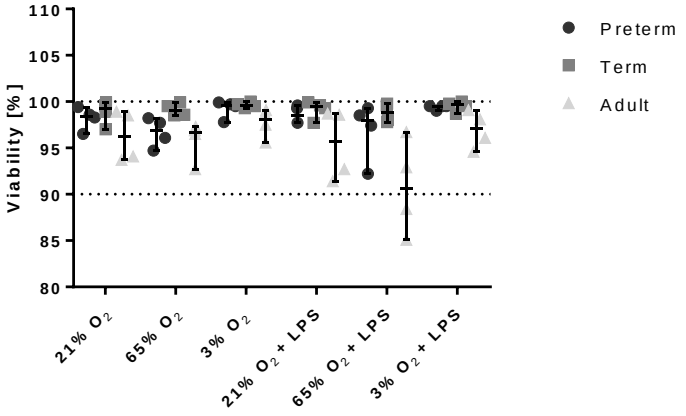


**Figure 7-1: Viability of preterm, term and adult macrophages after 72 h of LPS stimulatation and various $O_2$ concentrations and the double-hits.** Percentage of frequency of viable cells in all three groups assessed by flow cytometry using the double-hit model (n=4; Median with range).

### 7.1.2 Supplementary table

**Table 7-1: Clinical characteristics of patients for individual experiments**

| | Preterm | | | Term | | | Adult |
|---|---|---|---|---|---|---|---|
| | | GA | Weight | | GA | Weight | |
| **Experiment type** | **n** | **mean ± SD** | **mean ± SD** | **n** | **mean ± SD** | **mean ± SD** | **n** |
| Morphology | 4 | 33 ± 1 | 1815 ± 624 | 3 | 40 ± 1 | 3550 ± 170 | 3 |
| *Classical marker after differentiation* | | | | | | | |
| - CD14 panel | 3 | 32 ± 1 | 1663 ± 270 | 3 | 39 ± 1 | 3288 ± 528 | 3 |
| - CD68 panel | 3 | 32 ± 1 | 1730 ± 289 | 3 | 39 ± 1 | 3270 ± 500 | 3 |
| O2 sensing | 0 | | | 3 | 39 ± 1 | 3520 ± 401 | 3 |
| Surface marker after double-hit | 4 | 33 ± 1 | 2025 ± 313 | 4 | 38 ± 2 | 3175 ± 397 | 4 |
| *Cytokine secretion* | | | | | | | |
| - 52 h | 5 | 33 ± 2 | 2236 ± 752 | 5 | 38 ± 1 | 3598 ± 691 | 5 |
| - 72 h | 5 | 33 ± 1 | 1968 ± 317 | 5 | 39 ± 2 | 3748 ± 488 | 5 |
| Global transcriptom | 4 | 33 ± 2 | 1903 ± 216 | 4 | 39 ± 2 | 3713 ± 556 | 0 |
| Polarization of CD4+ cells | 4 | 33 ± 2 | 1925 ± 225 | 4 | 39 ± 1 | 3575 ± 344 | 4 |

## 7.2 Publications

**Twisselmann N**, Pagel J, Künstner A, Weinberg J, Weckmann M., Hartz A, Busch H, and Härtel C (2019) Dysregulated human preterm macrophage responses lead to exaggerated inflammation inducing a Th17/Treg imbalance due to age-dependent differences and key lung exposure factors (Manuscript in preparation)

**Twisselmann N**, Bartsch YC, Pagel J, Wieg C, Hartz A, Ehlers M, Härtel C. (2019) IgG Fc Glycosylation Patterns of Preterm Infants Differ With Gestational Age. Front Immunol. 2019 Jan 18; 9:3166. doi: 10.3389/fimmu.2018.03166. PMID: 30713537

Graspeuntner S, Waschina S, Künzel S, **Twisselmann N**, Rausch TK, Cloppenborg-Schmidt K, Zimmermann J, Viemann D, Herting E, Göpel W, Baines JF, Kaleta C, Rupp J, Härtel C, Pagel J. (2018) Gut Dysbiosis With Bacilli Dominance and Accumulation of Fermentation Products Precedes Late-onset Sepsis in Preterm Infants. Clin Infect Dis. 2018 Oct 06; doi: 10.1093/cid/ciy882. PMID: 30329017

Göpel W, Drese J, Rausch TK, **Twisselmann N**, Bohnhorst B, Müller A, Franz A, Ziegler A, Härtel C, Herting E. (2018) Necrotizing enterocolitis and high intestinal iron uptake due to genetic variants. Pediatr Res. 2018 Jan; 83(1-1):57-62. doi: 10.1038/pr.2017.195. PMID: 28820869

McCarthy MK, Procario MC, **Twisselmann N**, Wilkinson JE, Archambeau AJ, Michele DE, Day SM, Weinberg JB. (2015) Proinflammatory effects of interferon gamma in mouse adenovirus 1 myocarditis. J Virol. 2015; 89(1):468-79. doi: 10.1128/JVI.02077-14. PMID: 25320326

## 7.3 Conference contributions

### 7.3.1 Talks

Twisselmann N, Pagel J, Weckmann M, Göpel W, and Härtel C. Modulation of Macrophage Functions to Prevent Chronic Morbidity in Highly Susceptible Preterm Infants. Kick off-Retreat IRTG1911, Boltenhagen, SH, Germany, 10/2016

### 7.3.2 Posters

Twisselmann N, Pagel J, Weckmann M, Weinberg JB, and Härtel C. Immune response of macrophages from preterm infants with a focus on chronic lung disease. 2nd International Symposium “Allergy Meets Infection”, Lübeck, SH, Germany, 09/2018.

Twisselmann N, Bartsch YC, Pagel J, Wieg C, Hartz A, Ehlers M, and Härtel C. Gestational age-dependent IgG glycosylation pattern in preterm infants. 5th European Congress of Immunology, Amsterdan, Netherlands, 09/2018.

Twisselmann N, Pagel J, Weckmann M, Weinberg JB, Laumonnier Y, and Härtel C. *Ex-vivo* double-hit model for tissue-specific lung immaturity. Immunology Retreat CCHMC, Deer Creek, Ohio, USA, 10/2017.

Twisselmann N, Weckmann M, and Härtel C. Modulation of Macrophage Functions to Prevent Chronic Morbidity in Highly Susceptible Preterm Infants. On-site-review IRTG1911, Lübeck, SH, Germany, 01/2017.

Twisselmann N, Pagel J, Göpel W, and Härtel C. Modulation of macrophage functions to prevent chronic morbidity in highly susceptible preterm infants. 4th Translational DZIF-School, Lübeck, SH, Germany, 09/2016.

Twisselmann N, Pagel J, Göpel W, and Härtel C. Modulation of macrophage functions to prevent chronic morbidity in highly susceptible preterm infants. HZI/DZIF Summer School on Infection Research, Eiterfeld, HE, Germany, 06/2016.

## 7.4 Curriculum vitae

### Personal data

| | |
|---|---|
| Name | Nele Twisselmann |
| Date of birth | 17.02.1987 |
| Place of birth | Kaltenkirchen |
| Nationality | German |

### Education

| | |
|---|---|
| Since 10/2015 | PhD candidate<br>University of Lübeck, Lübeck, Germany<br>Department of Pediatrics<br>Associated to the International Research Training IRTG1911<br>Supported by a scholarship of the Friedrich-Ebert-Stiftung |
| 10/2012 - 05/2015 | Master of Science Infection Biology (Final grade 1.6)<br>University of Lübeck, Lübeck, Germany<br>Department of Infectious Diseases and Microbiology<br>Thesis: *Establishment of a genotype-specific model to study increased growth of Hepatitis C Virus under hypoxia.* |
| 10/2009 - 10/2012 | Bachelor of Science Molecular Life Science (Final grade 2.3)<br>University of Lübeck, Lübeck, Germany<br>Fraunhofer Research Institution for Marine Biotechnology and Cell Technology<br>Thesis: *Untersuchungen zum Einfluss der Kryokonservierung auf Stammzellen in einer 3D Matrix.* |
| 02/2006 - 12/2008 | Higher education entrance qualification<br>(Allgemeine Hochschulreife, final grade 1.5)<br>Abendgymnasium vor dem Holstentor, Hamburg, Germany |

**Experience and practical training**

| | |
|---|---|
| 11/2015 - 12/2015 | Student Assistant<br>University of Lübeck, Lübeck, Germany<br>Department of Pediatrics |
| 04/2014 - 06/2014 | Virology/Immunology research internship<br>Heinrich- Pette- Institute, Hamburg, Germany<br>Viral Zoonosis and Adaptation |
| 10/2013 - 01/2014 | Virology research internship<br>University of Michigan, Ann Arbor, USA<br>Department of Immunology and Microbiology |
| 10/2011 - 09/2012 | Student Assistant<br>Fraunhofer Research Institution for Marine Biotechnology and Cell Technology, Lübeck, Germany |
| 03/2011 | Work experience training in the field of microbiological food analysis<br>ALcontrol Laboratories, Newton Abbot, United Kingdom |

**Work experience**

| | |
|---|---|
| Since 01/2016 | Research Assistant (part-time)<br>University of Lübeck, Lübeck, Germany<br>Department of Pediatrics |
| 06/2015 - 08/2015 | Hospitality Service Specialist<br>Costa Crociere S.p.A., Genoa, Italy<br>Reception desk on the Costa Favolosa, North and Baltic Sea |
| 08/2005 - 09/2009 | Tax official<br>Tax office of Pinneberg, Germany |

**Languages**

| | |
|---|---|
| German | mother tongue |
| English | fluently |
| Spanish | basic knowledge |

## 8. Acknowledgements

In the process of preparing and writing this thesis, there have been many people who have guided and supported me in various ways and deserve appreciation.

First of all, I would like to thank my supervisor Prof. Dr. Christoph Härtel for the opportunity to be a member of his research group and to work on this interesting project. His continuous support and guidance, and the beneficial discussions not only on this thesis were very helpful throughout the last three years.

Secondly, I am very thankful to my mentor Dr. Julia Pagel for her scientific support and company during these years. I highly appreciate the valuable suggestions, helpful discussions and constructive comments on this thesis. With her constant positive mindset and encouraging way to face challenges, she always inspired me.

I also thank Prof. Dr. Egbert Herting for hosting this thesis at the Department of Pediatrics and Prof. Dr. Wolfgang Göpel for supporting my research, also with resources from the German Neonatal Network.

I would like to thank Dr. Axel Künstner and Prof. Dr. Hauke Busch from the group Systems Biology at the Institute for Experimental Dermatology in Lübeck for the great collaboration, and their support and analysis of the RNA sequencing data.

I am very greatful that Prof. Dr. Jason B. Weinberg from the Department of Microbiology and Immunology at the University of Michigan and Dr. Markus Weckmann from the Department of Pediatrics at the University of Lübeck were my second and third supervisors and supportively discussed all generated data and analysis-strategies with me. Specially, I thank Jason B. Weinberg for his thoughtful revision of my thesis.

I want to thank my colleagues Dr. Annika Hartz and Dr. Martin Demmert for helpful discussions about clinical- and science-related questions and their good advice. Moreover, I like to thank Dr. Annika Hartz for critically proof-reading my thesis.

I like to acknowledge Stefanie Prien and Gabriele Feldhoff for their manifold help with all kinds of technical issues, the great teamwork, and fun hours together.

I am very greatful to those involved in the process of sample collection for the data generated during my PhD study, which adresses parents, patients and blood donors, as well as nurses and physicians. In addition, I thank all medical students who supported the sample collection.

I am greatful that Prof. Dr. Jan Rupp of the Department of Infectious Diseases and Microbiology gave me the opportunity to work in his laboratories and participate in scientific meeting of the department. This gave me the chance to work together with

another group of colleagues. Therefore, I am very thankful to Dr. Nathalie Loeper, Dorinja Zapf, Dr. Simon Graspeuntner, Dr. Kensuke Shima, Dr. Dirk Friedrich and Dr. Nadja Käding for helpful scientific discussions, support in the laboratory, and of course the enjoyable atmosphere every day. I would like to emphasize my thanks to Dr. Simon Graspeuntner for always giving me advice on statistical analysis, and Dr. Dirk Friedrich and Dorinja Zapf for critically revising parts of this thesis. A special thanks goes to Dr. Nathalie Loeper, who became a life-long very good friend and will always be the first person who convinced me that cardio-training is a very good therapy for everything. In addition, I thank Angela Gravenhorst, Anke Hellberg, and Siegrid Pätzmann for their technical assistance.

I also want to acknowledge Prof. Dr. Jörg Köhl, Dr. Julia Figge and Dr. Nadine Höft from the Institute for Systemic Inflammation Research of the University of Lübeck to associate my PhD project to the International Research Training Group 1911. Moreover, I also like to acknowledge PD Dr. Yves Laumonnier and Dr. Tillman Vollbrandt, from the Cell Analysis Core, for their support in planning and performing flow cytometry experiments.

I am very greatful to the Friedrich-Ebert-Stiftung for their financial support (scholarship) and various opportunities to engage in social and political activities.

My family and friends deserve a big thank you for their unlimited support during my studies and PhD. Their continuous encouragement and love, also throughout some stressful times, helped me to succeed.

Because my father Jan Twisselmann passed away too soon suddenly in December 2017, I specially want to thank him for his support and love my whole life. I am deeply sad that he cannot be here for my graduation. Since this was a challenging time for me, I could not have made it through without the loving support of my mother Ingrid Twisselmann and my sister Lina Twisselmann. In addition, I would like to mention a few friends in particular. I am deeply thankful to Arno Wenderlein, who is not only a life-long friend, but was also there for me every day during the illness of my father and the grief afterwards. I am very greatful to Mariessa Stademann for our endless discussions about our dreams and hopes. I want to let her know, that I consider her my sister in heart and soul, too. I would also like to thank Dr. Alexander Heuer for our countless discussions on his balcony about the future and his uncontitional support and close friendship. Lastly, I would like to thank Dr. Nils-Owe Hansen for his constant caring, and thoughtful support and encouragement during my writing phase.